# Effect of stope construction parameters on ore dilution in narrow vein mining

By

Hind Zniber El Mouhabbis

A thesis submitted to McGill University in

Partial fulfillment of the requirements for the

Degree of Master of Engineering

Department of Mining and Metals and Materials Engineering

McGill University

Montreal, Quebec, Canada

February 2013

# Abstract

Ore dilution has an important influence on mining costs and hence on the viability of a mining operation. Costs associated with ore dilution with barren waste or material below the cut-off grade are linked to all mining and milling stages. Several research efforts were made in the past to help better understand the causes of ore dilution, and some of these led to the development of empirical formulae for the estimation of ore dilution in different mining environments. Stope geometry was identified as one of the principal factors influencing ore dilution attributed to stope wall overbreak. This thesis examines the effects of stope geometric parameters on ore dilution – namely the stope width and strike length, as well as stope undercutting and the orebody dip angle. The study uses nonlinear finite element modelling as the analysis tool. Numerical model predictions are compared, whenever possible, with surveyed stope profile obtained from field measurements. The scope of the thesis is a case study of the Lapa Mine of Agnico Eagle Mines Limited, a gold mining operation situated in the Abitibi region of Quebec. The Lapa orebody is a narrow vein, steeply dipping deposit with varying width, and is extracted with longitudinal retreat mining method.

# Résumé

La dilution a une influence importante sur les coûts de minage et de la viabilité d'une opération minière. Les coûts associés à la dilution provenant du stérile ou du marginal sont générés de toutes les étapes de minages et de procédé. Plusieurs efforts de recherche ont été déployés afin de mieux comprendre les causes de la dilution d'ailleurs ces recherches ont conduit à développer des formules empiriques pour différents environnements miniers. La géométrie des chantiers a été identifiée comme un facteur principal influençant la dilution provenant des épontes. Cette thèse examine l'effet de la géométrie sur la dilution dont la largeur et la longueur du chantier, mais aussi la sur-excavation des épontes et enfin le pendage du gisement. L'étude utilise comme outil la modélisation numérique avec éléments finis non linéaire. Les prédictions des modèles numériques sont comparées si possible à l'arpentage réel des profils obtenus après le minage. Cette thèse est basée sur l'étude de la Mine Lapa d'Agnico Eagle Mines Limited, une opération aurifère située en Abitibi au Québéc. Le gisement de Lapa est composé de veine étroites dont le pendage est sub-vertical avec des épaisseurs variables. L'extraction du gisement se fait avec la méthode de retrait longitudinal.

# Acknowledgment

I wish to thank my supervisor, Professor Hani Mitri, for his technical guidance and moral support throughout my study. I express my sincere gratitude to the engineering department at Lapa Mine of Agnico Eagle for their help and contributions, most notably Eric Lecomte – the Mine Manager. This work was supported by a joint research grant from Agnico Eagle Mines Ltd and Natural Science and Engineering Research Council of Canada. I am grateful for their support. Finally, I thank all my colleagues at McGill - McGill Mine Design Group for their continued support and encouragement.

# Table of contents

# List of Figures

# List of Tables

# Nomenclature

DD dilution density

D damage factor

c cohesion

$E_{rm}$ young's modulus of elasticity of the rock mass.

$E_i$ young's modulus of elasticity of intact rock.

ELOS equivalent linear overbreak/slough

$J_n$ joint set number

$J_r$ joint roughness number

$J_a$ joint alteration number

$J_w$ joint water reduction

GSI geological strength Index

RMR rock mass rating

RQD rock quality designation

SFR stress reduction factor

$\gamma$ material unit weight

$\rho$ material density

$\sigma_c$ Uniaxial compressive strength

$\sigma_t$ tensile strength

$\sigma_1$ major principal stress

$\sigma_3$ minor principal stress

$\psi$ angle of dilation

$\phi$ internal angle of friction

# Chapter 1 Introduction

## 1.1 Introduction

Dilution is defined as the contamination of ore with either barren waste or material with the minerals of interest below the cut-off grade. The importance of dilution on the profitability of a mining operation is related to unexpected extra costs. The costs associated with a mine experiencing dilution is a function of ore grade, dilution material grade, metal price, and the degree of acceptable dilution which differs from one mining operation to another. Dilution is present at all stages of mining including the first step of stope mining where waste is extracted intentionally in order to insure excavation stability or equipment fitting within the drift. Numerous factors influence the occurrence of dilution.

Empirical models have been developed based on several tunneling surveys and previously mined stopes to assess the amount of dilution that had taken place. These models evaluate the occurrence of dilution without providing a confidence interval for its quantification.

## 1.2 Study problem

Ore dilution or overbreak increases the cost of production and reduces the profitability of a mining operation. The unfavourable economic impact is related to all the extra costs associated with the mining cycle and processing of waste rock or low grade ore generated from either the hanging-wall or the footwall or both. Ore dilution is a main concern at the Lapa Mine in northern Quebec, and it is caused mainly due to the low quality of the host rockmass. Thus, this study will concern itself with better understanding the response of the stope walls to ore extraction and how this process influences the stability of these walls.

## 1.3 Scope and objectives

The main objective of this study is to provide a better understanding of the influence of stope design parameters and stope settings on the stability of the stope walls. As the unstable stope walls fail into the mined stope – thus experiencing overbreak, ore dilution occurs. More specifically, the objectives of this thesis are:

- Review the current methods for the quantification of ore dilution.
- Review and identify the primary factors influencing ore dilution.
- Conduct a detailed numerical modelling study to assess the effect of stope undercutting effect, stope width, stope strike length, and ore body dip on ore dilution.
- Validate whenever possible the numerical modelling trends with field measurements of surveyed stope profiles.

**Thesis Outline**

Chapter 1 presents the scope of the study and its objectives.

Chapter 2 is a detailed literature review of ore dilution.

Chapter 3 provides a description of Lapa Mine including mining method and backfill practice.

Chapter 4 describes the rock mechanics parameters at the Lapa Mine collected from various sources. A preliminary database was created to compile this information.

Chapter 5 reports a study on the effect of stope undercutting on ore dilution applied to Lapa Mine with multiple mining stages.

Chapter 6 examines the effect of stope width, strike length and ore dip on ore dilution.
Chapter 7 provides conclusions and a summary of the work done.

# Chapter 2 Ore dilution in narrow stope vein mining

## 2.1 Introduction

Ore dilution is divided into two types: planned and unplanned. Planned ore dilution is defined as non-ore material (barren or below the cutoff grade) taken into account in ore reserves estimation and operating costs. Planned ore dilution meets the design limits where factors such as the orebody complexity (i.e. narrow vein) and mining method govern the amount of planned ore dilution assumed in forecasting the costs. In the literature, planned ore dilution is referred as intentional or primary dilution. Unplanned ore dilution, commonly known as overbreak, is the unexpected non-ore material (barren, below the cut-off grade, and fill) added to the mucked tonnage, as can be seen in Figure 2.1 below. It is the extra waste not assumed in the mine planning that comes from the stope or adjacent fill. The economic consequences can be significant on the profitability of a mining project.

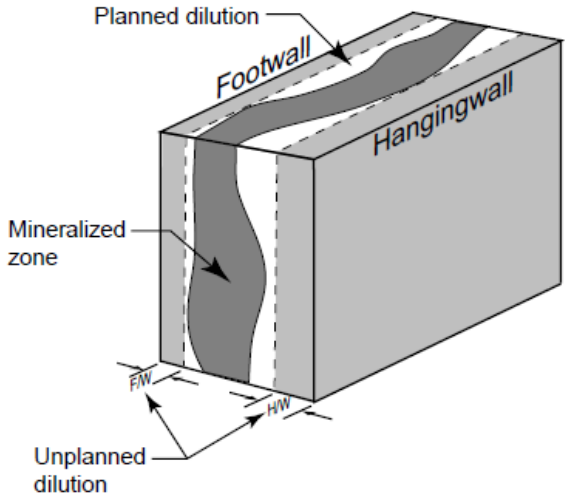


**Figure 2.1** Schematic illustration of different types of dilution

Unplanned ore dilution is usually reported in the literature as secondary dilution. Factors inducing dilution have been summarized by de la Vergne (2000), and they have been presented in Figure 2.2 below

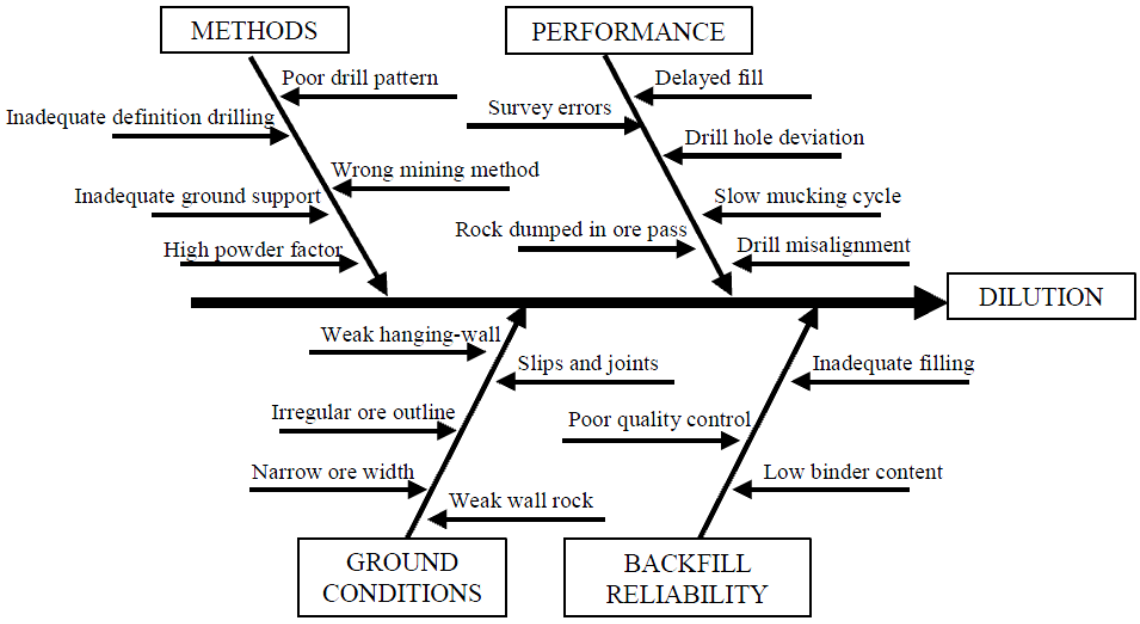


**Figure 2.2** Fishbone chart resuming factors inducing dilution (de la Vergne 2000)

## 2.2 Dilution measuring

Dilution can be measured by a non-reflecting laser instrument called the cavity monitoring system (CMS). It was developed jointly by the Noranda Technology Center and Optech Systems. The device is placed on a pole at the stope overcut. Two points are surveyed on the pole in order to match the mine coordinates with the volume measured. The laser is attached to a horizontal boom then inserted into a cavity. The range finder rotates around the boom to survey the opening where the data are sent to a data logger. The laser on the device rotates at 360 degrees angle around the boom axis and up to 135

degrees about the pivot axis, making a sphere of 270 degrees. The capacity of the CMS to survey stope voids is up to 100 meters in height; however, in an irregular shaped stope, the effective range is within 20 meters. The accuracy range is around 2cm and maximum reading is 100,000 points. The degree of rotation can be selected by the surveyor depending on the precision needed. The saved information in the remote device is loaded in a CAD program where a primary wire mesh is constructed (see Figure 2.3).The major advantage of the system is that it gives a realistic 3D volume of the stope, allowing stope reconciliation and stope overbreak or underbreak evaluation with precise measurement of walls and backs caving. Moreover, it is possible to monitor backfill placement, blast efficiency, and extent of rockburst damage, as well as quantifying and minimizing dilution (illustrated in Figures 2.4 and 2.5).

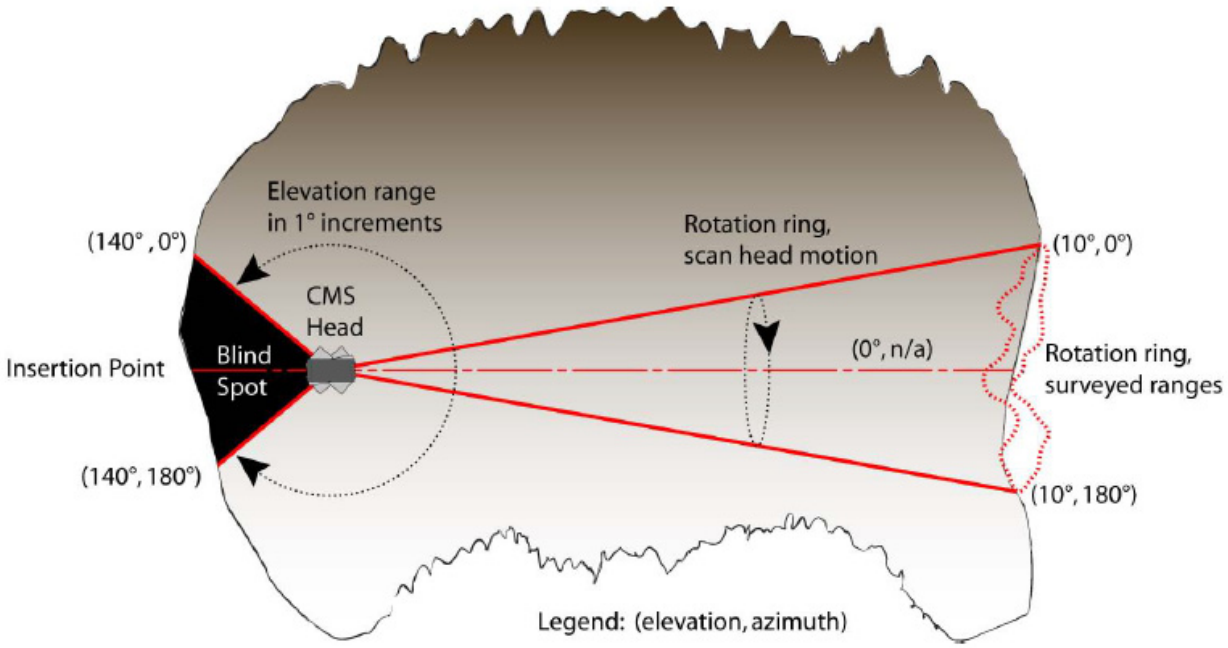


**Figure 2.3** Cavity monitoring system (CMS) in a drift (Optech-CMS advertising)

Nonetheless, some limitations cause difficulties in rendering the volume true shape or volume calculation such as the muck remaining at the bottom of the stope, set-up errors by the surveyor, and hidden or blind spots in the geometry of the stope. Moreover, the distance, density of suspended dust, blasting smoke, and humidity are factors controlling the cavity monitoring system efficiency.

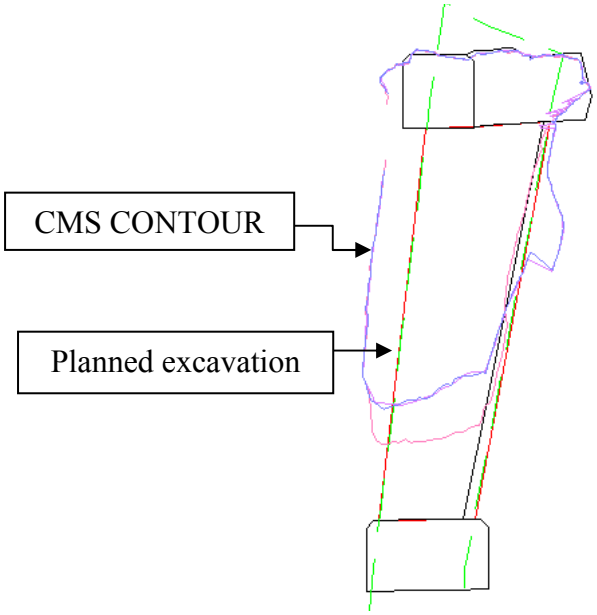


**Figure 2.4** CMS stope survey and planned excavation at Lapa Mine

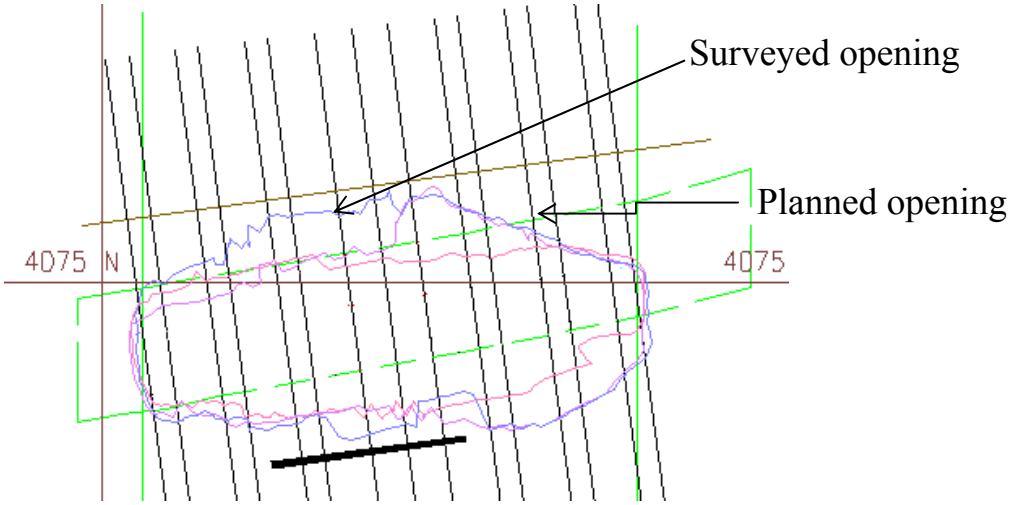


**Figure 2.5** Horizontal cross section at stope mid-height at Lapa Mine

## 2.3 Dilution reporting

A survey in Canadian mines was conducted by Pakalnis (1986) to collect dilution reporting. Nine equations were compiled; and Scoble and Moss (1994) showed that the equations listed below are the widely used in defining ore dilution in Canadian mines. The first equation will be used for calculating in this thesis.

**Dilution** =(Tonnes waste mined)/(Tonnes ore mined)

**Dilution** =(Tonnes waste mined)/(Tonnes ore mined + Tonnes waste mined)

Moreover, Conners et al (1996) introduced a dilution reporting independent from ore stope width, entitled "Equivalent Linear Overbreak / Slough (ELOS)". It was defined as the average meter of sloughage per square meter of wall ($m/m^2$) where the volume measured by the CMS is converted into an average sloughage over the stope surface, as can be seen in Figure 2.6.

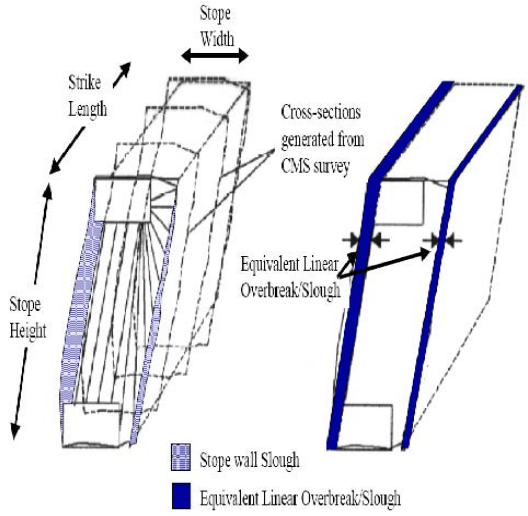


**Figure 2.6** ELOS schematic representation (Clark and Pakalnis 1997)

ELOS is defined by the equation below:

$$\text{ELOS} = \frac{\text{Volume of overbreak}}{\text{stope height} \times \text{wall strike length}}$$

Clark and Pakalnis (1997) defined an ELOS table where design zones are separated according to number ranges. Table 2.1 shows this classification.

**Table 2.1** ELOS ranges within design zones

| ELOS RANGE | ELOS DESIGN ZONES |
|---|---|
| **< 0.5m** | Blast damage only, the surface is self-supporting |
| **ELOS = 0.5m - 1m** | Minor sloughing: some failure from unsupported stope wall should be anticipated before stable configuration is reached |
| **ELOS = 1m -2m** | Moderate sloughing from unsupported stope walls is anticipated before stable configuration is reached |
| **ELOS > 2m** | Severe sloughing: large failures from unsupported stope wall should be anticipated. Wall collapse is possible. |

ELOS gives a value of dilution; however, it does not indicate whether the hanging-wall or the footwall wall suffers from sloughage. Additionally, factors such as in-situ stress and stope depth are not taken into account in ore dilution reporting.

## 2.4 Planned ore dilution

Planned dilution is defined as the intentional waste added to operating costs and to annual reserves estimation. Ore deposits have different shapes and geometry.

Therefore, different mining methods and equipment fleet selection could be adopted according to the ore dilution tolerance limits defined in the planning and stope design.

### 2.4.1 Mining method

Mining method selection dictates the amount of resulting dilution. Bulk mining allows for extra dilution in massive ore deposits; and on the other hand selective methods are chosen to limit the effectiveness of ore dilution when mining a narrow vein. In the case of conventional narrow vein mining, a minimal stope width has to be respected. Table 2.2 summarizes dilution measurements for a variable ore width in a minimal drift width, considered 1.2m. By comparing the results, the dilution in a narrow vein deposit increases significantly with smaller ore width.

**Table 2.2** Minimum stope width vs primary dilution (SME 2001)

| Ore width | Dilution width | Minimum stope width | Dilution |
|---|---|---|---|
| 0.15 m (0.5 ft) | 1.05 m (3.5 ft) | 1.20 m (4.0 ft) | 700% |
| 0.30 m (1.0 ft) | 0.90 m (3.0 ft) | 1.20 m (4.0 ft) | 300% |
| 0.45 m (1.5 ft) | 0.75 m (2.5 ft) | 1.20 m (4.0 ft) | 167% |
| 0.60 m (2.0 ft) | 0.60 m (2.0 ft) | 1.20 m (4.0 ft) | 100% |
| 0.75 m (2.5 ft) | 0.45 m (1.5 ft) | 1.20 m (4.0 ft) | 60% |
| 0.90 m (3.0 ft) | 0.30 m (1.0 ft) | 1.20 m (4.0 ft) | 33% |
| 1.05 m (3.5 ft) | 0.15 m (0.5 ft) | 1.20 m (4.0 ft) | 14% |
| 1.20 m (4.0 ft) | 0 | 1.20 m (4.0 ft) | 0% |

However, in the case of medium ore thickness, the longitudinal stope mining is ideal. Waste or material below the cut-off grade are mined and are included in mining drilling and blasting plans.

### 2.4.2 Mining operation

Stope width is a function of ore width, equipment size, mining method, and the equipment clearance imposed by law. As an example in drilling activities, a minimum space is needed from a wall to the drill boom to start the hole. In addition, another example is shown in Figure 2.7 where, two ore deposits with different dips and an LHD chosen randomly are sketched. As can be seen, the ore deposit dip has an influence on the drift size geometry where the size in the steep deposit is smaller than the drift designed size in the case of an inclined deposit.

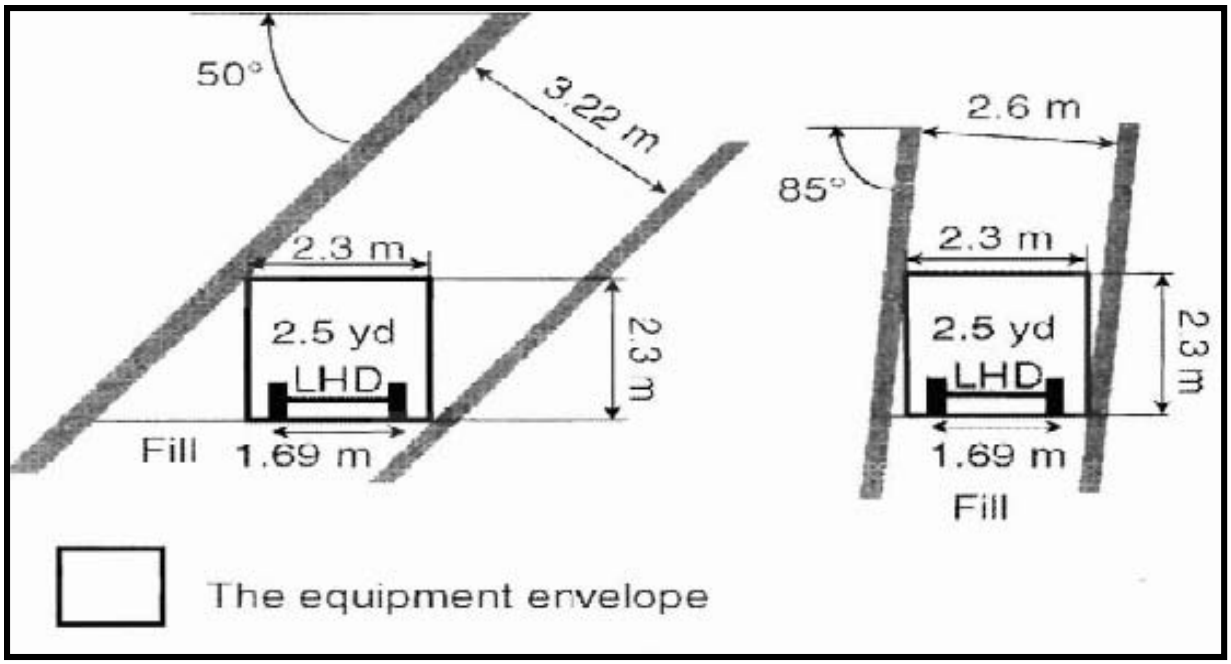


**Figure 2.7** Stope width for differently dipping ore deposits (SME 2001)

## 2.5 Unplanned ore dilution

Unplanned ore dilution has a major influence on the mine's life and the profitability of the operation. If extra waste is mined, additional costs will be encountered leading to the inaccuracy of the forecasted costs associated. Numerous factors affect the occurrence of unplanned ore dilution. Several operating mines attempt to distinguish its causes in stopes.

Unplanned ore dilution is generated occasionally by inexperienced surveyor or worker. Some examples could be mentioned as an inaccurate drill set-up, drill hole deviation, unskilled labor (i.e., loading holes not marked on the blasting pattern). Also, errors in mucking where waste can be dumped in an ore pass and vice-versa.

The stope design influences the effectiveness of unplanned ore dilution. Stope dimensioning, ground conditions, inadequate ground support, and drill and blasting patterns are factors leading to stope overbreak. For example, failure of free faces into the mined ore after a blast as a consequence may be the result of the backfill not completely having cured. Henning and Mitri (2007) demonstrated that the mining depth has no effect on the unplanned ore dilution based on $\sigma_3$ iso-contours. In addition, the rock mass quality influences the overbreak where the lower the rock quality the more the overbreak is significant.

### 2.5.1 Time effect

The stope cycle has to be well studied where a delay can affect the wall's integrity. As time pass by, the exposed walls fail into the stope. If the stope is not mucked and walls are weak, boulders cave on the muck leading to a recovery problem.

Ran (2002) conducted a study on an opened stope where surveys were done and a comparison with the original stope contour is plotted on Figure 2.8.The study showed that hanging-wall progressive sloughing is related to the time wall exposure.

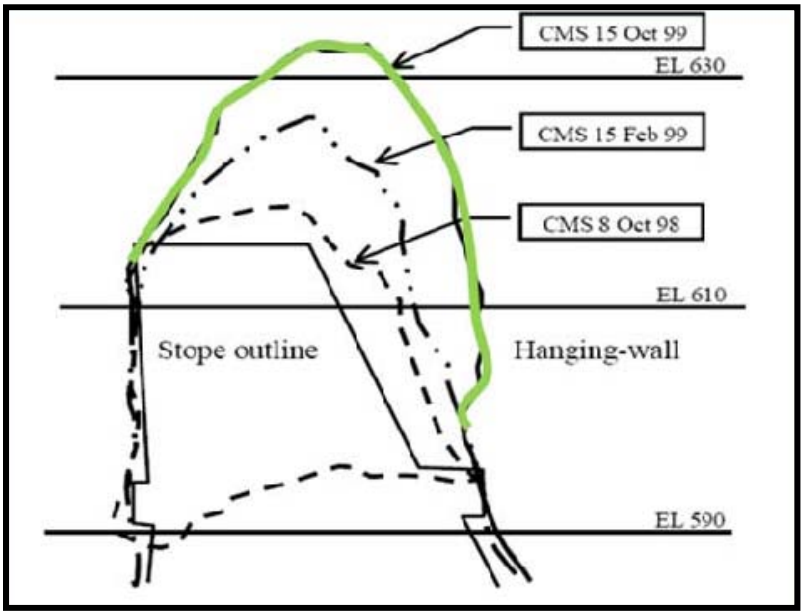


**Figure 2.8** Open stope caving (Ran 2002)

### 2.5.2 Stope category

In long-hole mining, stopes are either surrounded by rock on both sides or rock on one side and backfill on the other side or backfill on both sides. Henning and Mitri (2007) introduced the terminology illustrated in Figure 2.9. The primary stope is subjected to high stresses as a result of confinement that tends to distress the adjacent rock mass.

Location within the mining sequence has an influence on the overbreak occurrence. Unsettled backfill and inappropriate stope sequencing can have a severe consequence on unplanned stope dilution.

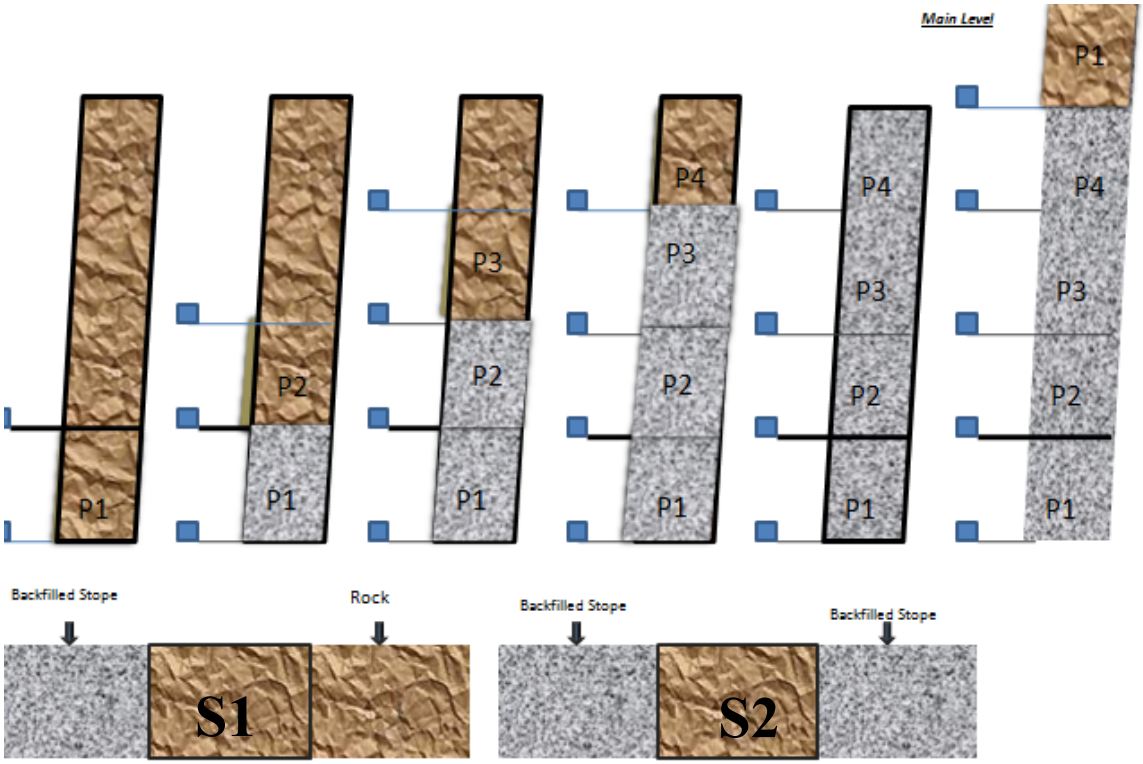


**Figure 2.9** Stope categories within the mining block

### 2.5.3 Stope height and complexity

Stope height and complexity affects the wall stability and specially the hanging wall. Several cases were studied and Perron (1999) reported that high stopes (60m height) at the Langlois Mine had to be re-designed to decrease the dilution. Sub-levels were mined to reduce the stope span, and improve the stability. Besides, stope complexity is a factor influencing dilution where the irregularities in the stope geometry and ore body strike changes results in wall sloughed.

### 2.5.4 Stope undercutting

Undercutting interrupts the continuity of a rockmass where a relaxation zone, a near-zero stresses condition tangential to the opening, is created. Wang (2004) examined the effect of undercutting on wall stability and when bedding and foliation are within the rockmass (Figure 2.10).

Stope undercutting could be represented in three scenarios, undercutting the hanging wall, or footwall or both.

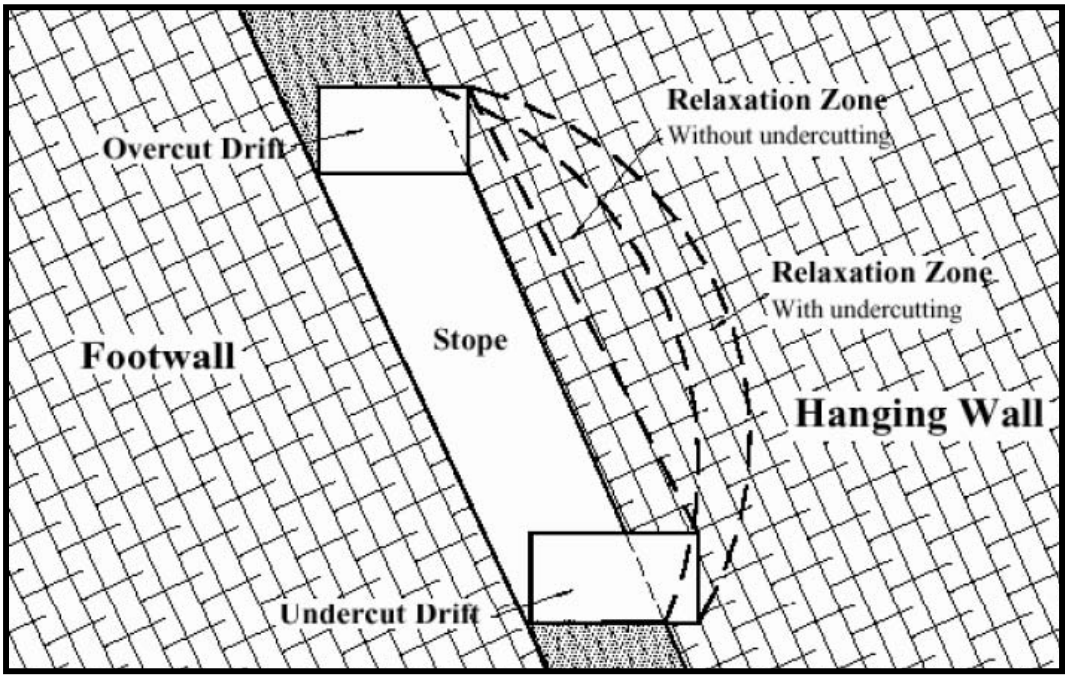


**Figure 2.10** Influence of wall undercutting on stope relaxation (Wang et al. 2002)

### 2.5.5 Hanging-wall dip angle

Unplanned ore dilution is sensitive to the ore dip. Henning and Mitri (2007) noted that with the steep hanging-wall dip, the disturbance of low $\sigma_3$ stress can relieve an unstable wedge. Moreover, with an inclined hanging wall dip, the dilution has the tendency of increasing under the gravity effect.

### 2.5.6 Stress environment

Dilution is a result of rockmass relaxation. It is defined as a reduction in stress state parallel to wall excavation. Dilution occurs when the minor principal stress is below or equal to zero, Martin et al (1999) as illustrated on Figure 2.11.

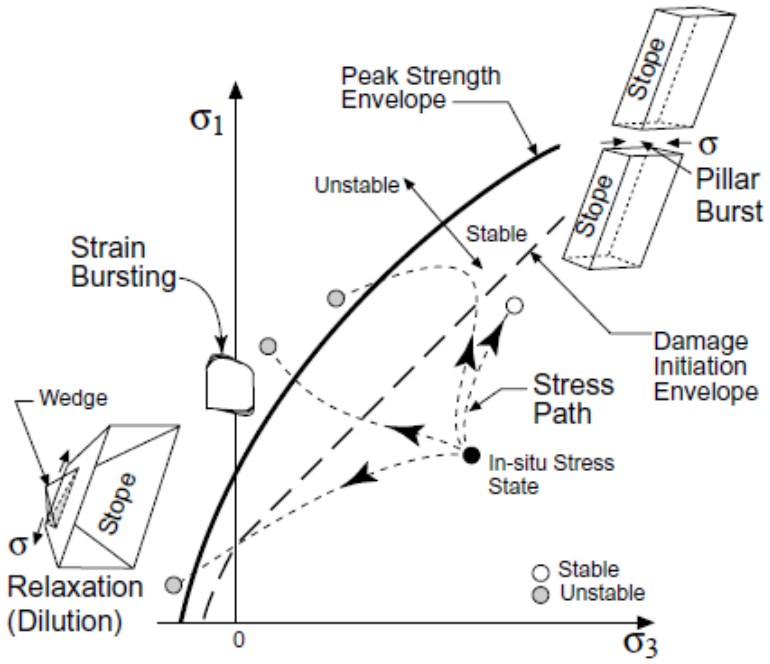


**Figure 2.11** Possible stress path for a stope (Martin et al. 1999)

The severity of sloughage is related directly to the rock tensile strength. However, rockmass has a self-supporting capacity depending on the material properties and geological structures. Tensile strength criterion can be used to assess hanging wall stability and dilution potential that has been reported by Mitri et al. (1998).

### 2.5.7 Orezone width

Dilution is critical when mining a narrow stope according to Pakalnis et al. (1995). As illustrated in Figure 2.12, when a 3m stope width having a 1.7m wall sloughage, a 55% dilution is expected. However, a 7m stope with same amount of wall sloughage will experience a 25% unplanned ore dilution.

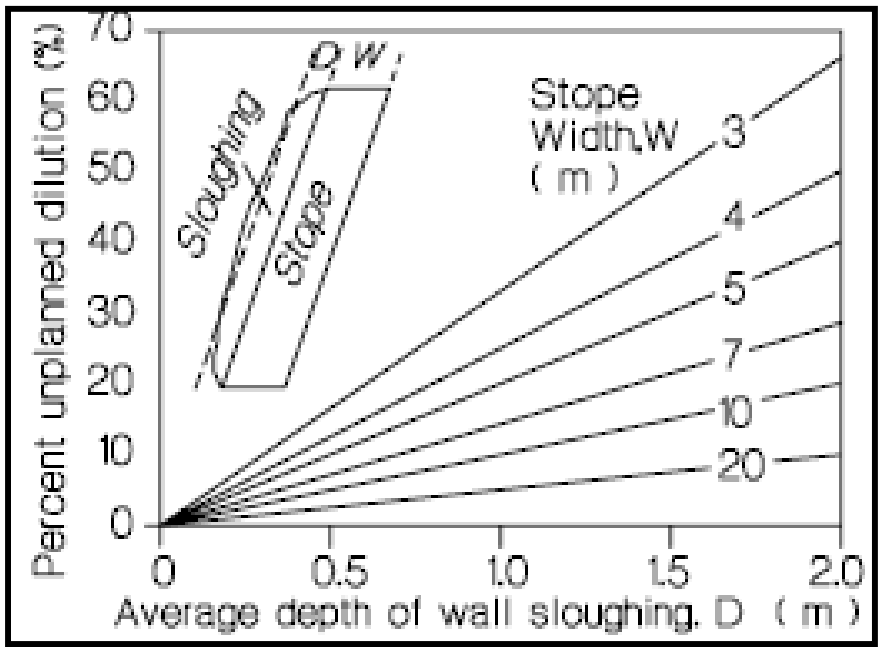


**Figure 2.12** Dilution vs sloughing and span (Pakalnis et al. 1995)

## 2.6 Prediction of dilution

Various empirical models have attempted to predict dilution based on stope width or ore width. However the estimate is qualitative and not quantitative and does not give an accurate prediction since numerous factors affect dilution. The widely used prediction tool is the stability graph method, described in the following section. The stability graph method is an empirical method developed by Matthews et al (1981) and refined by Potvin

(1988) where the prediction curve was updated with more data. Studied cases are 228 of unsupported open stopes and 163 stopes where cable bolts were installed.

The stability graph method associates the modified number of stability to the hydraulic radius of a stope. Figure 2.13 represents the stability graph method. The graph helps to assess the stability of an opening according to the stope hydraulic radius. The stability number is calculated by the following equation.

$$\mathbf{N'=Q' \times A \times B \times C}$$

N' = Stability Number

Q' = Modified Tunneling Quality Index (NGI) with stress reduction factor

A =Stress Factor estimated from Figure 2.14.

B = Joint Orientation Factor estimated from Figure 2.15.

C = Gravity Factor, estimated from Figure 2.16.

HR = Hydraulic Radius = Surface Area/Perimeter

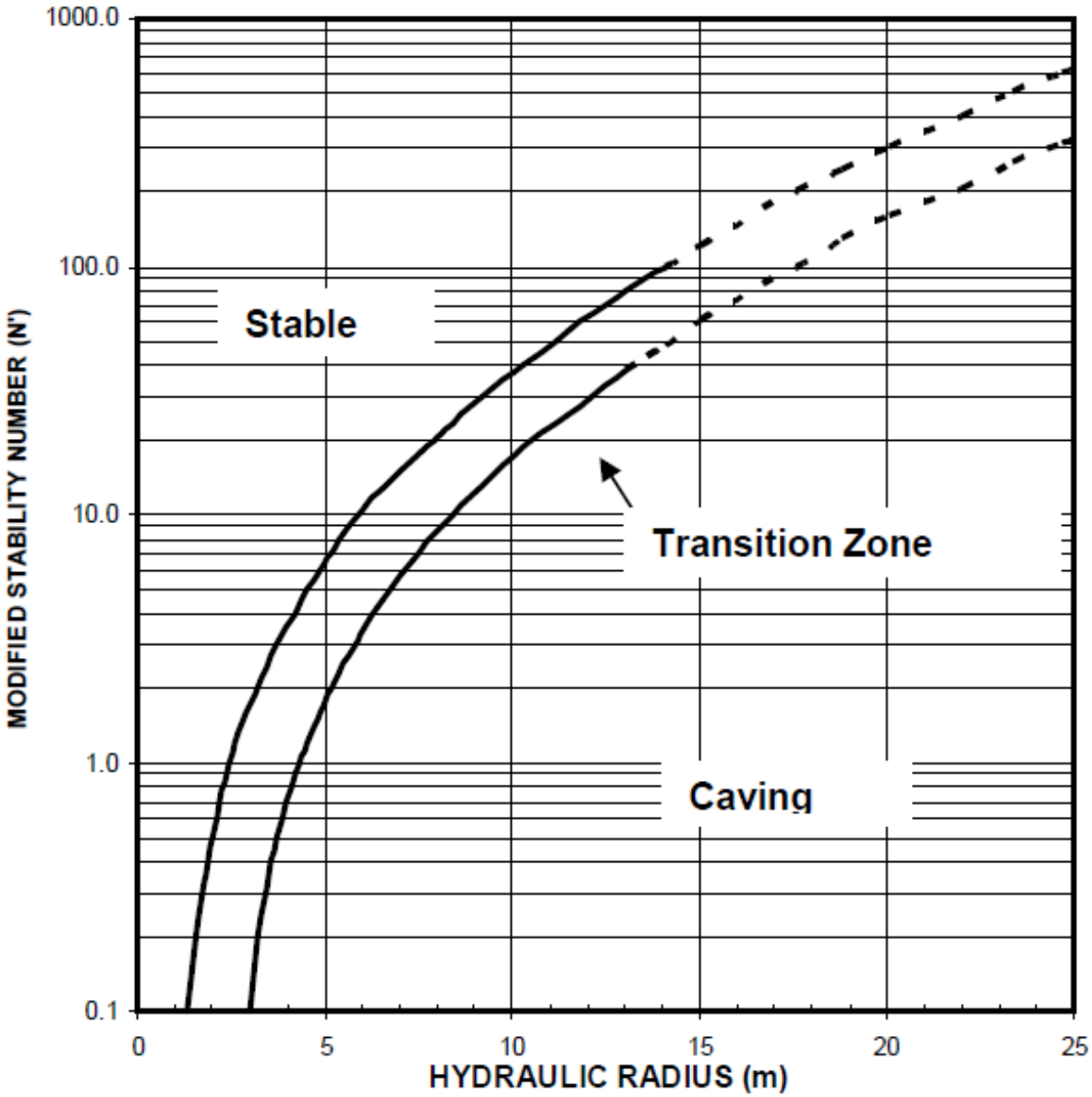


**Figure 2.13** Modified stability graph (Potvin et al 2001

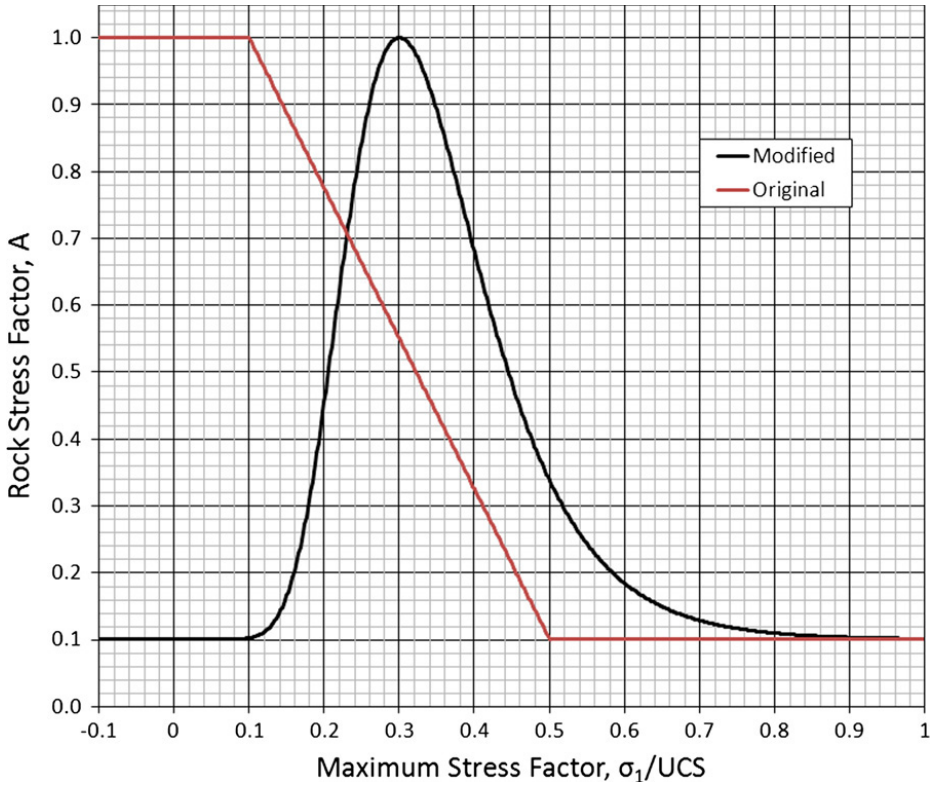


**Figure 2.14** Modified stress factor A, (Mitri et al. 2011)

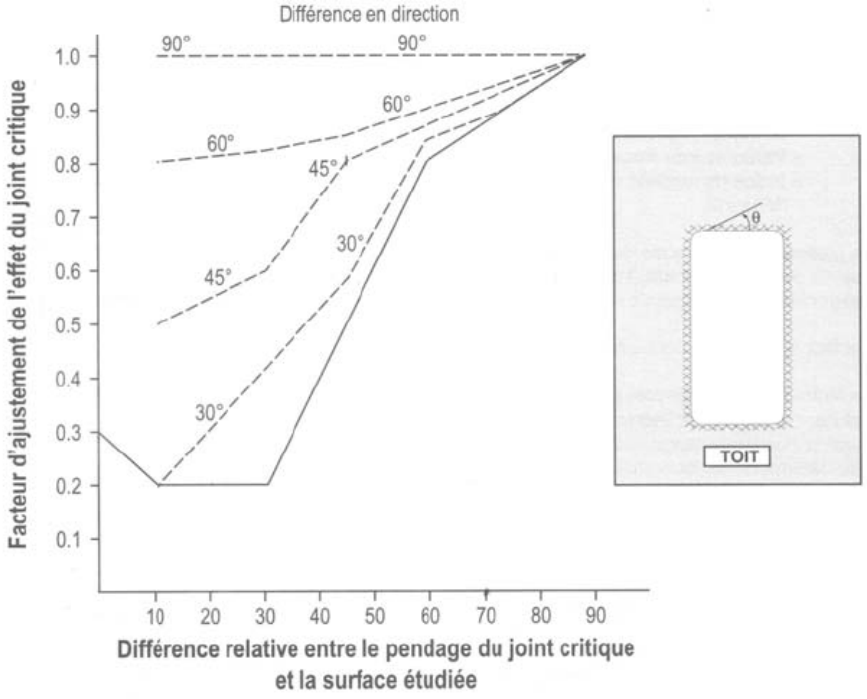


**Figure 2.15** B factor evaluation

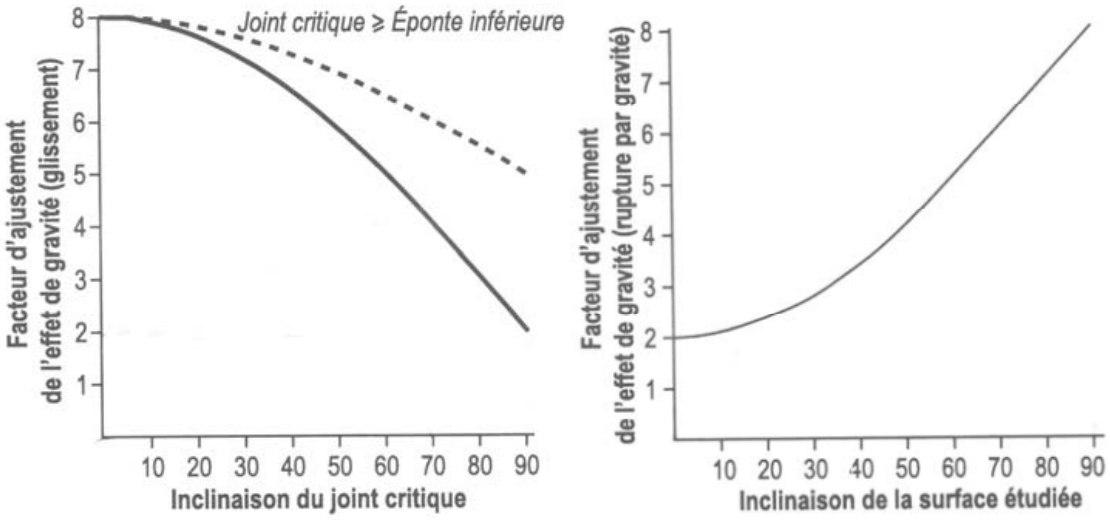


**Figure 2.16** C Factor – case with instability by sliding or gravity instability

Moreover, the stability graph is a handy tool that can be used easily to assess the situation when the factor A is already known by a numerical model. Three models are represented with the stability graph method: safe, unstable, and caving. These three types represent an increasing importance of occurring dilution. Planned dilution is accepted on purpose to simplify opening geometry for blasting and materials handling. It is represented within the stable zone of stability graph method. Unplanned ore dilution, overbreak, occurs in the caving and instable zones. According to Pakalnis (1995), dilution can be determined, from a modified stability graph assuming a 5m ore width (Figure 2.17).

The stability graph method is limited to the same case scenario. Abutment relaxation, stress changes magnitudes and orientation, blasting effect, time exposure, stress induced damages, and variation in stope construction and design are not considered. In addition, the graph is not appropriate for stiff rock or creeping rock mass.

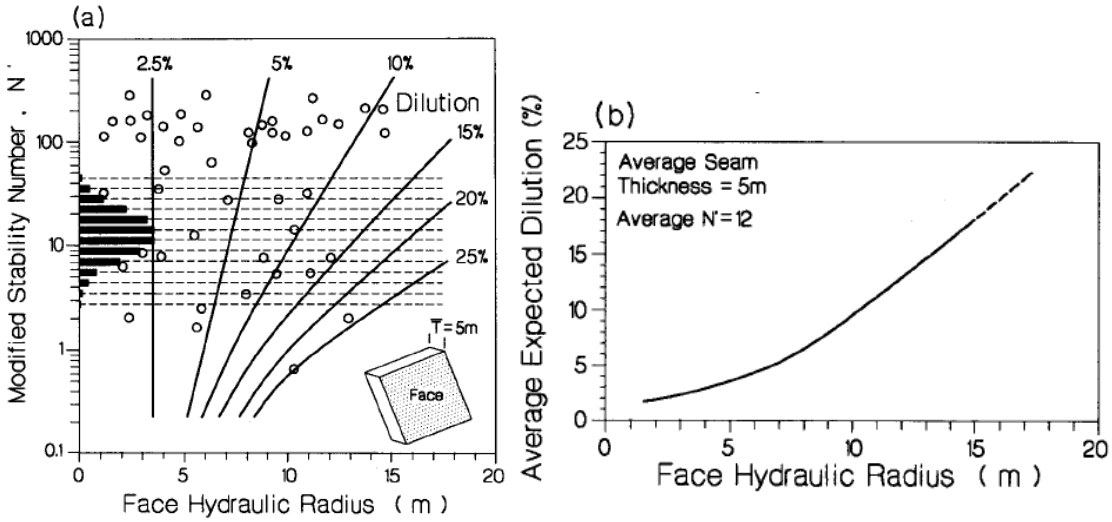


**Figure 2.17** Average dilution at Canadian mines (Palkanis 1995)

The main limitation of the stability graph method use for predicting dilution is that the model does not give a quantification of ore dilution but only helps in assessing the occurrence of dilution.

## 2.7 Quantification of dilution

A methodology was developed by Henning and Mitri (2007) to evaluate the potential overbreak from a 3-dimensionnal numerical model where the size of the overbreak area was typically represented in the zero stress contour ($\sigma_3$= 0 MPa) or the rockmass tensile strength contour ($\sigma_3$= $\sigma_t$) are used to define the boundary of the overbreak area.

The volume of the potential hanging-wall relaxation for a mined stope was represented as the volume of half ellipsoid and expressed by the following formulation:

$$V_{pe} = \frac{2}{3}\pi \times r_1 \times r_2 \times r_3$$

where,

$r_1$, $r_2$, $r_3$: radial distances from the centre of stope to $\sigma_3$ iso-contour, illustrated on Figure 2.18.

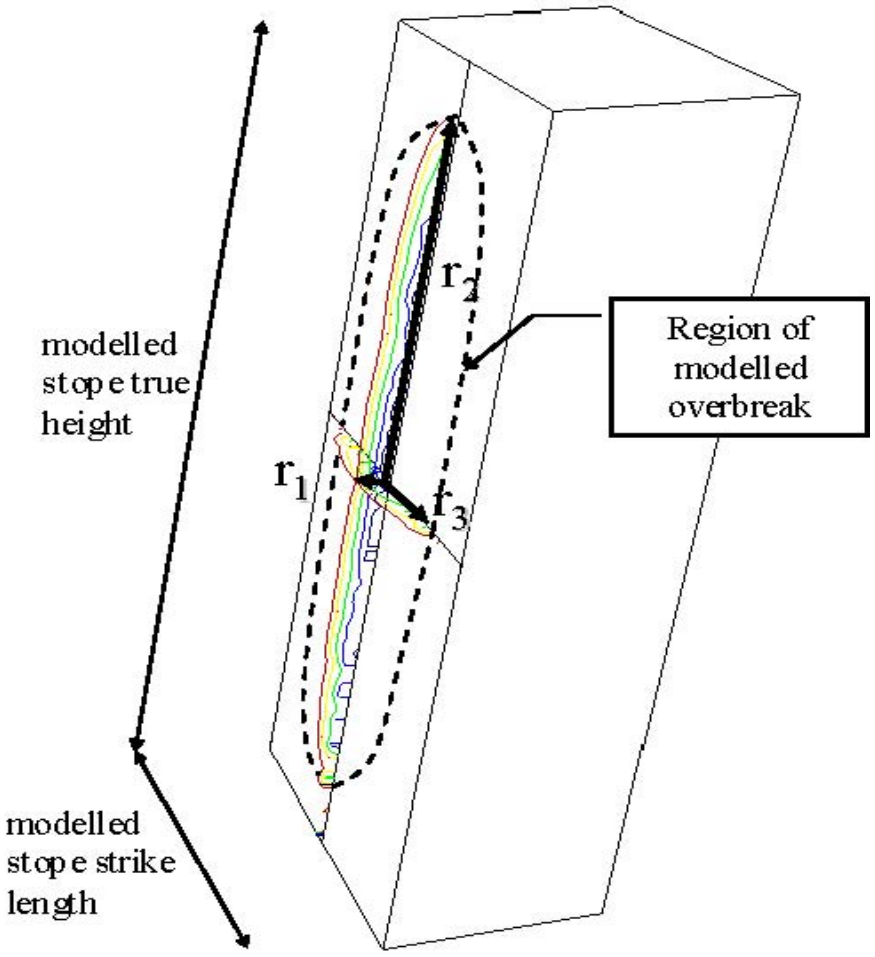


**Figure 2.18** Representation of the half ellipsoid (Henning and Mitri 2007)

In order to quantify ore dilution from a 3-dimensional model, the ore dilution density (DD) terminology is used and its unit is meter. It predicts the probable sloughage in any in the mining stope walls.

$$DD = \frac{Vpe}{Surface\ area\ exposed\ m^2}$$

In the case of using the CMS, measured dilution density (DD cms) can be defined as

$$DD\ cms = \frac{Unplanned\ Volume\ m^3}{Surface\ area\ exposed\ m^2}$$

The dilution density along the stope wall is defined as DD=0 and is maximum at the stope centre such as DD = $r_1$, which is the height. The dilution density DD is similar to the parameter ELOS defined previously.

Advantages of this new terminology are that the dilution density is not examined only as a function of stope width or either RMR. It takes into consideration stope dimensions, in-situ stress, stope location, wall dip, depth and it is calibrated by the CMS. Both values of density dilution (measured and predicted) can be used jointly to assess the importance of dilution occurrence. Quantification of dilution density can be done at any location in the stope wall where the DD is not constant over the surface area examined.

## 2.8 Control of ore dilution

Ore dilution can be controlled by a number of good practices and it is listed below:

- Reduce maximum stope height
- Reduce stope undercutting
- Good drilling practice (e.g. deviation)
- Good blasting practice ( e.g. vibration control)
- Installation of a ground support system as cable bolts where cost of cable bolting is small compared to the loss provoked by dilution, as can be seen in Figure 2.19 below

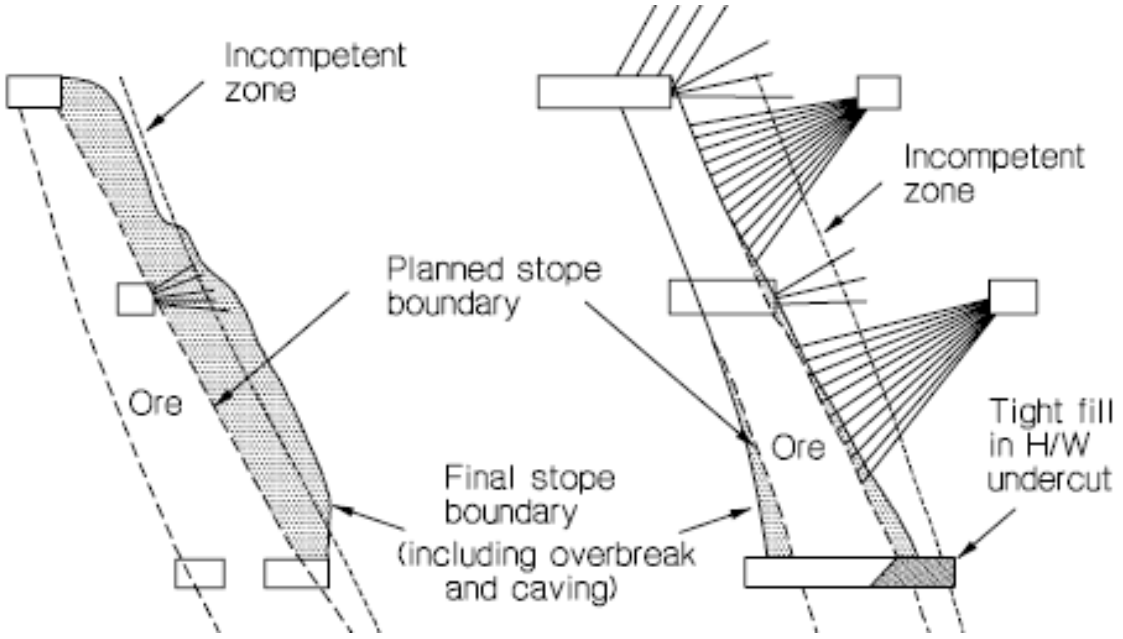


**Figure 2.19** Cable bolting pattern at Helmo mine (after Anderson and Grebenc 1995)

## 2.9 Impact of dilution on operation profitability

Unplanned dilution due to sloughing walls can make a mining project non-profitable. Improvement can be attempted by modifying the stope design, blasting practices and ground support, Bawden (1995). The economical consequence of unplanned ore dilution can be severe and may lead to closing the operation. When unplanned ore dilution is excessive, the profitability of the project is at peril, and the discounted cash flow rate is affected, as illustrated in Figure 2.20.

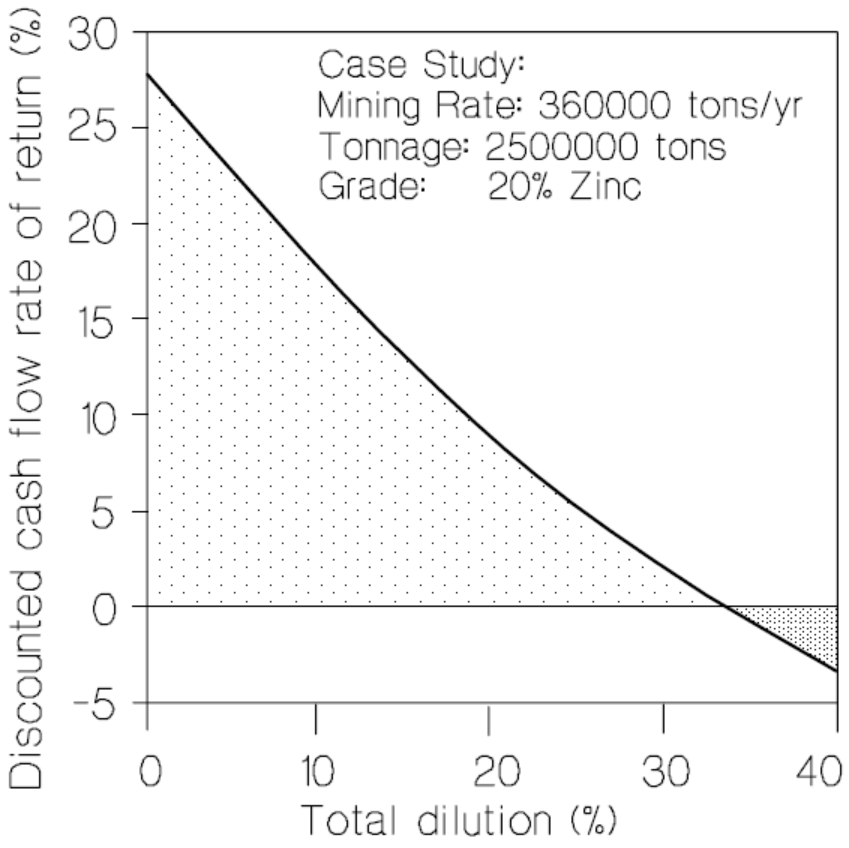


**Figure 2.20** Economic impact of dilution (Bawden 1993)

## 2.10 Conclusion

Dilution has an influence on the profitability of a mining operation and is divided onto planned and unplanned categories. Planned dilution is accounted for in mine planning and design and its sources are well defined. On the other hand, the unplanned ore dilution is affected by several factors such as stope height, in-situ stressed or hanging-wall dip. Empirical models based on case studies are used to predict dilution but do not quantify its significance. The quantification can be a result of a 3-dimesionnal numerical model based on the dilution density method (DD) and calibrated by CMS measurements. Ore dilution can be controlled by good practices such as ground support installation or blasting

# Chapter 3 Mine description

## 3.1 Location

The Lapa Mine is located in northwestern Quebec, in the Abitibi region near the town of Cadillac. It is 54 km west of Rouyn-Noranda. The deposit is situated approximately 11 km from the LaRonde mine as can be seen Figure 3.1.

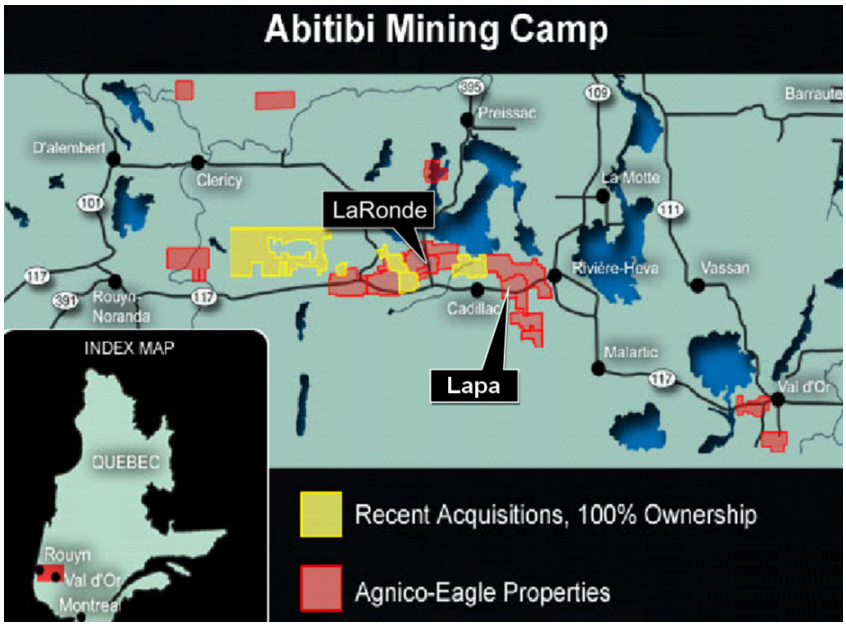


**Figure 3.1** Lapa Mine location map

In 2002, Agnico-Eagle permitted exploration drilling and mineral processing test at Lapa. A year later, it took acquisition of Lapa and budgeted sinking an exploration shaft. In 2006, it was concluded that the Lapa project was feasible and results were considered being favourable to a project development. In 2007, a shaft was sunk to 1,370m below

surface. In 2009, the first gold brick was produced and the expected annually production is 115,000 ounces of gold over seven years.

## 3.2 Geology

The main mineralization is within the contact zone located between 490m and 1280m below surface. The contact zone is found at the deformed intersection between the volcanic Piché Group and the sedimentary Cadillac Group. The mineralization zone is approximately 3 meters wide but it can reach 8 meters as can be seen in Figure 3.2. The average vein thickness varies between 3 and 5m.

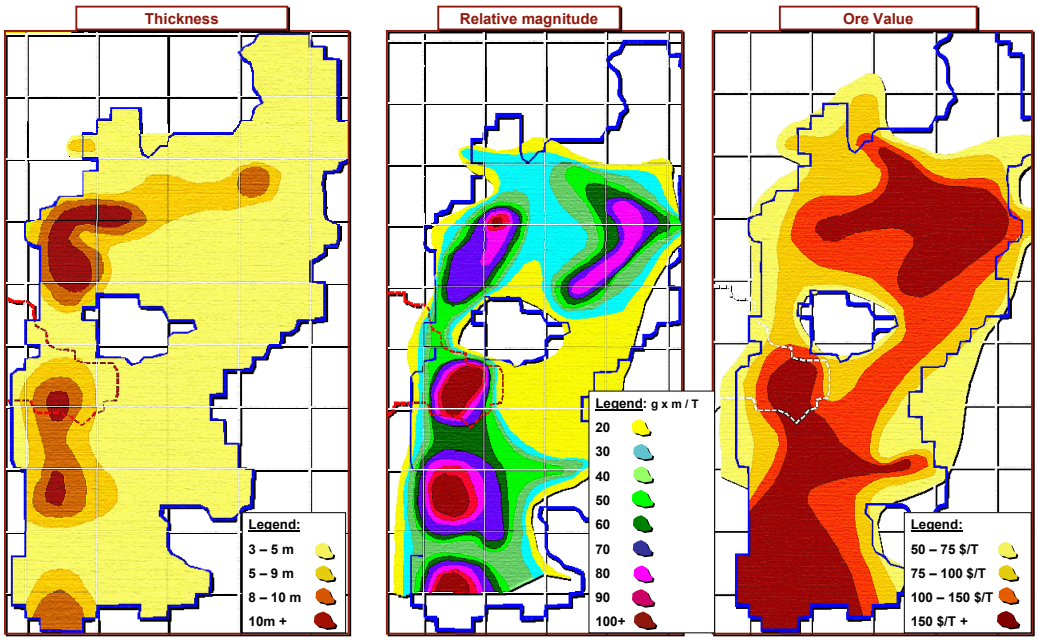


**Figure 3.2** Characteristics of Contact zone

Resources and reserves data were based on the block model released on December 2009. The average reserves grade is 8.33 g/t as presented in Table 3.1. The deposit holds 3.2 millions tonnes including the probable and proven reserves with an average grade of 8.2g/t.

The total amount of gold that would eventually be produced from Lapa is 843,000 ounces. The life of mine is approximated until 2015.

**Table 3.1** Mineral resources and reserves in 2009

| | g/t | t (000s) | oz (000s) |
|---|---|---|---|
| Proven Reserves | 8.33 | 897 | 240 |
| Probable Reserves | 8.09 | 2319 | 603 |
| Indicated Resources | 4.63 | 1672 | 249 |
| Inferred Resources | 7.9 | 393 | 100 |

## 3.3 Mine overview

The Lapa Mine infrastructure is trackless where levels and sub-levels are connected by a ramp system. The ramp is located between the two areas using different mining methods, i.e., transverse mining sub-levels and longitudinal Eureka mining sub-levels. Figure 3.3 illustrates the access ramp and the separation between eureka mining and Primary/ secondary mining.

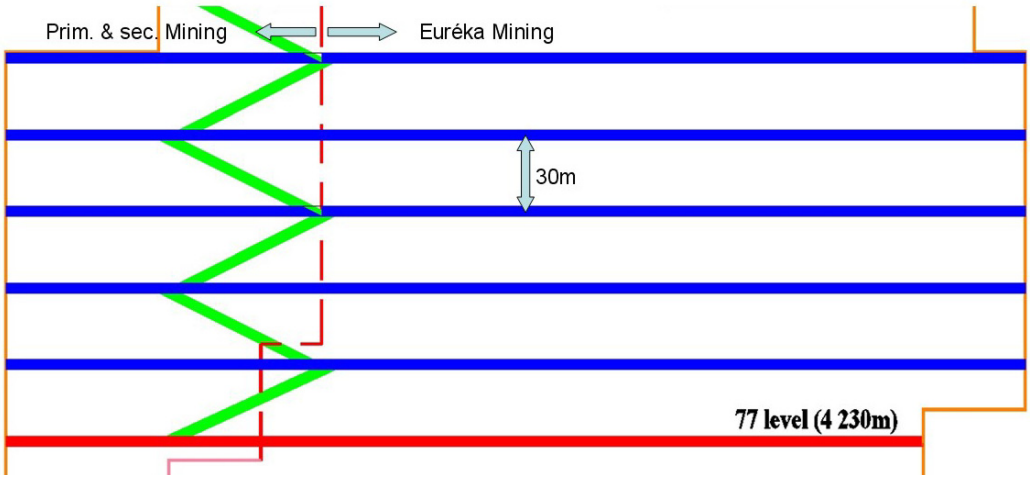


**Figure 3.3** Longitudinal view showing sub-levels

Levels are connected to the shaft and sub-levels by the ramp system. Levels were constructed every 120m vertically. The services in levels are illustrated in Figure 3.4.

Sub-levels are spaced by 30m vertically and have no exit to the shaft. A system of ore and waste pass is installed into each sub-level for materials handling as illustrated in Figure 3.5.

The loading station is located at a depth of 1,290 meters depth with an intermediate station is located at a depth of 810 meters depth.

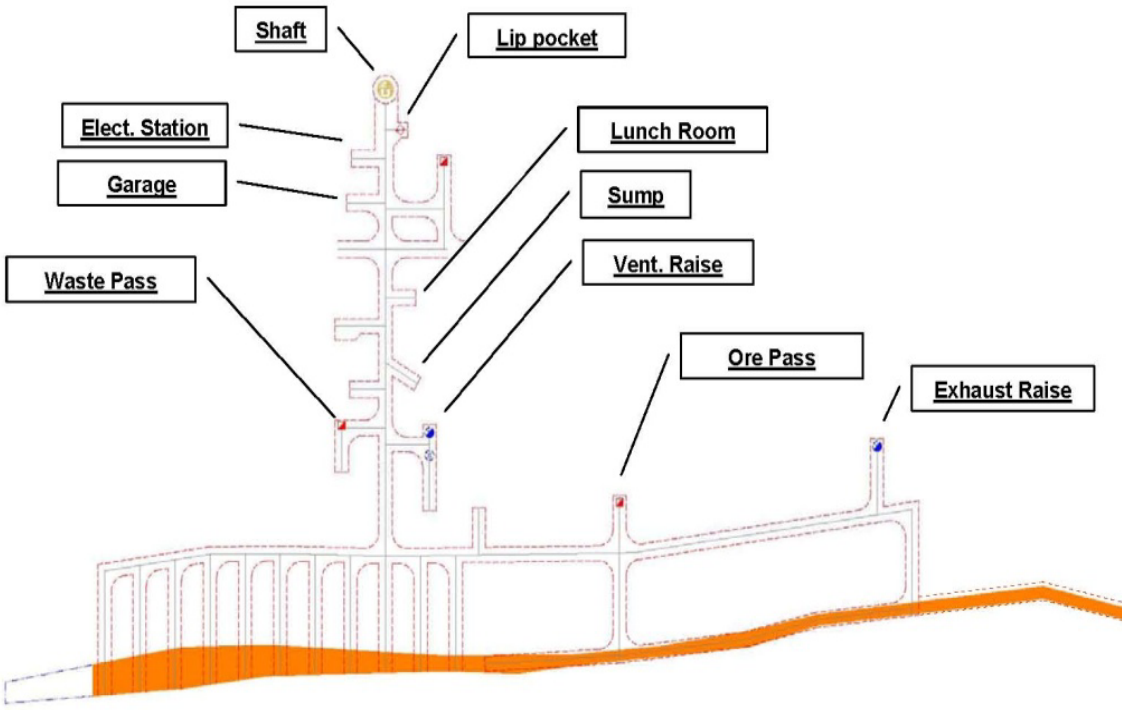


**Figure 3.4** Typical underground services in each level at Lapa, level 800

Waste development drifts were sized to fit medium size equipments. The ramp is an arched 4.5m x 4.5m and the access drift is 4m x 4m developed into waste.

Drift size in the ore zone is guided by the vein thickness where the minimum width is 3.6m fitting to the smallest scoop size. The back is supported with rebars and the walls with split sets: a screen #9 gage is also used.

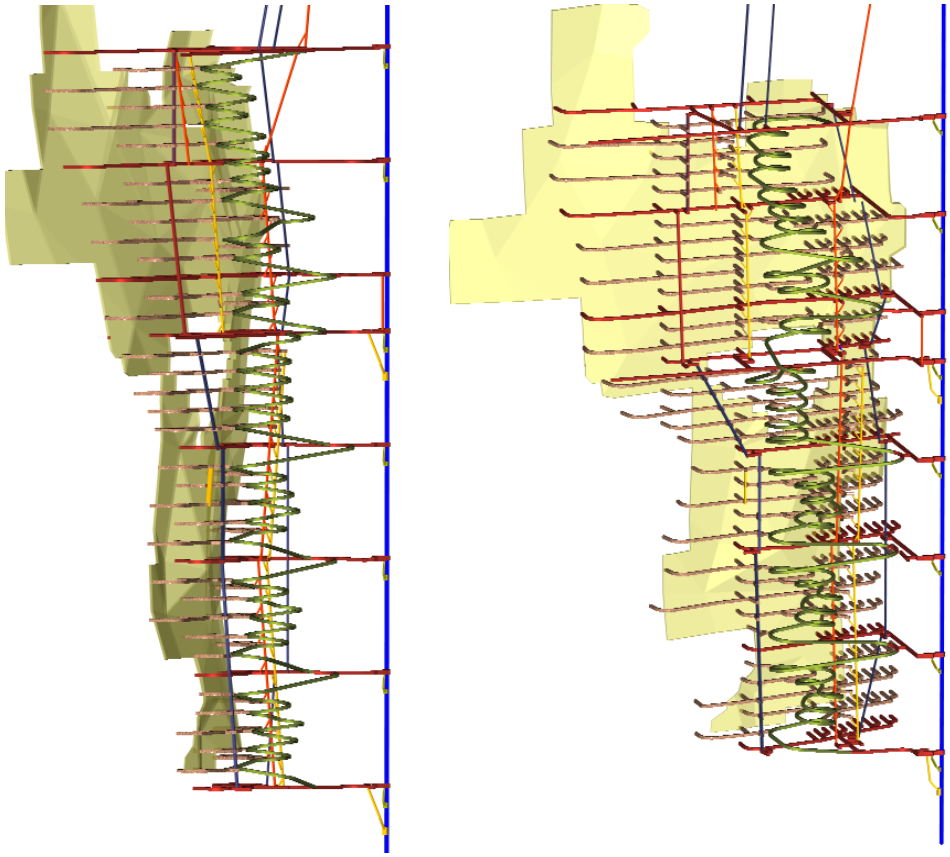

**Figure 3.5** Ore and waste pass

The shaft is sunk at a depth of 1,370m below ground surface with a diameter of 4.9m. The shaft is downcast and its size allows a double-duty production hoist, man-way, and a ventilation duct. The ventilation system capacity is 300,000 CFM with an expected production averaging 1,500 tpd.

## 3.4 Mining method

Two mining methods were selected. The first one is a longitudinal retreat, also called Eureka, with delayed backfill on sublevels of 30m intervals. Stope dimensions are 12m along the strike, 30m in height (without the overcut), and have variable width between 3m and 7m following the vein thickness using an inverse double pyramidal sequence. The hydraulic radius is 4.4 based on 12m width and 34m height as is illustrated in Figure 3.6.

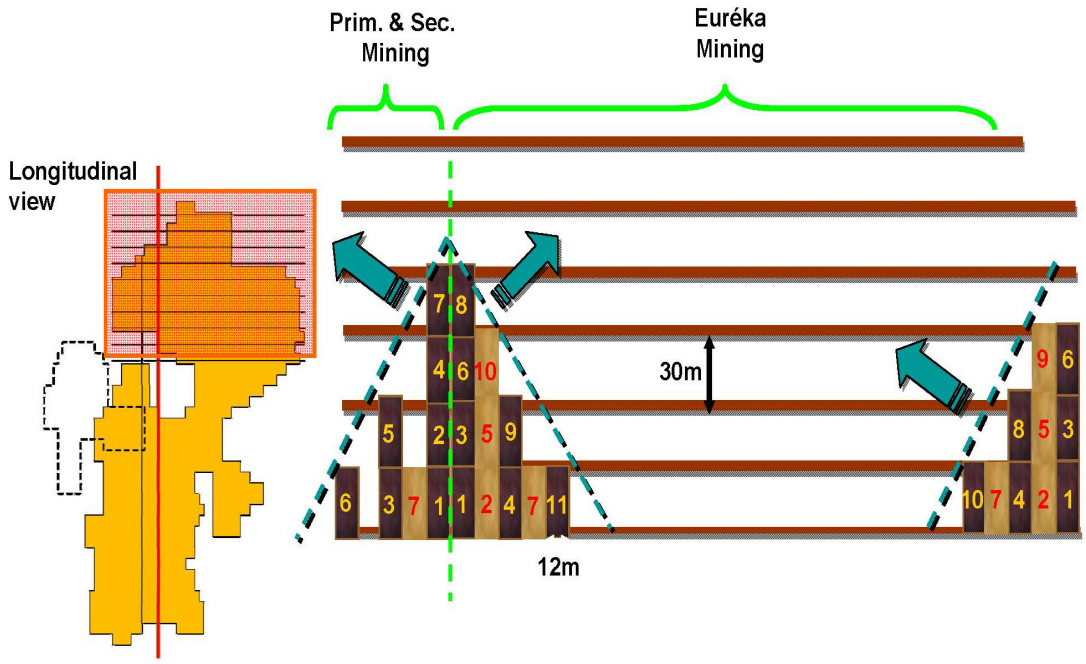


**Figure 3.6** Combination of Eureka and the Primary/Secondary mining methods

The longitudinal retreat mining method is cost effective where significant savings are achieved by the reduced developments in the host rock. Ore is blasted using the long-hole method and mucking is done on each sublevel from a longitudinal undercut. Once stope mucking is completed, it is filled with cemented rock backfill, as shown on Figure 3.7.

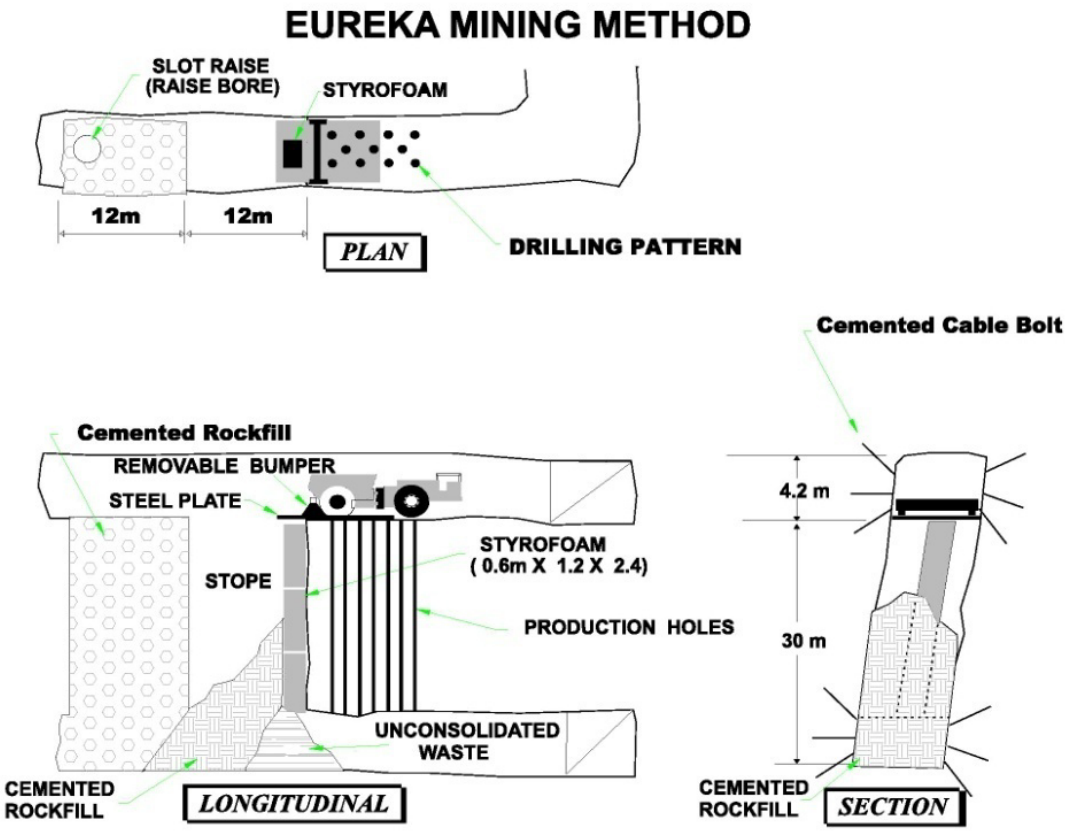


**Figure 3.7** Eureka mining method

The main advantages of the Eureka method is drift development in mineralization, following the minimum vein thickness, and no draw point excavated in hanging-wall causing dilution. The main disadvantage, on the other hand, is the reduced productivity, which is a consequence of the long hauling distance.

The second mining method is the transversal primary and secondary. The method is used in areas where the mining width is continuously 6m. Stope dimensions are 12m along the strike, 30m in height and the hydraulic radius is 4.4m like the Eureka mining method.

An example of the mining sequence is illustrated in Figure 3.8. Primary stopes are filled with cemented rock fill at 5% binder while the secondary stope would be filled with rock fill only.

The transversal primary and secondary presents high recovery with low to moderate dilution. Good production rate and multiple production faces are two strong advantages of the transversal primary/secondary method. However, higher mining costs have to be expected, and there is the necessity of a good quality backfill in primary stopes.

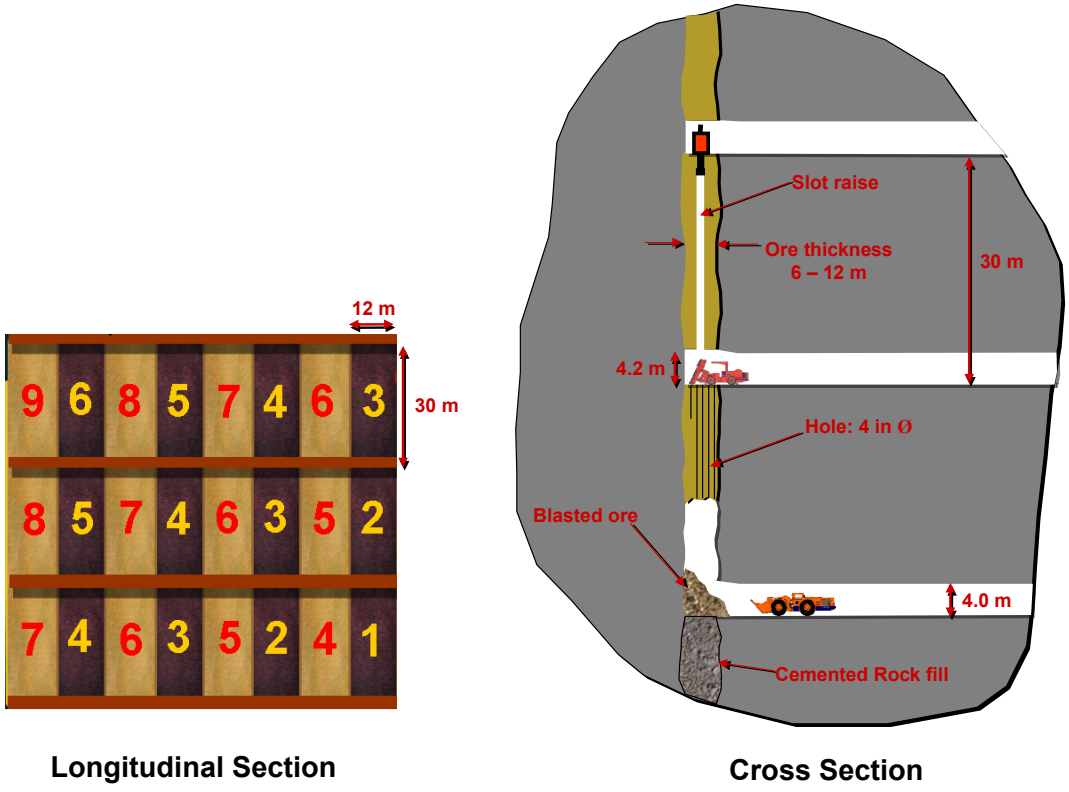


**Figure 3.8** Transversal Primary and Secondary mining method

The average dilution anticipated in the feasibility study is expected to be 30% which was estimated according to the thickness of the ore zone. An approximation of 0.8m of caving was attributed to the footwall and 0.4m attributed to hanging-wall.

## 3.5 Backfilling

Initial rock fill is provided from waste development and from the surface waste stockpile produced during the mine development. It is dumped from surface, and then distributed to the production level with the fill raise. Stope backfilling is done with 6 yards scooptram and the cement content in rock fill used in both mining methods is 5%. The backfilling in secondary stopes in transverse mining is rock fill without the addition of cement.

As the mining rate increases and to avoid filling delays, additional fill material will be required from LaRonde Mine and the imported waste rock will be taken from the non-acid generating rock.

# Chapter 4 Rock mechanics properties

## 4.1 Introduction

Rock mechanics studies were conducted by Itasca and Georock to assess stopes dimensioning, joint classification and ore dilution. Face and drift mapping were conducted to correlate with consultant results of the consultant's report in the summer 2009. Diamond drill holes information was plotted against planned mined stopes for 2009 and 2010. All the collected data were used to have the closest properties approximation and these were summarized in a preliminary database.

## 4.2 Rock mass properties

### 4.2.1 Joints classification

#### 4.2.1.1 Sediments Wacke (S3)

The dipping direction is 0º and the dip is between 85º and 90º. The foliation spacing is from 1 to 5 cm and it reaches 10 cm in some mine sections.

Joint set 2 dips between 70º and 90º. The dipping direction varies from 35º to 55º and spacing is between 30 and 50 cm. The joint length is longer than the opening height. The secondary family 1 has no alteration.

Joint set 3 is sub-horizontal and less present than the other two families. The dipping direction is 90º and the dip is between 0º and 20º. Spacing is 1m and the joint trace length is 0.5 to 2m and no alteration is remarkable on joint surface.

#### 4.2.1.2 Schist chlorite (M8)

The principal joint family has a high schistosity with a dipping direction 0º with 85º to 90º dip. Spacing between the foliation is within the millimeter scale. The join surface is highly altered. The contact with water causes a joint expansion acting as lubricant facilitating sliding between joints.

Joint set 2 is dips between 70º and 90º and the dipping direction is 35º to 55º. Joint spacing varies from 30 to 50 cm and the length is higher than the opening height. Alteration is absent from observation.

Joint set 3 has the same properties as the secondary family 2 observed on the Wacke S3.

### 4.2.2 Unconfined compressive strength test

Unconfined axial tests were performed on hanging-wall (23 samples) and footwall (20 samples) rocks. The hanging wall $\sigma_c$ results show a strength of approximately 90 MPa while the results of the footwall are highly variable with $\sigma_c$ is lying between 2.9MPa and 91.7 MPa.

Tri-axial test were not performed on any core samples and therefore Mohr-Coulomb properties had to be approximated for the database.

### 4.2.3 RQD classification

RQD is defined as the degree of fracturing of the rock mass. Drilling cores were taken from the first 5m from both walls.

Two methods were used in order to assess the RQD classification. The first method is based on the core logging where the number of available core was limited.

The second method is based on the volumetric joint count using the following equation:

RQD = 115-3.3 Jv (Palmström 1982)

Jv is obtained by adding the number of joints in 1m for each joint family.

#### 4.2.3.1 Sediments Wacke (S3)

Table 4.1 below summarized used the drilled cores used assess the average RQD for hanging-wall composed by wacke S3. Drilled cores were taken from the first 5 meters from the wall.

**Table 4.1** Hanging-wall RQD classification per drilling hole

| Section | Drilling hole | RQD | Length |
|---|---|---|---|
| 5520E | 118-03-09 | 60 | 5 |
| 5520E | 118-03-13A | 40 | 3 |
| 5520E | 118-03-13A | 80 | 2 |
| 5520E | LA06-49-7 | 50 | 2.5 |
| 5520E | LA06-49-7 | 75 | 2.5 |
| 5520E | 118-03-19B | 40 | 5 |
| 5600E | 118-03-43 | 60 | 3 |
| 5600E | 118-03-43 | 85 | 2 |
| 5600E | 118-03-39B | 60 | 1.5 |
| 5600E | 118-03-39B | 90 | 3.5 |
| 5600E | 118-03-39A | 55 | 5 |
| 5600E | 118-03-39 | 70 | 5 |
| 5600E | LA06-49-6 | 60 | 2.5 |
| 5600E | LA06-49-6 | 50 | 2 |
| 5600E | LA06-49-6 | 60 | 0.5 |
| 5440E | 118-03-04C | 50 | 5 |

Based on the table above, the average RQD for the hanging-wall is 60. The results of the second method which was based on the field observations are summarized in Table 4.2. The average RQD is 60 for the Wacke S3, which is similar to the value obtained by the core drilling method.

**Table 4.2** Jv according to field observation on Wacke S3

| | |
|---|---|
| Spacing family 1 | 7.5 cm |
| Spacing family 2 | 40 cm |
| Spacing family 3 | 100 cm |
| $J_v$ | 17 joints/m³ |

4.2.3.2 Schist chlorite (M8)

Table 4.3 summarized RQD values of drilled cores within the first 5m of the Schist chlorite (M8) inthe footwall.

**Table 4.3** Footwall RQD classification per drilling hole

| Section | Drilling hole | RQD | Length |
|---|---|---|---|
| 5520E | 118-03-09 | 60 | 5 |
| 5520E | 118-03-13A | 85 | 5 |
| 5520E | LA06-49-7 | 15 | 5 |
| 5520E | 118-03-19B | 55 | 2 |
| 5520E | 118-03-19B | 55 | 3 |
| 5600E | 118-03-43 | 70 | 2 |
| 5600E | 118-03-43 | 10 | 1 |
| 5600E | 118-03-43 | 0 | 1.5 |
| 5600E | 118-03-43 | 25 | 0.5 |
| 5600E | 118-03-39B | 80 | 1.5 |
| 5600E | 118-03-39B | 50 | 2 |
| 5600E | 118-03-39B | 15 | 1 |
| 5600E | 118-03-39B | 75 | 0.5 |
| 5600E | 118-03-39A | 75 | 1 |
| 5600E | 118-03-39A | 25 | 4 |
| 5600E | 118-03-39 | 80 | 1.5 |
| 5600E | 118-03-39 | 75 | 1.5 |
| 5600E | 118-03-39 | 85 | 2 |
| 5600E | LA06-49-6 | 50 | 3.5 |
| 5600E | LA06-49-6 | 70 | 1.5 |
| 5440E | 118-03-04C | 10 | 5 |

Based on the table, the average RQD for schist chlorite is 48. As shown in the Table 4.3 the RQD varies greatly between 10 and 85 depending on the drilling core intersection.

The second method results, based on the field observations, are summarized in the Table 4.4. The average RQD is similar to the value obtained above.

**Table 4.4** $J_v$ according to field observation on schist chlorite

| | |
|---|---|
| Spacing family 1 | 0.4 cm |
| Spacing family 2 | 40 cm |
| Spacing family 3 | 100 cm |
| $J_v$ | 253 joints/m³ |

According to the $J_v$, the RQD is null. The difference between the field observation and the core drilling logs is quite significant. Hence, it was concluded that the schist quality deteriorate when creating an opening.

On the whole, the hanging wall was composed of rocks of better quality than the schist chlorite on the footwall side.

### 4.2.4 NGI Classification

The Q-method is based on 6 parameters that can be obtained by geological mapping, Barton et al (1974). High value indicates a good stability and low values indicates poor stability as shown on Table 4.5.

$$Q=\frac{RQD}{J_n} \text{ X } \frac{J_r}{J_a} \text{ X } \frac{J_w}{SFR}$$

where,

$\frac{RQD}{J_n}$ is block size

$\frac{J_r}{J_a}$ is inter block shear strength

$\frac{J_w}{SFR}$ is the active stress

Field observation and core logging were used to assess the NGI parameters of the hanging wall. Based on the Q system value the hanging wall Wacke sediment has an average quality however the footwall schist chlorite quality is very poor.

**Table 4.5** NGI parameters for hanging wall and footwall

| | Wacke | Schist chlorite |
|---|---|---|
| RQD | 60 | 48 |
| $J_n$ | 9 | 9 |
| $J_r$ | 1 | 1 |
| $J_a$ | 1.5 | 2.5 |
| $J_w$ | 1 | 1 |
| SFR | 1 | 1 |
| Q | 4.5 | 2.1 |

### 4.2.5 Stope dimensioning

A preliminary study was conducted by Itasca to assess the maximum span allowed and Georock did a similar study based on field observations. The Matthews-Potvin empirical method was used for stope dimensioning and Georock came up with the data listed in Table 4.6. The typical span proposed is 11m by 11m and it was noted that the stability number N' of schist chlorite will decrease when the rock will be exposed with time.

**Table 4.6** Hanging wall and footwall stability number (Georock study 2006)

| | Wacke | Schist chlorite |
|---|---|---|
| Q' | 4.5 | 2.1 |
| A | 0.9 | 0.2 |
| B | 0.3 | 0.3 |
| C | 8 | 8 |
| N' | 9.6 | 1 |

Critical walls assessed by Itasca were the back and walls within the weak rocks units and the back was less critical since the vein is narrow. Table 4.7 summarizes the different rock units and their spans.

**Table 4.7** Hydraulic radius and typical spans in meters (Feasibility study 2006)

| Rock Unit | Location | RMR | N' | HR | Typical Spans |
|---|---|---|---|---|---|
| Pontiac Sediments | | 41 | 1.4 | 3 | 12 x 12 |
| Pontiac Sediments | | 46 | 2.5 | 3.5 | 14 x 14 |
| Piché- Chlorite Schist | F/W | 38 | 1 | 3 | 12 x 12 |
| Piché Chlorite. schist | F/W | 33 | 0.6 | 2.5 | 10 x 10 |
| Cadillac Greywacke | H/W | 55 | 6.8 | 5 | 20 x 20 |
| Cadillac Conglomerate | H/W | 71 | 40 | 10.1 | 40 x 40 |
| Cadillac Conglomerate | H/W | 61 | 13 | 6.7 | 27 x 27 |

In both the studies conducted, the hanging wall was in good condition and the footwall was more prone to instability. Therefore, major infrastructures were built on the hanging wall zone to alleviate potential instability issues.

## 4.3 Data approximation

Most of the data was not available during the period of study for this thesis. Diamond drilling cores, field observations, and the data collected from the feasibility and Georock studies listed on the previous sections were used instead. Empirical rock mechanics formulas were considered to assign properties to each stope and RocLab software was used in this part.

### 4.3.1 RQD stope approximation

The diamond drilling core was plotted in Datamine. RQD scale was separated into 4 ranges from 1 to 25, 25 to 50, 50to 75, and 75to 100. It was observed that RQD values vary drastically on a short length section as seen in Figure 4.1. It has to be noted that only few levels had a good frequency intersection with the diamond drilling program as illustrated in Figure 4.1. Table 4.8 summarized the approximations made for each stope.

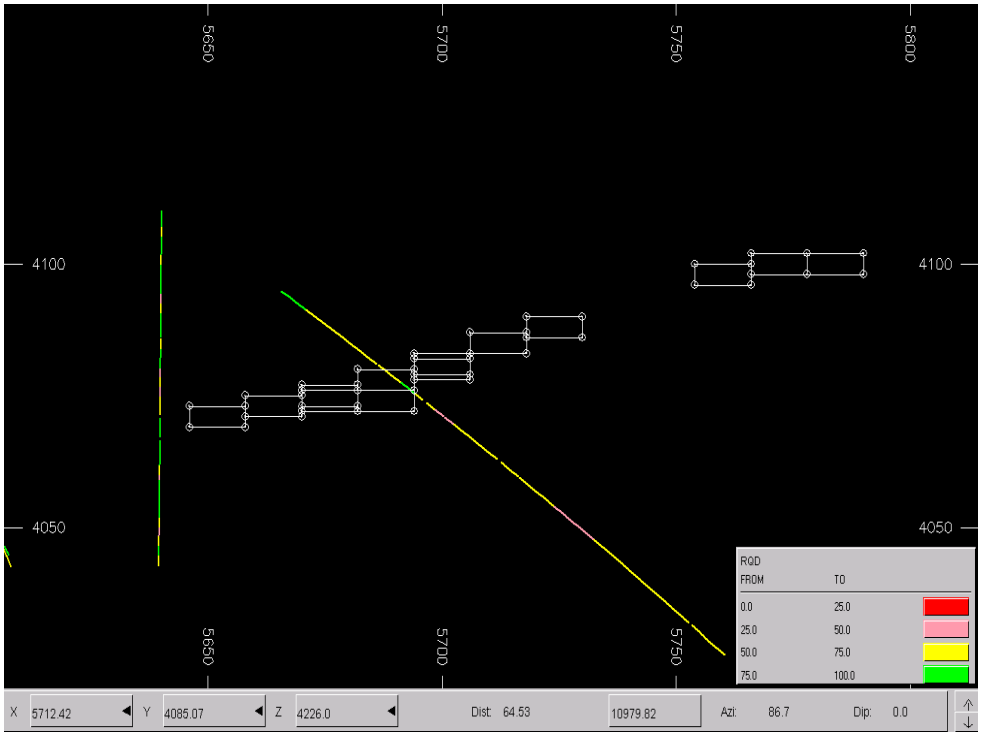


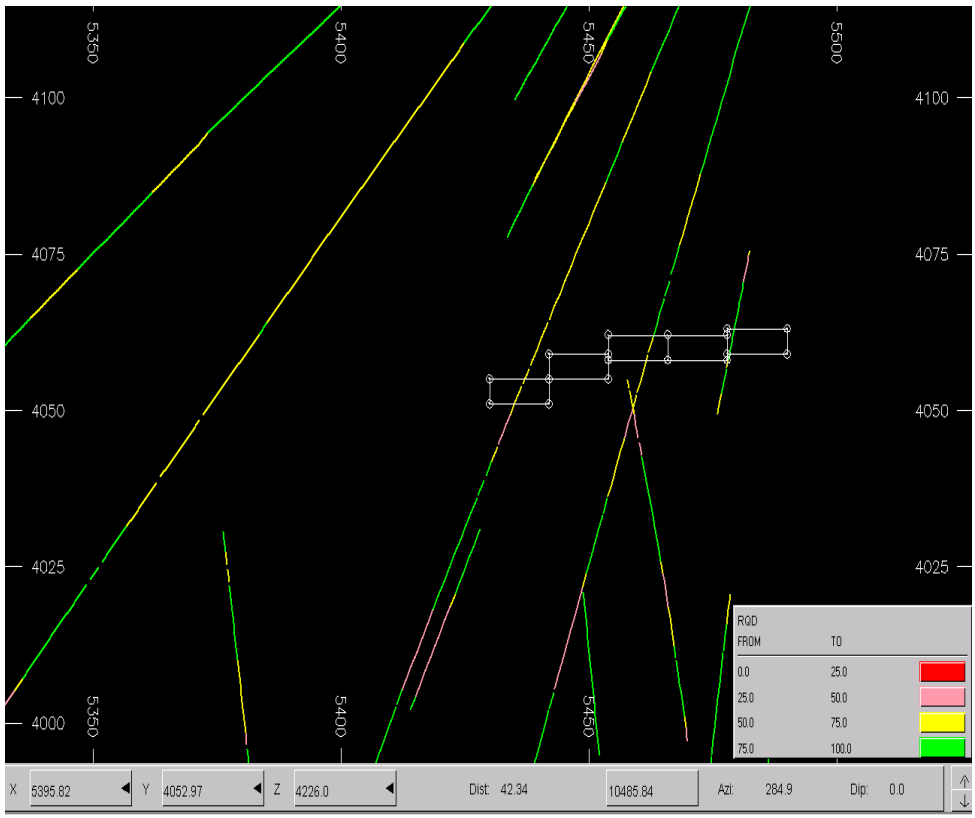


**Figure 4.1** Diamond drills holes plotted and stopes in Datamine

**Table 4.8** RQD per stope approximation

| Stope | Dist FW | Near FW RQD | Ore RQD | Near HW RQD | Dist HW |
|---|---|---|---|---|---|
| 7128 | | 50 | 50 | 75 | 6.01 |
| 7428 | 5.75 | 0 | 25 | 25 | 9.72 |
| 7429 | 5.75 | 0 | 25 | 25 | 9.72 |
| 7430 | 5.75 | 0 | 25 | 25 | 9.72 |
| 7449 | 3.75 | 50 | 25 | 25 | 11.9 |
| 7728 | 5.75 | 0 | 25 | 25 | 9.72 |
| 7729 | 5.75 | 0 | 25 | 25 | 9.72 |
| 7730 | 5.75 | 0 | 25 | 25 | 9.72 |
| 7731 | 7.69 | 50 | 25 | 25 | 14.21 |
| 7747 | 9.1 | 75 | 50 | 25 | 11.45 |
| 7748 | 9.1 | 75 | 50 | 25 | 11.45 |
| 7749 | 8.35 | 25 | 50 | 50 | 15.21 |
| 7750 | 8.35 | 25 | 50 | 50 | 15.21 |
| 7757 | 15.84 | 25 | 50 | 75 | |
| 8028 | 9.5 | 25 | 50 | 50 | |
| 8029 | 9.5 | 25 | 50 | 50 | |
| 8030 | 7.1 | 50 | 50 | 75 | 14.21 |
| 8031 | 5.28 | 75 | 75 | 75 | 7.63 |
| 8032 | 6.75 | 50 | 75 | 75 | 7.4 |
| 8046 | 6.57 | 75 | 50 | 25 | 8.47 |
| 8047 | 6.57 | 75 | 50 | 25 | 8.59 |
| 8048 | 6.63 | 25 | 50 | 50 | 13.25 |
| 8049 | 6.63 | 25 | 50 | 50 | 13.25 |
| 8050 | 6.63 | 25 | 50 | 50 | 13.25 |
| 8051 | 6.63 | 25 | 50 | 50 | 13.25 |
| 8052 | 6.63 | 25 | 50 | 50 | 13.25 |
| 8055 | 15.84 | 25 | 50 | 75 | |
| 8056 | 15.84 | 25 | 50 | 75 | |
| 8057 | 15.84 | 25 | 50 | 75 | |
| 10432 | 19.71 | 50 | 50 | 75 | |
| 10434 | 19.71 | 50 | 50 | 75 | |
| 10435 | 19.71 | 50 | 50 | 75 | |
| 12826 | 11.3 | 50 | 50 | 50 | 4.85 |
| 12834 | | 50 | 75 | 50 | 7.17 |
| 12835 | | 50 | 75 | 50 | 7.17 |
| 12845 | 11.5 | 25 | 50 | 25 | 10.96 |
| 12846 | 11.5 | 25 | 50 | 25 | 10.96 |

Field observations demonstrated that the footwall deteriorated rapidly with exposure and blasting. Hence, a concept of near footwall, which was a 1m thick of the exposed wall thickness, was used to fit with field observations in the case of stope undercutting.

### 4.3.1 Rock mass quality

Several rock mass classification method were examined such as rock quality designation Q-system (Barton et al 1974), rock mass rating RMR (Bieniawski 1976), and GSI (Hoek et al. 2002).

GSI was chosen for rock mass classification at the Lapa Mine. The poor rock quality noticed in mine opening was a factor to select the GSI since it does not take RQD into consideration. GSI decreases when the interlocking between rock pieces decreases and with the surface quality deteriorates see Figure 4.2. Block size description is summarized in Table 4.9 and GSI classes given in Table 4.10.

GSI can be approximated from RMR and Q as shown below (Hoek et al. 2002)

$GSI = RMR_{1976}$

$GSI = RMR_{1989}-5$, (Bieniawski 1989)

$GSI = 9 * \ln Q' + 44$

**Table 4.9** GSI Rock mass structural descriptions of block size (Hoek et al. 2000)

| **GSI description** | **ISRm designation** | **Jv, joints/m$^3$** | RQD % |
|---|---|---|---|
| Blocky | Medium tolarge blocks | <10 | 90-100 |
| Very blocky | Small tomedium blocks | 10-30 | 60-90 |
| Blocky/folded/faulted | Very small to small blocks | >30 | 30-60 |
| Crushed | Crushed rock | >60 | <30 |

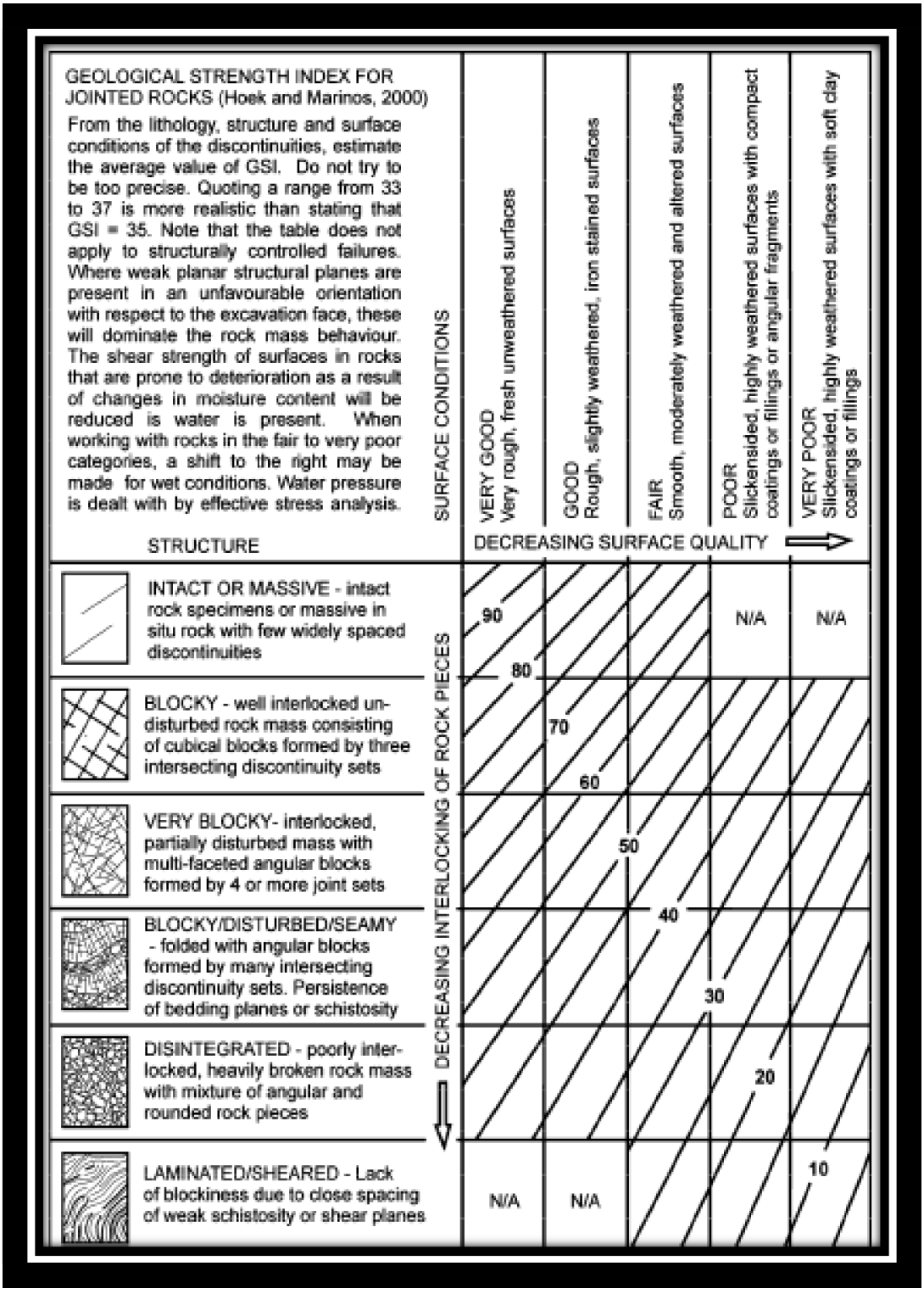


**Figure 4.2** Geological strength index GSI classifications (Hoek et al. 2002)

**Table 4.10** Rock mass classes determined from GSI

| GSI value | 76-95 | 56-75 | 36-55 | 21-35 | <20 |
|---|---|---|---|---|---|
| Rock mass quality | Very good | Good | Good fair | Poor | Very poor |

## 4.4 Rock mass modulus

The rock mass modulus was derived from the empirical relation suggested by Hoek and Diederichs (2006)

$$E_{rm} = E_i \left( 0.02 + \frac{1 - D/2}{1 + e^{((60+15D-GSI)/11)}} \right)$$

where,

D is a factor which depends upon the degree of disturbance to which the rock mass has been subjected by a stress relaxation and blast damage.

D = 1 when rock mass is very disturbed

D = 0 when rock mass is undisturbed

In Lapa Mine case, D was chosen to be 0.6 for the near footwall when conducting the study of stope undercutting. The footwall, when exposed, becomes weak with time exposure and deteriorates significantly. In order to reflect the reality, the damage parameter was added to the database sheet.

## 4.5 Hoek and Brown parameters and tensile strength

Uniaxial compressive strength was used to calculate the properties of the intact rock sample $E_i$, $\sigma_{ci}$ then the Hoek and Brown parameter $m_i$ from the Rocklab program of Rockscience. The following equations were used (Hoek et al 2002):

Hoek and Brown parameter, reduced $m_i$: $m_b = m_i e^{\left(\frac{GSI-100}{9-3D}\right)}$

Rock mass constant: $a = \frac{1}{2} + \frac{1}{6}\left(e^{-GSI/15} - e^{-20/3}\right)$

Rock mass constant: $s = e^{((GSI-100)/(9-3D))}$

$\sigma'_{3n} = \sigma'_{3\max} / \sigma_{ci}$

$\sigma'_{3\max} = 0.47\sigma'_{cm}\left(\frac{\sigma'_{cm}}{\gamma H}\right)^{-0.94}$

Global rock mass strength: $\sigma'_{cm} = \sigma_{ci}\left[\frac{(m_b + 4s - a(m_b - 8s))(m_b/4 + s)^{a-1}}{2(1+a)(2+a)}\right]$

Uniaxial rockmass compressive strength: $\sigma'_c = \sigma_{ci} s^a$

Tensile strength:

$$\sigma_t = -\frac{s\sigma_{ci}}{m_s}$$

## 4.6 Mohr-Coulomb properties

As the elasto-plastic analysis is carried out with the Mohr-Coulomb yield function, it was necessary to convert the above mentioned Hoek-Brown parameters of the rock mass to those of Mohr-Coulomb (Hoek et al. 2002). The following equations were then used:

$$c = \frac{\sigma_{ci}\left[(1+2a)s + (1-a)m_b\sigma'_{3n}\right](s + m_b\sigma'_{3n})^{a-1}}{(1+a)(2+a)\sqrt{1 + \frac{\left(6am_b(s + m_b\sigma'_{3n})^{a-1}\right)}{(1+a)(2+a)}}} \qquad \phi = \sin^{-1}\left[\frac{6am_b(s + m_b\sigma'_{3n})^{a-1}}{2(1+a)(2+a) + 6am_b(s + m_b\sigma'_{3n})^{a-1}}\right]$$

## 4.7 Data compilation

A database was built in Excel with the aim of putting available information together and approximating missing rock properties by using equations presented on the previous section. The preliminary database enclosed the limited stopes data available and all the cells were linked. The first step was to enter stope information (ID, type, sequence, RMR, RQD, Rock type,etc.). Based on that, rock mechanics properties were calculated with the defined formulas. Certain stopes had the same values since the lack of information in the early mining stages obliged the use of diamond drill information. Table 4.12 shows an example of tables from the database. The second step was to detail the stope geometry with the undercutting being is measured from a survey conducted of the actual overcut and undercut drifts. The undercutting in blasting rows was measures according to the planned sections as presented on Table 4.11.

**Table 4.11** Measured stope undercutting (m) of 8049 stope

| Stope 8049 | | |
|---|---|---|
| **Row** | **HW** | **FW** |
| 1 | 1.2 | 2.3 |
| 2 | 1.4 | 2.2 |
| 3 | 1.7 | 2 |
| 4 | 1.8 | 2.1 |
| 5 | 1.6 | 2.1 |
| 6 | 1.5 | 2.1 |
| 7 | 1.6 | 1.9 |
| 8 | 1.4 | 1.3 |
| 9 | 1.4 | 0.8 |
| 10 | 1.4 | 0.4 |
| 11 | 1.4 | 0.4 |
| 12 | 1.4 | 0.6 |
| 13 | 1.1 | 0.7 |
| 14 | 0.2 | 1 |
| 15 | 0.2 | 1.1 |

**Table 4.12** 12846 stope information in the preliminary data base

| | | | |
|---|---|---|---|
| Scheduled Month | oct-09 | Height (m) | 26 |
| Stope Type | P1 | Strike (m) | 12 |
| Depth (m) | 1280 | Ore Tichkness (m) | 2.9 |
| t. diluated/ 95% rec. | 3902 | Au Grade g/t | 5.99 |
| Stope dip | 85 | Sequence | 12 |
| | ***Hanging-wall*** | ***Ore*** | ***Footwall*** |
| Rock Type | Cadillac | Contact | Piche |
| ρ (MN/m3) | 0.0272 | 0.0292 | 0.0292 |
| RMR 76 | 58 | 52 | 45 |
| RQD | 25 | 50 | 25 |
| ν | 0.16 | 0.18 | 0.18 |
| $\sigma_{ci}$ (MPa) | 86,2 | 42 | 30.9 |
| GSI | 58 | 52 | 45 |
| mi | 18 | 13 | 10 |
| D | 0 | 0 | 0 |
| $E_i$ (GPa) | 44.7 | 21.1 | 15.2 |
| $m_b$ | 3.02 | 2.34 | 0.60 |
| s | 0 | 0 | 0 |
| a | 0.50 | 0.50 | 0.51 |
| c (MPa) | 4.24 | 3.08 | 1.59 |
| φ ° | 38,2 | 29,9 | 17.9 |
| $\sigma_t$ | -0.13 | -0.09 | -0.02 |
| $\sigma_c$ | 5.75 | 2.84 | 0.64 |
| $\sigma_{cm}$ | 20.20 | 8.66 | 3.11 |
| $E_{rm}$ | 21.2 | 7.3 | 33.9 |
| $\sigma_{3max}$ | 15.84 | 16.09 | 15.13 |
| $\sigma_{3n}$ | 0.18 | 0.38 | 0.49 |
| Dilation | 9.54 | 7.46 | 4.47 |

The third step was the prediction of dilution based on the dilution density $DD_{max}$. DD was calculated for each row section according to the drilling pattern; "x" is the distance from the beginning of a stope to "Ri". It must be noted that "R" refers to "row'' and ''i'' is the row number. The fourth step is the reporting of the dilution in the database when

the stope is mined and the ELOS value is calculated. Hanging-wall and footwall overbreak are measured from the CMS. Table 4.13 presents the third and fourth steps.

**Table 4.13** Example of stope summary in the database spreadsheet

| Stope 8049 | | | |
|---|---|---|---|
| Planned Volume | 894 | m3 | |
| Ore left | 92 | m3 | |
| Mined ore | 803 | m3 | |
| Overbreak south | 371 | m3 | |
| Overbreak north | 151 | m3 | |
| Total volume | 1323.93 | m3 | |
| | | | |
| ELOS TOTAL | 1.45 | m | |
| Hangingwall | 0.42 | m | |
| Footwall | 1.03 | m | |
| **Dilution Density max** | **2.77** | **m** | |
| **DD Average** | **1.45** | **m** | |
| **Hanging-wall** | | | |
| R 2, DD max | 0,32 | x= | 0.5 |
| R 3, DD max | 0,56 | x= | 1.7 |
| R 4, DD max | 0,62 | x= | 2.2 |
| R 5, DD max | 0,72 | x= | 3.4 |
| R 6, DD max | 0,75 | x= | 3.9 |
| R 7, DD max | 0,79 | x= | 5.1 |
| R 8, DD max | 0,80 | x= | 6 |
| R 9, DD max | 0,79 | x= | 6.9 |
| R 10, DD max | 0,75 | x= | 8.1 |
| R 11, DD max | 0,72 | x= | 8.6 |
| R 12, DD max | 0.62 | x= | 9.8 |
| R 13, DD max | 0.56 | x= | 10.3 |
| R 14, DD max | 0.35 | x= | 11.4 |
| R 15, DD max | 0.00 | x= | 12 |
| | | | |

| Footwall | | | |
|---|---|---|---|
| R 8, DD max | 1.967 | x= | 6 |
| R 2, DD max | 0.79 | x= | 0.5 |
| R 3, DD max | 1.37 | x= | 1.7 |
| R 4, DD max | 1.52 | x= | 2.2 |
| R 5, DD max | 1.77 | x= | 3.4 |
| R 6, DD max | 1.84 | x= | 3.9 |
| R 7, DD max | 1.94 | x= | 5.1 |
| R 9, DD max | 1.94 | x= | 6.9 |
| R 10, DD max | 1.84 | x= | 8.1 |
| R 11, DD max | 1.77 | x= | 8.6 |
| R 12, DD max | 1.52 | x= | 9.8 |
| R 13, DD max | 1.37 | x= | 10.3 |
| R 14, DD max | 0.86 | x= | 11.4 |
| R 15, DD max | 0.00 | x= | 12 |

By using the database information, DD and ELOS are plotted against the CMS in Figure 4.3 below. Afterwards, a back analysis is done to deduce the cause of dilution.

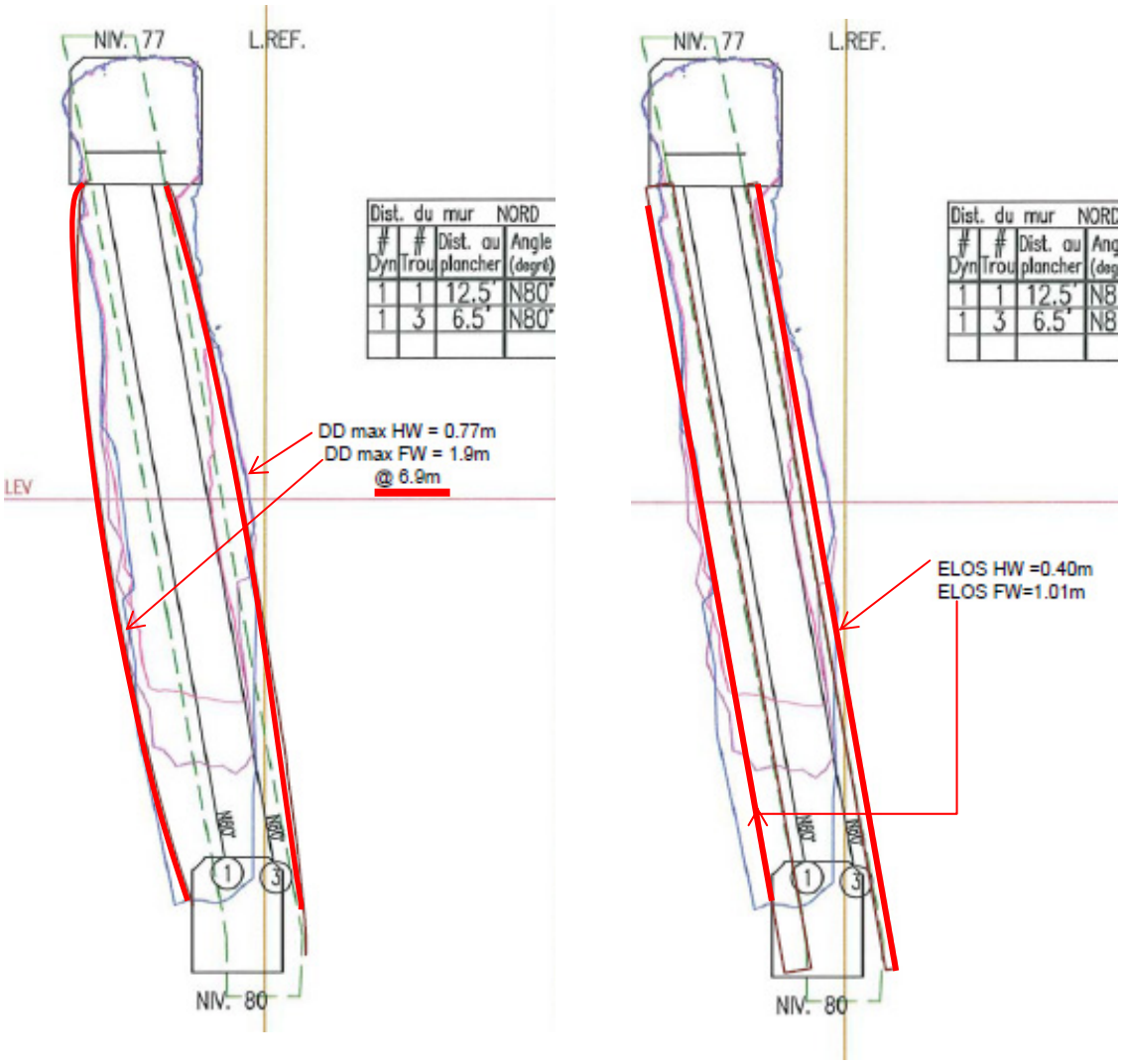


**Figure 4.3** 8049 mid-stope DDmax and ELOS plotted

A summary tab was created to enclose all different stope information (rock properties, sequencing, undercutting, dilution, and comments) as shown on Figure 4.4. The preliminary database was refined by Rory Hughes with additional and more accurate data.

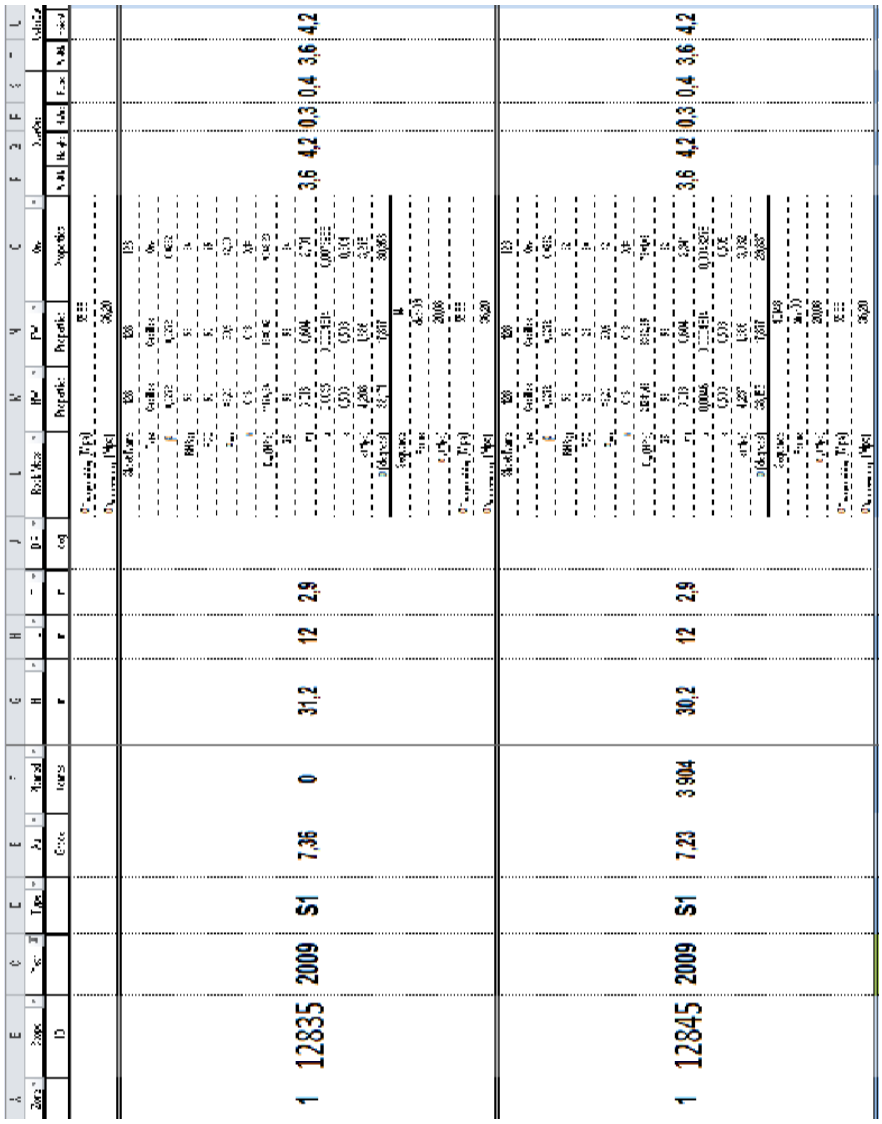

**Figure 4.4** Stope summary

## 4.8 Conclusion

Data collection from field and reports were necessary to compile specific stopes rock mechanics properties in one preliminary database. Several approximation equations were used and the stope geometry was measured from CAD files. Gathered information with plotted stopes became an excellent tool to define the cause of dilution.

# Chapter 5 Effects of stope undercutting[1]

## 5.1 Introduction

Henning and Mitri (2007) examined the factors causing stope wall overbreak in a blasthole stoping environment, with transverse, primary and secondary stopes. Mining depth, in situ stresses as well as stope geometry and orientation were among the factors studied. The current project concerns itself with ore dilution associated with longitudinal mining, where stope extraction follows a retreat sequence along the orebody strike, and stope access is provided through longitudinal overcut and undercut drifts through the orebody. Such mining system may require that the stope walls be undercut to provide necessary space for production drills and mucking equipment. This chapter presents a numerical model parametric study to examine the influence of stope undercutting on its wall overbreak using geomechanical data from the Lapa mine of Agnico Eagle Mines Limited. The study compares two scenarios of stope undercuts namely 1m and 0.4m to a hypothetical case of no undercut; see Figure 5.1. Numerical modeling is carried out with elastoplastic finite elements using the finite element software Phase2. Overbreak is estimated by comparing mining induced stresses in the stope walls to the tensile strength of the rock mass. The study demonstrates the role that stope undercut could play on wall overbreak, and hence ore dilution.

[1] This chapter was published in proceeding 43rd us Rock Mechanics Symposium held at Ashville in 2009

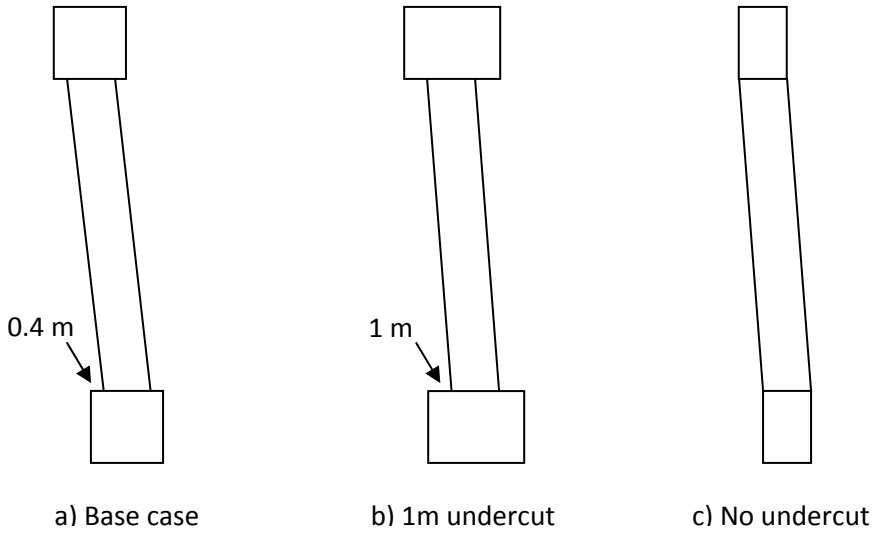


**Figure 5.1** Scenarios of stope undercuts studied

## 5.2 Previous work

Many authors have recognized that stope undercut is one of the factors contributing to the instability and dilution of the stope hanging-wall. Stope undercutting could be performed for the hanging wall, the footwall or both walls. It was reported that stope undercutting reduces stability through the disintegration of the rockmass that would otherwise have formed a solid continuation along either the foliation or bedding planes. Confirmation of this phenomenon has come through several case histories that have underlined the importance of this factor in the occurrence of hanging-wall breakage. A typical undercutting process would result in the hanging-wall sloughing to the depth of the undercut. Factual investigations have shown that dilution levels above 5% were to be found at the Detour Lake Mine that were produced exclusively by undercuts, Dunne et al (1996). The stability graph method was used to assess dilution due to wall overbreak. It was reported that stope walls with low stability number N' values are extremely

vulnerable to undercutting. This and other empirical methods, however, do not take into account the effect of critical parameters such as the depth of the stope undercut.

The geometric and geomechanical data are obtained from the Lapa Mine of Agnico Eagle Mines Limited to examine the influence of stope undercut on the stability of its walls. While 2-dimensional modeling is approximate, it is acceptable for studying cross sections in longitudinal mining systems such as the one at Lapa mine. The study demonstrates the role that the depth of stope undercut could play on wall overbreak as stope extraction and backfilling progresses upward.

## 5.3 Geomechanical data

The stope undercutting study was carried out on a typical 2-dimensional section of the orebody taken in the Zone Contact between levels 710 m and 800 m, where typically three stopes at levels 800, 770 and 740 are to be mined out and backfilled; refer to Figure 46. Based on the RQD data, it was determined that the footwall is highly foliated and is therefore more prone to damage due to blasting. As illustrated in Figure 5.2, the footwall was divided into two parts, which are designated as near and far, in which the rock masses have different geomechanical properties. The near footwall material is weaker and represents the disturbed rock adjacent to the stope. In addition, the hanging wall was considered as comprised of undisturbed material since it is in better condition. The orebody is steeply dipping with an average dip angle of 87º.

Thus, the modeled section is characterized by four regions: far footwall, near footwall, ore, and hanging wall. The thickness of the near footwall is variable, and was estimated by importing the RQD drill holes information obtained from the mine into Datamine

Studio software. A thickness of 1m for the near footwall was taken for the purpose of the model parametric study.

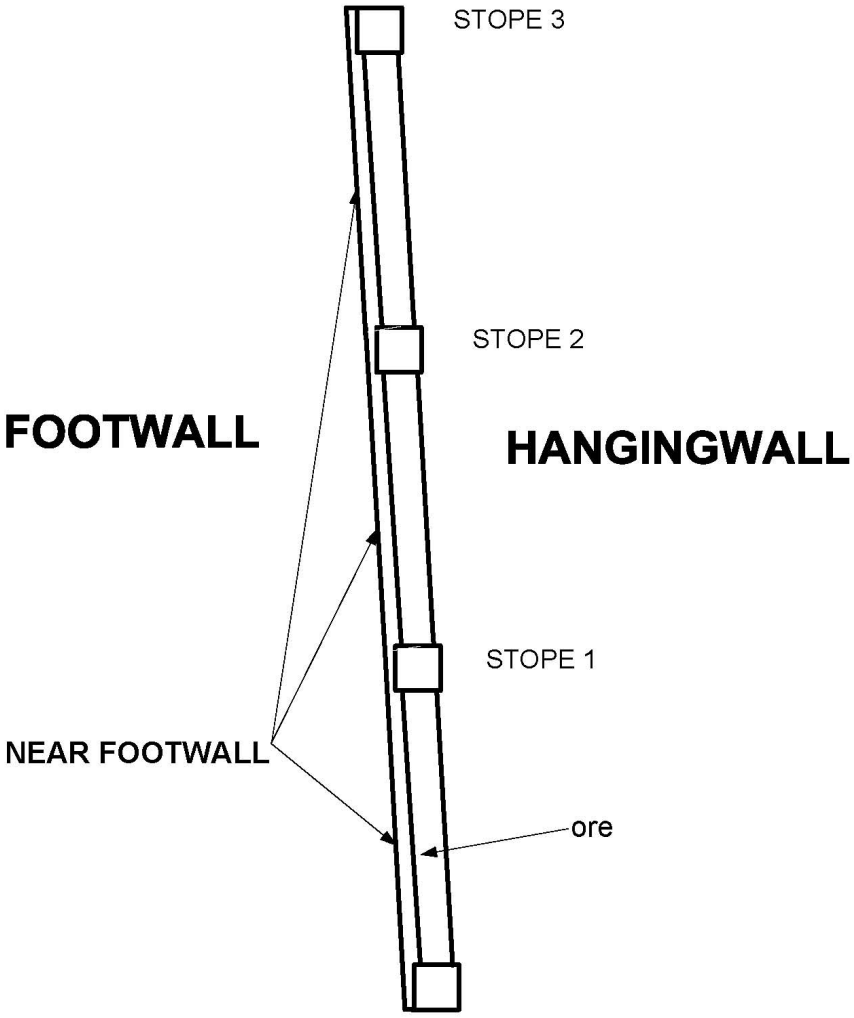


**Figure 5.2** Two-dimensional section modeled

The mechanical properties of the four rock masses modeled are presented in Table 5.1. The angle of dilation $\psi$ was taken equal to $\varphi/4$.

As the finite element model considers the simulation of mine backfill, it was necessary to use suitable data for cemented rockfill. These are given in Table 5.2.

**Table 5.1** Rock mass mechanical properties

| Rock mass | GSI | $E_{rm}$ GPa | $\sigma_t$ MPa | c MPa | φ ° | ψ° | ν |
|---|---|---|---|---|---|---|---|
| Hanging wall | 60 | 23.2 | 8.6 | 3.67 | 44.7 | 11.2 | 0.16 |
| Footwall | 56 | 15.9 | 6.5 | 2.93 | 41 | 10.2 | 0.18 |
| Ore | 56 | 9.1 | 0.12 | 3.26 | 34.7 | 8.7 | 0.18 |
| Near Footwall | 56 | 2.7 | 0.07 | 1.5 | 25.2 | 6.3 | 0.18 |

**Table 5. 2** Numerical model parameters for cemented rockfill

| **Backfill parameter** | **Material value** |
|---|---|
| Modulus of elasticity, E (GPa) | 2.5 |
| Cohesion, c (MPa) | 0.1 |
| Friction angle, φ (°) | 35 |
| UCS,(MPa) | 3 |
| Poisson's ratio, ν | 0.35 |
| Unit weight (kN/m$^3$) | 23 |
| Dilation angle, ψ (°) | 0 |

## 5.4 Numerical modeling study

Phase2 is a 2-dimensional elastoplastic finite element code for calculating stresses and displacements around underground openings. It can be used to solve a wide range of mining and geotechnical engineering problems. The program can simulate the sequence of excavation and backfilling in modeling stages and is thus suitable for the current case study. A four-node quadrilateral element was chosen to generate the finite element mesh.

In the first place, a mesh sensitivity analysis was performed to arrive at a suitable mesh for each of the three scenarios presented in Figure 5.3, namely stope with the planned undercut of 0.4 m, stope with 1m undercut, and stope with no undercut. In the mesh sensitivity analysis, stope wall closure is compared for a number of generated meshes of increasing density until no significant change in wall closure is observed. Figure 46 depicts the results of the mesh sensitivity analysis, which show the monotonic convergence of wall closure for each of the three cases tested. It can be seen that the model with no undercut exhibits smaller closure than the other two models, as expected.

An elasto-plastic study was performed based on Mohr-Coulomb criterion where the residual strength parameters are equal to the peak parameters, defining an ideally elastoplastic material. It should be noted that the Mohr-Coulomb is preferred over Hoek-Brown in this study as the latter is believed to be more suitable for high confinement applications, which is not the case herein.

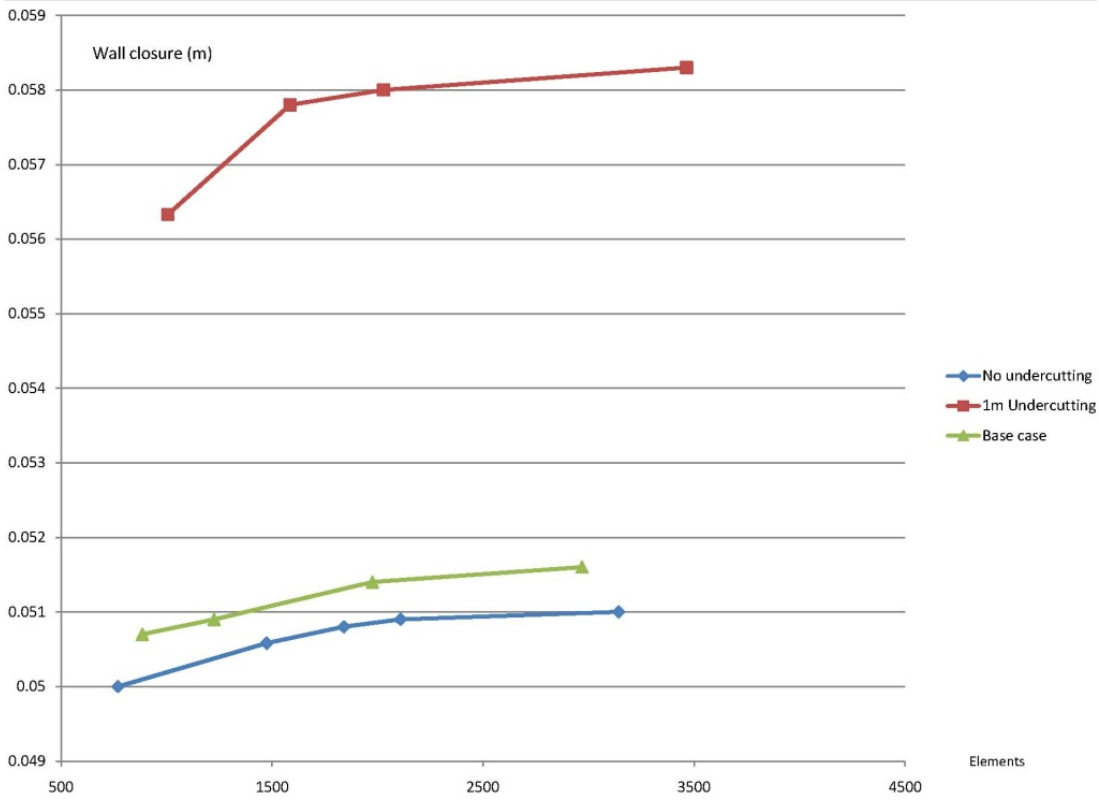


**Figure 5.3** Mesh sensitivity analysis for each of the three models analyzed

In this study, the extent of yielding into the stope walls is used as an indicator of wall overbreak. Yield failure takes place in the form of either shear or tensile failure. In the case of wall overbreak, yielding is predominantly attributed to the mining induced stress relaxation in the walls, which produces tensile stresses. Thus, a criterion based on tensile stress is adequate and has shown to give good correlation with field observations.

Figure 5.4 illustrates this behavior; it shows the stress trajectories around the first (lowest) stope for the base case of 0.4 m undercut, overlapping the minor principal stress contours. As can be seen, the blue zones in the walls representing low stress regimes (including tensile stresses) surround the stope walls. Thus, the model parametric study

adopted the criterion of yield progression into the walls as the basis for the estimation of dilution or overbreak.

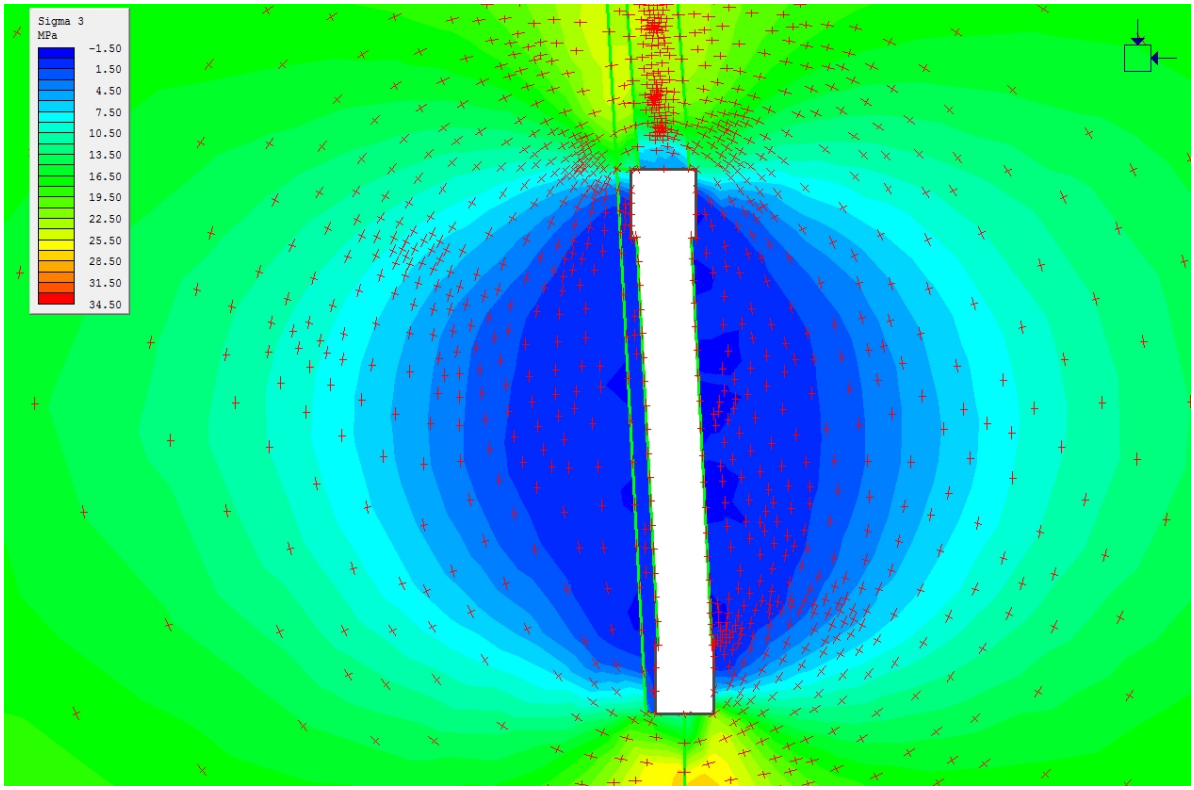


**Figure 5.4** Stress trajectories around the first stope

## 5.5 Model results

Modeling of the section shown in Figure 44 with Phase 2 software was conducted in seven stages starting with the excavation of all four level drifts, followed by the mining and filling of each stope going upward. The results are displayed in terms of displacements and yielding. Figure 5.5 presents a comparison of the total displacement contour lines around the first stope for the three scenarios analyzed. As can be seen, wall closure characterized by the green and yellow zones show higher values for the case of 1 m undercut (Figure 5.5 c) compared to the other two cases. Thus, it can be said that the

depth of wall undercut has a significant influence on its deformation.

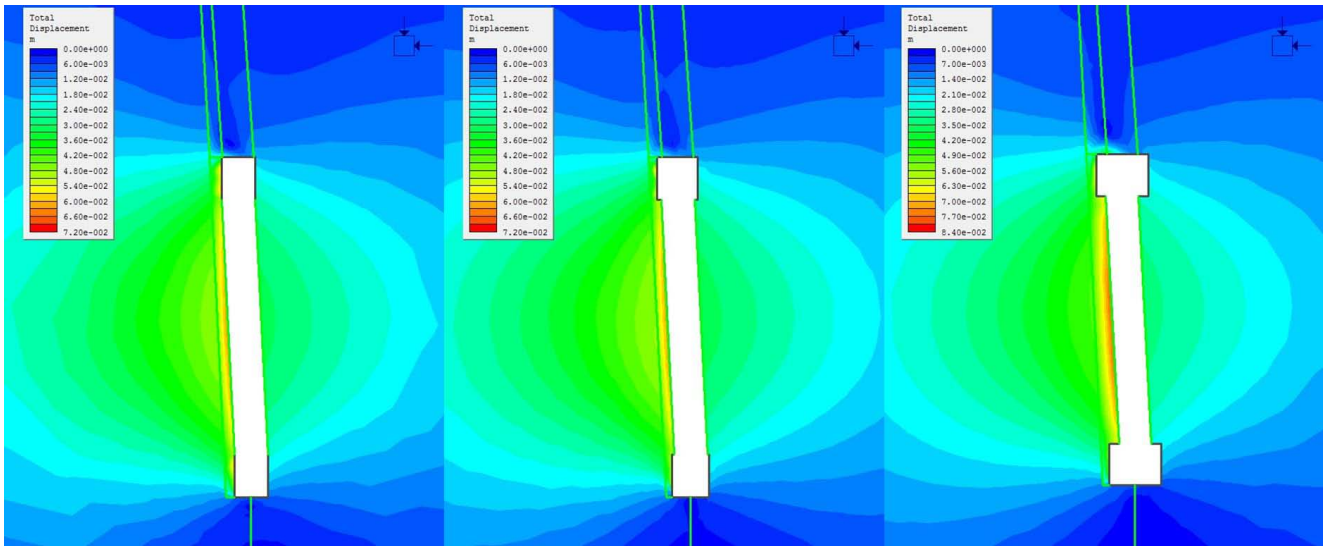


**Figure 5.5** Displacements around the first (lowest) stope

Model results in terms of yield zones are presented in Figures 5.6 to 5.8, whereby the red zones around the excavation represents 100% yielding. A number of interesting observations can be made in light of these results. The footwall appears to exhibit considerably larger yielding surface than the hanging wall for all cases analyzed, and at all three mining levels. While this observation is contrary to common belief, the footwall at Lapa mine is known to be highly foliated and its dilution is expected to be higher than that of the hanging wall.

A comparison between the base case result in Figure 5.6 and that of the 1m undercut in Figure 5.7, reveals clearly the adverse effects of deep stope undercut on the stability of its walls. On the other hand, it is seen from Figure 5.8 that the yield zones are reduced significantly when there is no undercut.

On the other hand, it appears from these results that wall stability is only slightly affected by previous mining and filling activities. This finding is based on the observation that the size and extend of yield zones in the footwall of the upper stopes are approximately equal to those of the first stope. This observation applies for all of the three cases analyzed. It is believed that the strength of mine fill could play a role in this respect. However, this is beyond the scope of the present study.

It should be noted however that the results obtained from this study are based on 2-dimensional analysis, which is effectively conservative. That is to say, deformations and yield zones are overestimated. Hence the analysis should be regarded only as qualitative. Nevertheless, the results have proven useful and have served to shed light on the effects of stope undercutting.

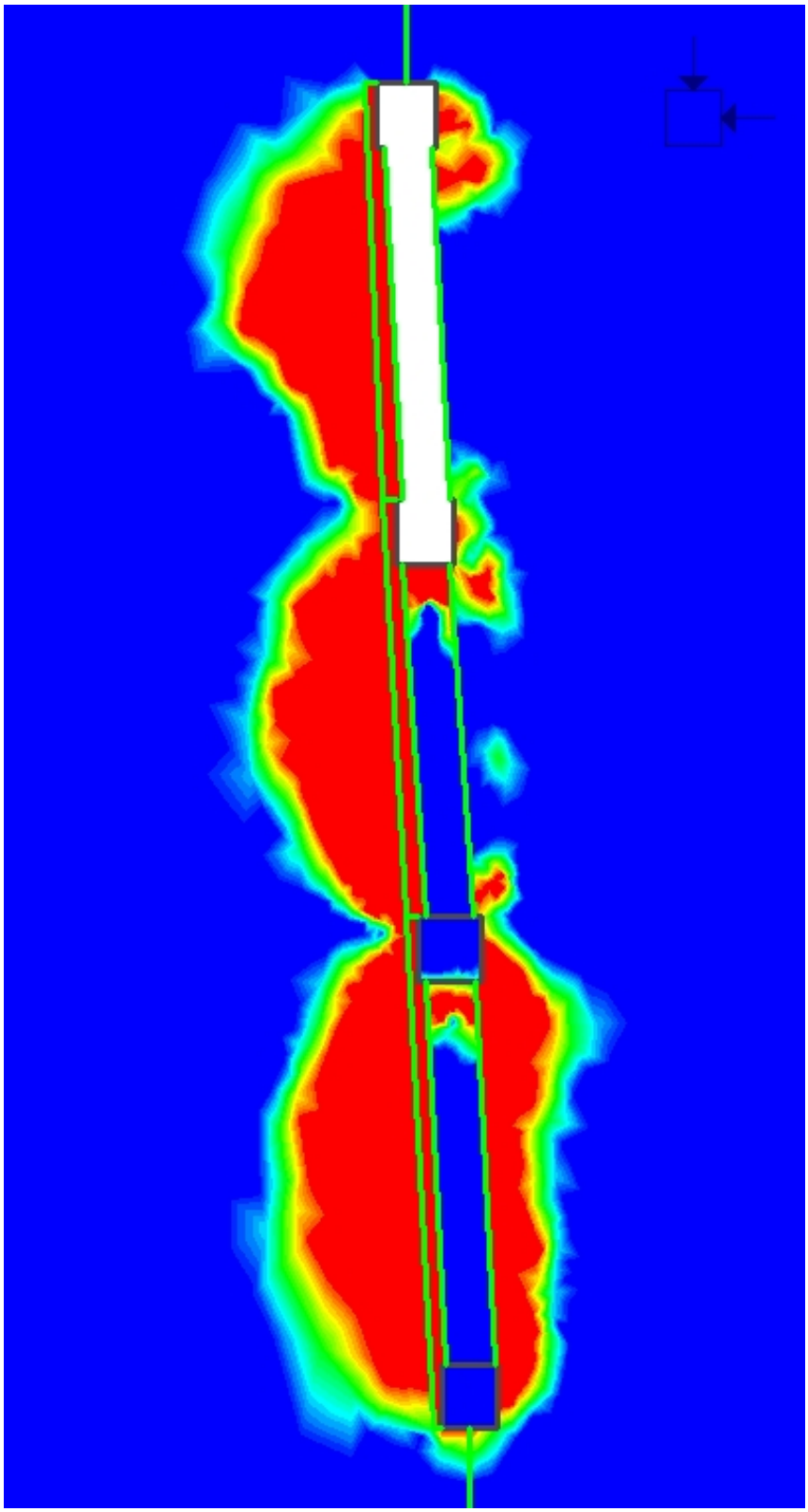

**Figure 5.6** Yield zones around stope with 0.4m undercut

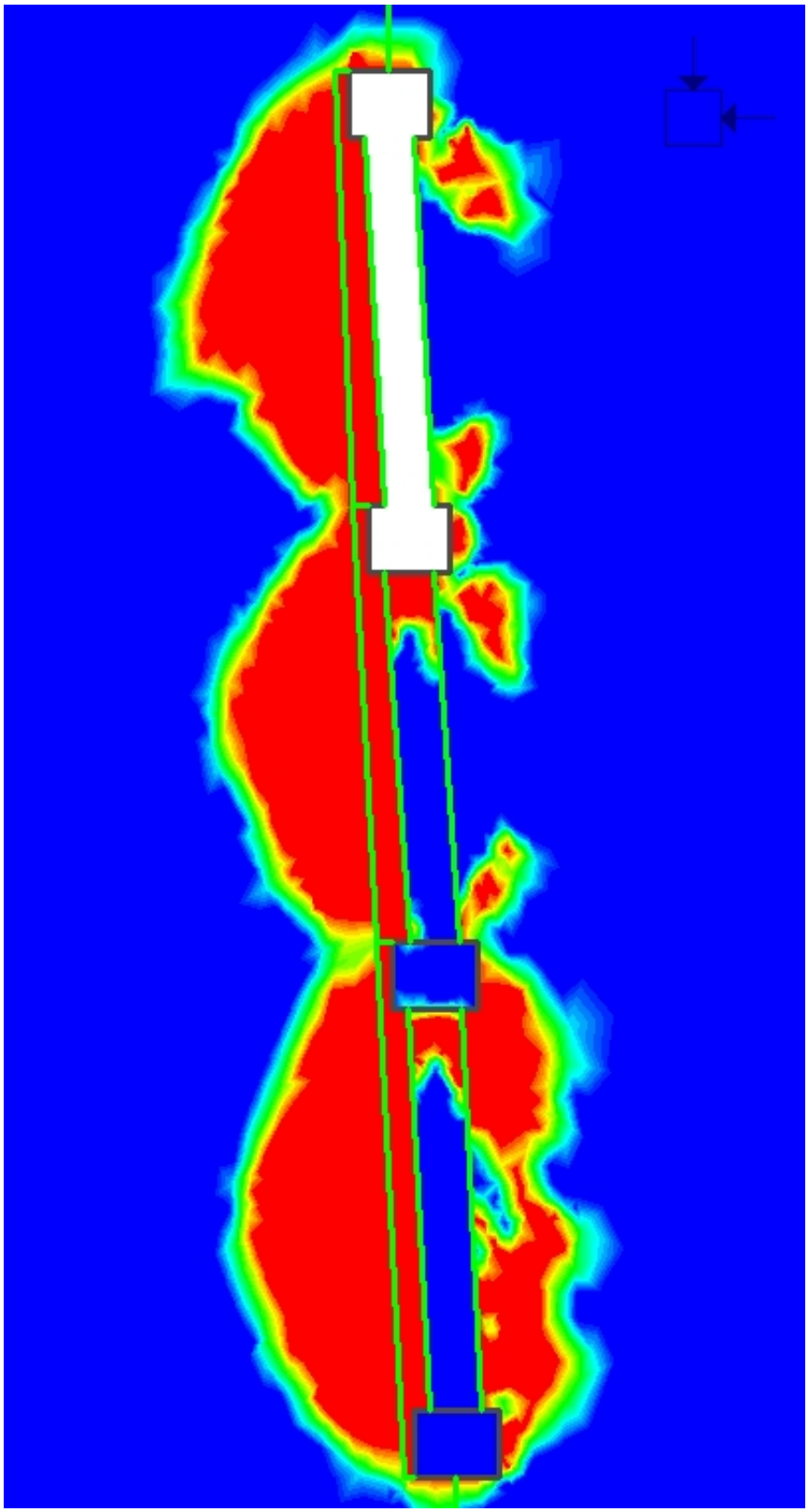

**Figure 5.7** Yield zones around the stopes - 1m undercut

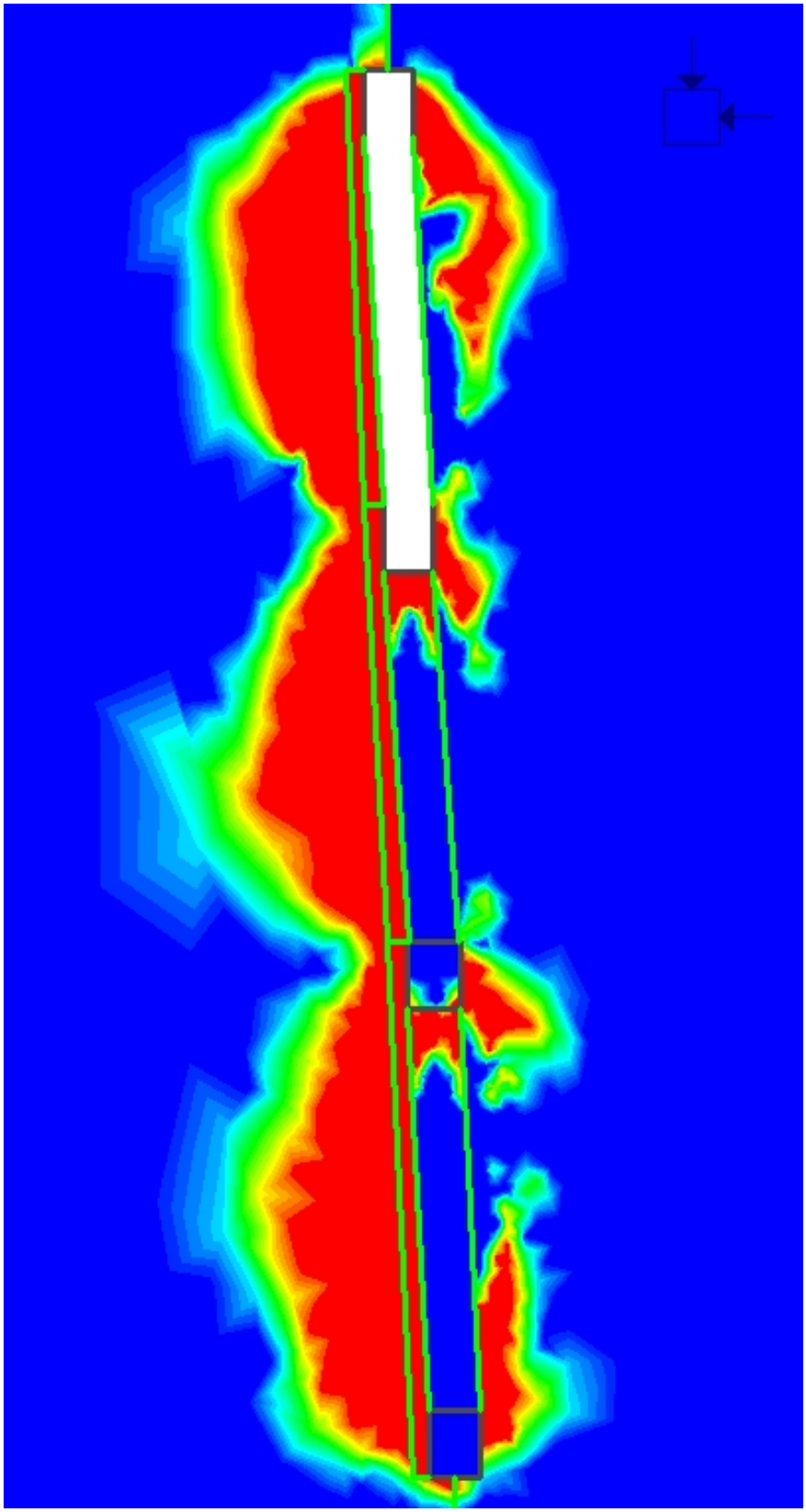

**Figure 5.8** Yield zones around the stopes - no undercut

## 5.6 Conclusions

Three scenarios were studied in the model parametric study of stope undercutting, in which the base case scenario of a 0.4m undercut is compared with two hypothetical scenarios with 1m undercut and no undercut. The finite element method was selected to conduct a two-dimensional, elastoplastic analysis with Phase2 finite element software.

A model parametric study has revealed that wall overbreak consistently increases with the depth of the undercut. Also, the footwall overbreak is found to be more significant than that of the hangingwall and this is attributed the lower quality of the footwall rockmass. It is also found the extent of yielding in the upper stopes is nearly similar to that around the lower stopes suggesting no significant increase in dilution as mining progresses upward.

# Chapter 6 Effects of stope construction on overbreak

## 6.1 Introduction

A study was conducted on the Lapa Mine where unplanned ore dilution or overbreak was observed. The actual average dilution experienced after mining the reserves stands at 50% while the feasibility study indicated an overbreak estimate of 30%**.** Figure 6.1 is a 2D section of a stope located on level 80. The total dilution was estimated to an average of 32% but dilution after mucking was at 66%.

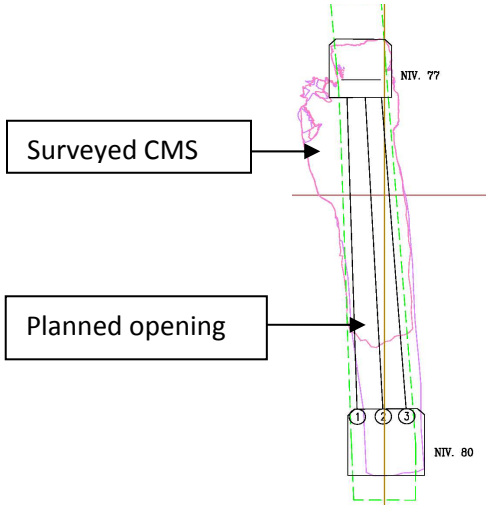


**Figure 6.1** 2D section of an 80 level stope at Lapa Mine

Numerous factors influence the occurrence of dilution such as the stope construction and ore geometry. In this chapter, parametric studies were conducted on strike length, ore dip, and ore width. An overbreak estimation criterion, based on the tension criterion used by Mitri et al (1998), was calibrated to the surveyed CMS, which assessed the occurrence of overbreak on stope walls.

The elastoplastic finites elements model was built on Phase2. An eight-node quadrilateral element was chosen to generate the finite element mesh. The mesh was graded and calibrated by performing a sensitivy analysis based on the stope wall closure. The study was achieved by using the Mohr-Coulomb criterion.

## 6.2 Overbreak criterion estimation

Mitri et al (1998) examined the no-tension rock method in cable bolts design using numerical modelling. The no-tension rock gives more realistic results and confirms the cavity monitoring system measurements of the mined stope. Hence, tension criterion estimating overbreak is used for calibrating the CMS measurements at Lapa Mine.

As an example of stopes dipping 80 degrees or less, stope 7748 located on level 77 at 770m depth and dipping 78° was chosen. The results of the numerical modeling are shown on Figure 6.2, and the first case examined is the $\sigma_3$=+0.05MPa.

Tension is seen to cover the surveyed CMS but slightly overestimates the quantities. The second case is taken at $\sigma_3$ = 0 MPa and the tension contours fit with the surveyed CMS. The last case is $\sigma_3$ = -0.1 MPa where the footwall is underestimated and the hanging-wall tension is distinguished at the undercut only. It could be concluded from the study of stope 7748 that for stopes that dip 80 degrees and less, overbreak is estimated for the footwall and hanging-wall by a no-tension criterion $\sigma_3$ = 0 MPa.

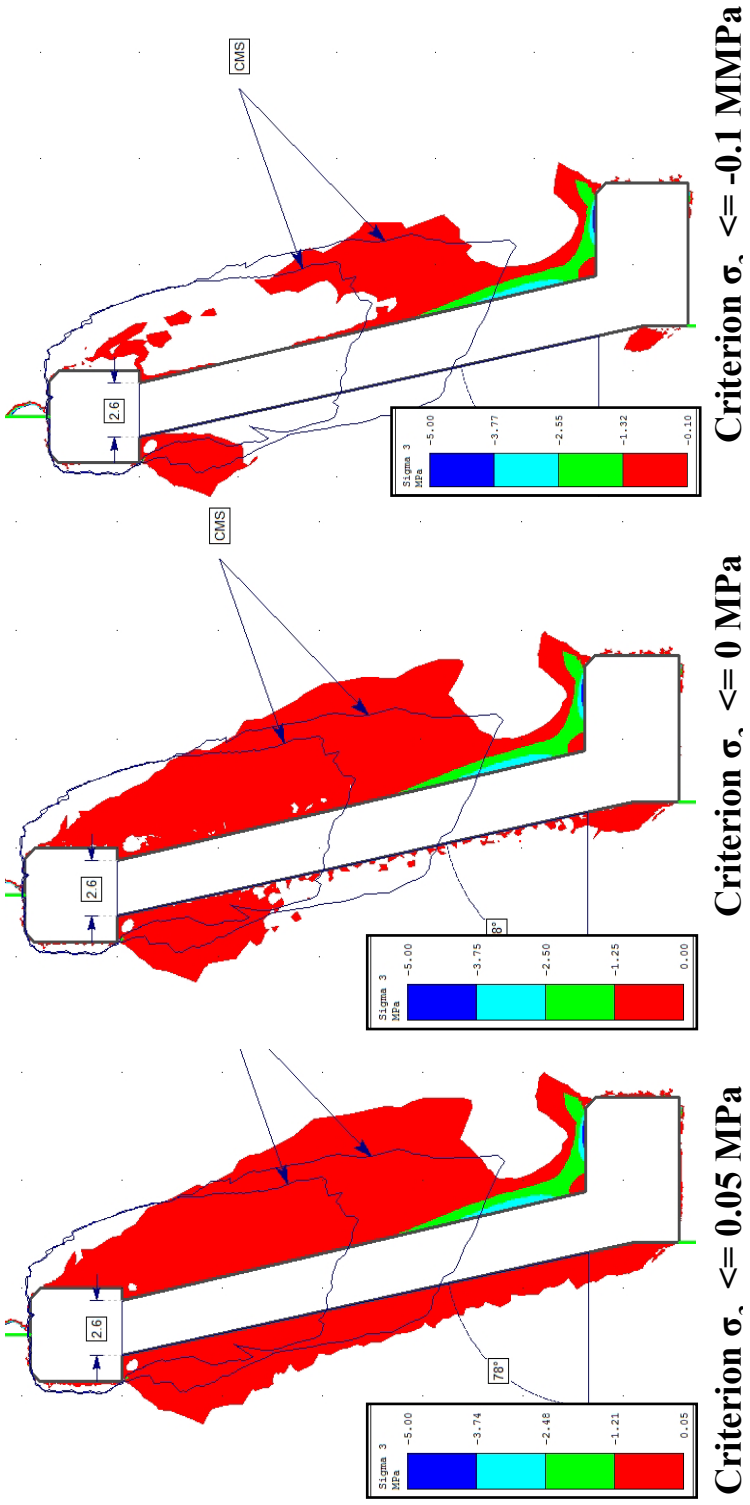


**Figure 6.2** $\sigma_3$ calibration with CMS, stope 7748

As an example of vertical or sub-vertical stopes, stope 8029 located in level 80 at 800m depth and dipping 89° was chosen. The results are summarized in Figure 6.2.

The first case examined is where $\sigma_3$ = +0.05MPa and tension is seen to cover the surveyed CMS but overestimates quantities for both footwall and hanging-wall.

The second case is $\sigma_3$ = 0 MPa and footwall tension contours fit with the surveyed CMS but still overestimate the hanging-wall.

The last case is $\sigma_3$ = -0.1 MPa where the footwall is underestimated. Since the hanging-wall is in a better geotechnical state than the footwall, it will not fail when $\sigma_3$=0 MPa due to a resistance on tension.

Consequently, $\sigma_3 \leq$-0.1 MPa is chosen as the overbreak criterion for hanging-wall and $\sigma_3 \leq$0 MPa for footwall.

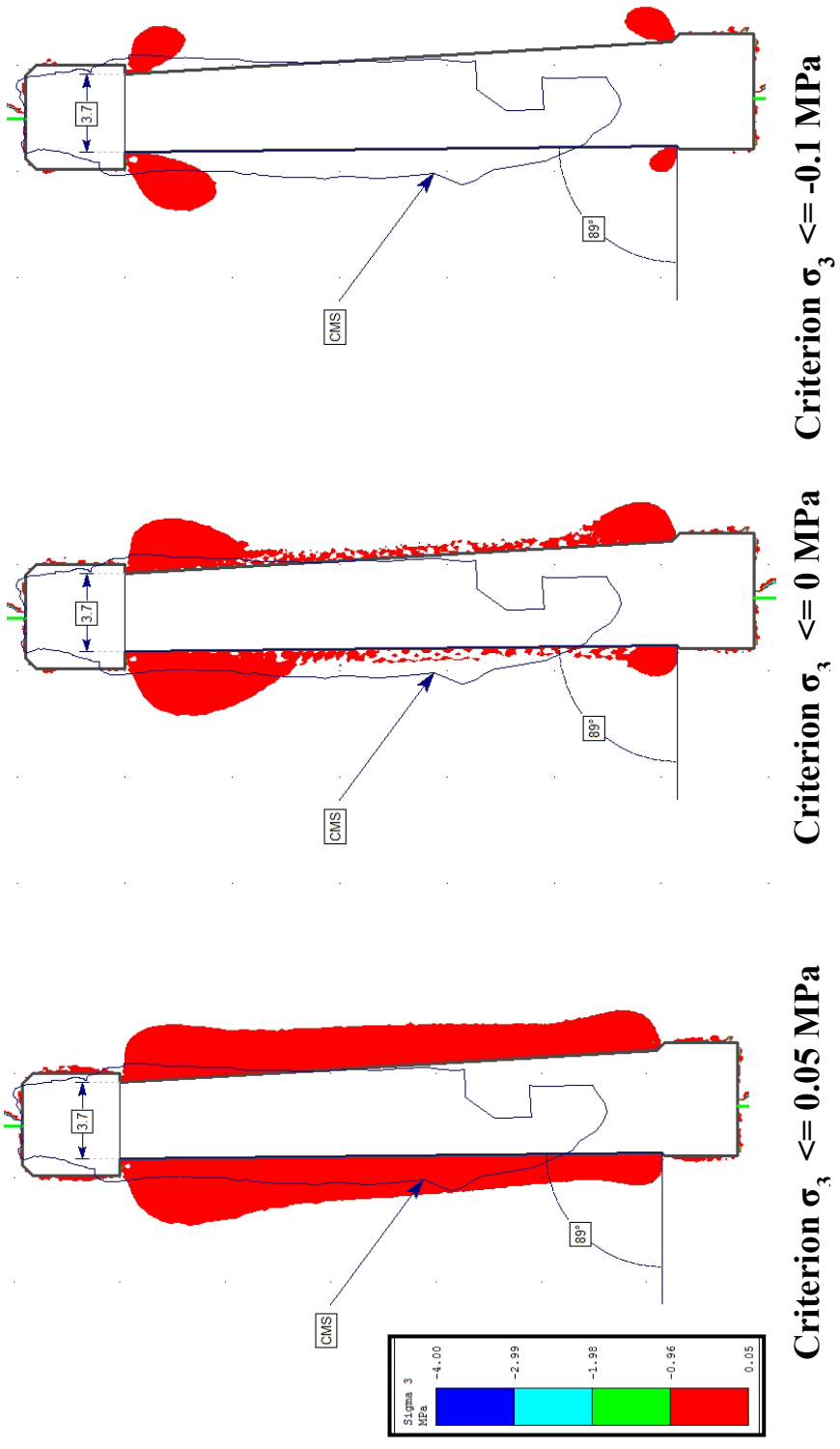


**Figure 6.3** $\sigma_3$ calibration with CMS, stope 8029

## 6.3 Effect of strike length

Increasing the productivity and the need for extra tonnes to muck are reasons inducing to change the strike length. However, it was demonstrated that changing this parameter has severe consequences on the wall stability, mucked tonnes, and hence not achieving the goal of production and cost control.

Strike length effect was examined by Henning and Mitri (2007) for various depths in Bousquet 2 mine located in the Abitibi region. It was noted from the study that dilution density is greater for longer strikes at a giving depth considering a perfect geometry (no changes in strike direction). Figure 6.4 illustrates results.

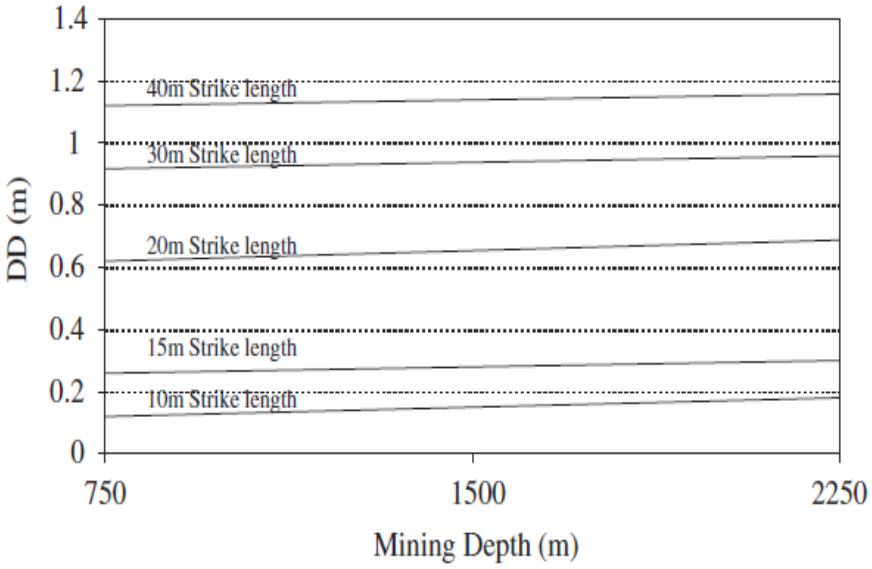


**Figure 6.4** DD vs mining depth and strike length, (Henning 2007)

To improve the wall stability, the strike length is a parameter that can be modified to control the overbreak.

### 6.3.1 Numerical modelling set-up

Level 104, located at 1040m depth,was selected for conducting the strike study at the Lapa mine. The tension criterion is used where footwall $\sigma 3 \leq 0$MPa and hanging-wall $\sigma 3 \leq -0.1$MPa. Three models were studied with strikes of 12m, 14m, and 10m. Tables 6.1 and 6.2 below summarize the geomechanical properties for walls and the cemented rock fill.

**Table 6.1** Geomechanical properties based on stope 10431

| Rock mass | GSI | $E_{rm}$ GPa | $\sigma_t$ MPa | c Mpa | φ ° | ψ° | v |
|---|---|---|---|---|---|---|---|
| Hanging wall | 48 | 13.17 | 0.1 | 2.89 | 32.89 | 8.22 | 0.2 |
| Ore | 54 | 11.66 | 0.1 | 2.81 | 32.56 | 8.14 | 0.2 |
| Footwall | 60 | 7.33 | 0.1 | 2.53 | 30.81 | 7.70 | 0.2 |

**Table 6.2** Cemented rockfill, (Hassani et al. 1998)

| **CRF properties** | Material value |
|---|---|
| Modulus of elasticity, E (GPa) | 2.5 |
| Cohesion, c (MPa) | 0.1 |
| Friction angle, φ (°) | 35 |
| UCS,(MPa) | 3 |
| Poisson's ratio, v | 0.35 |
| Unit weight (kN/m$^3$) | 23 |
| *Dilation angle, ψ (°) | 0 |

Three types of stope categories were identified. P1 is an isolated primary stope with rock on both sides and the secondary stope S1 has rock on one side and backfill on the other side. The secondary stope S2 has both side walls against backfill.See Figure 6.5.

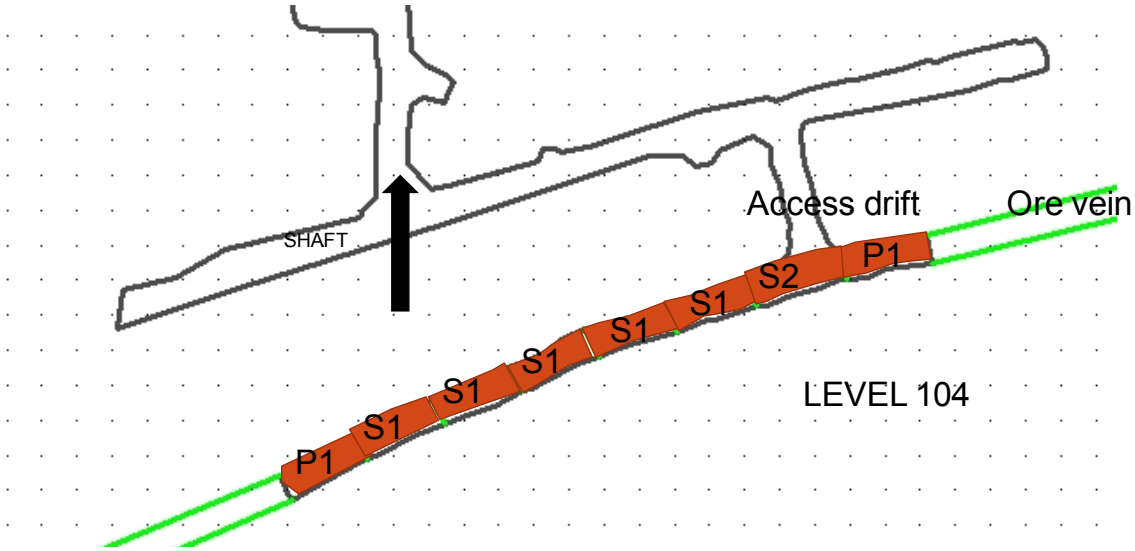


**Figure 6.5** Mining sequence at level 104

### 6.3.2 Model results

The overbreak experienced in the primary stope P1 increases with the strike length, as illustrated on Figures 6.6 and 6.9. Moreover, depending on the stope location, whether located between backfill or between rock and backfill, the amount of overbreak will be affected. The overbreak experienced in the secondary stope S1 increases with the strike length, and wall convergence increases with a longer strike, Figures 6.7 and 6.10. Overbreak in the secondary stope S2 is higher too with longer strike, see Figures 6.8 and 6.11

Tension is greater when mining 14m strike length. A 10m strike stope mined, the observed tension in a perfect geometry, in the three stopes type, would have been null. However, mining a 10m strike is not economical. In the case of Lapa, where the footwall is weak, the footwall is severally affected in the case of longer strike. The 12m strike is the best compromise between the two studied cases. It has to be noted that in a perfect geometry, the overbreak would have been less.

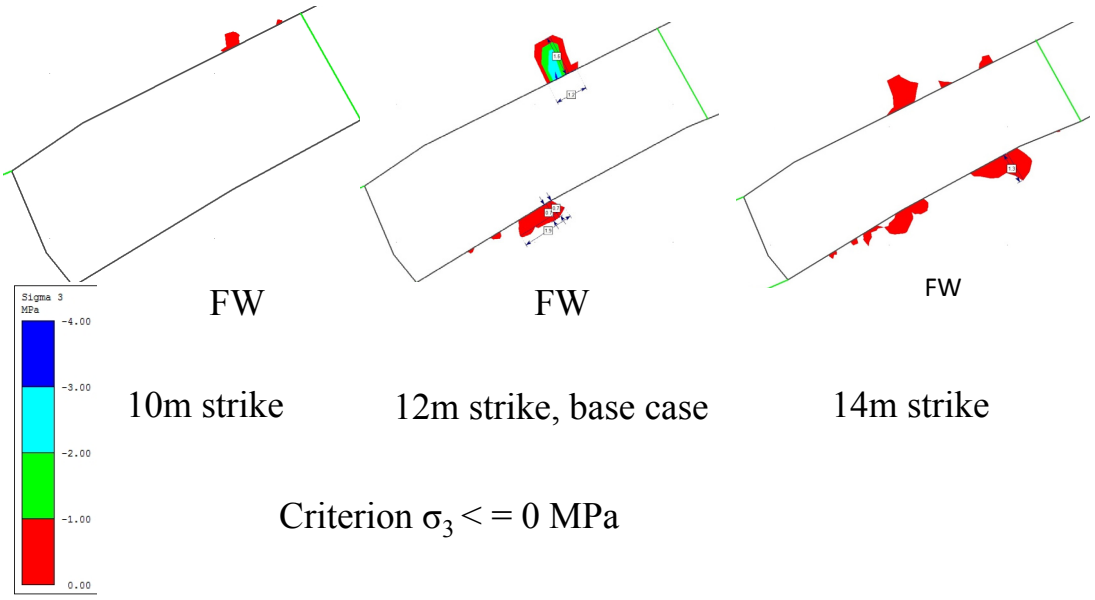


**Figure 6.6** P1 footwall comparison

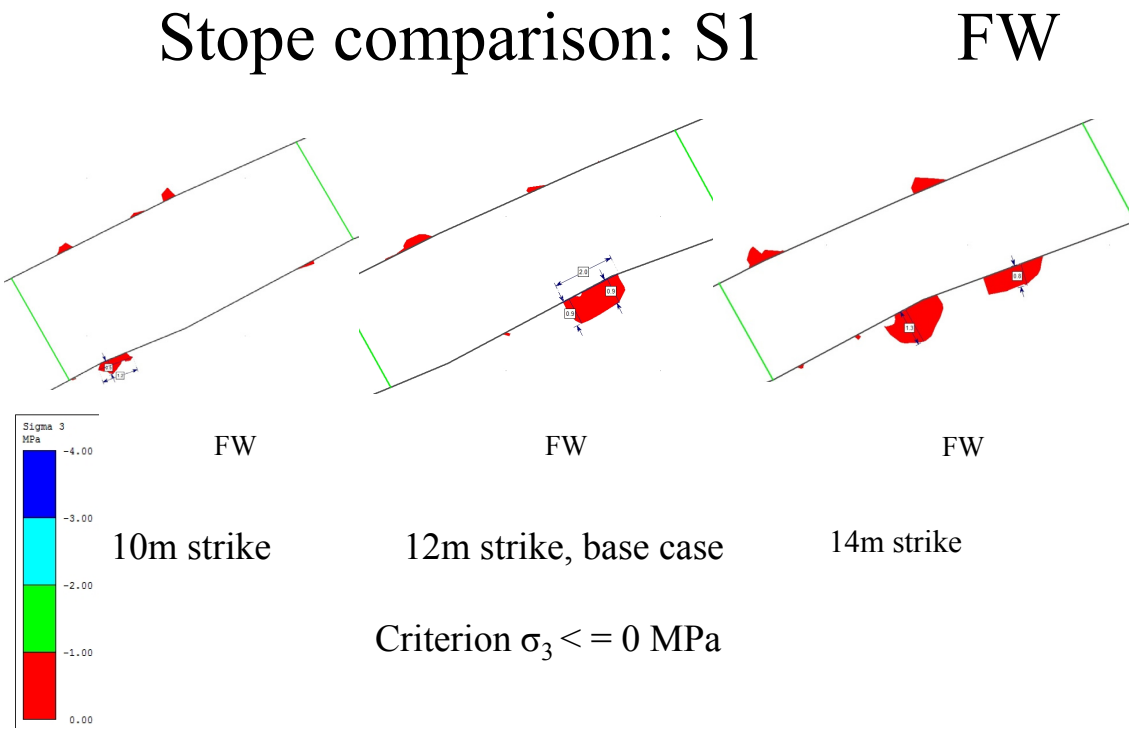


**Figure 6.7** FW comparison for S1

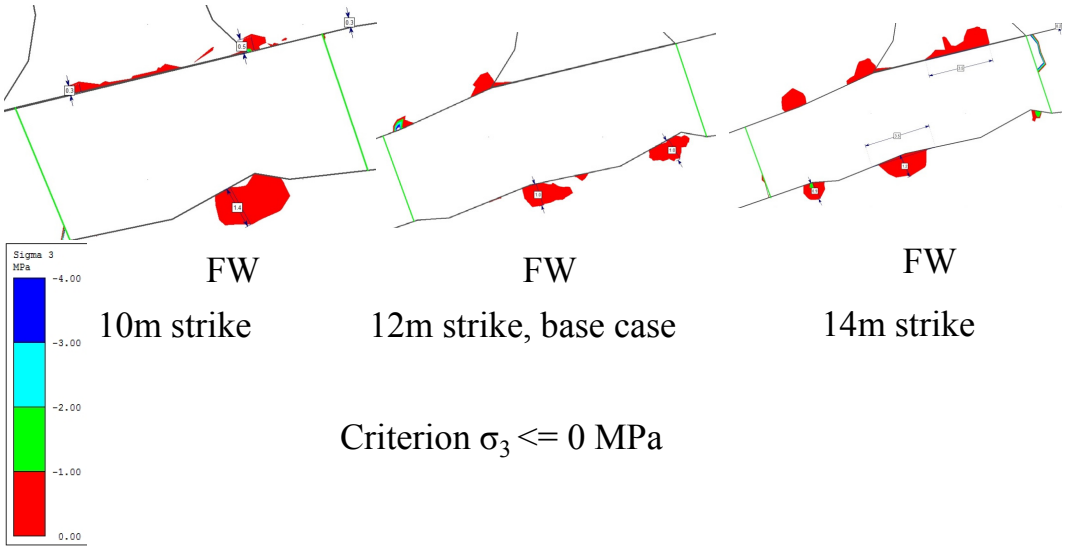


**Figure 6.8** FW comparison for S2

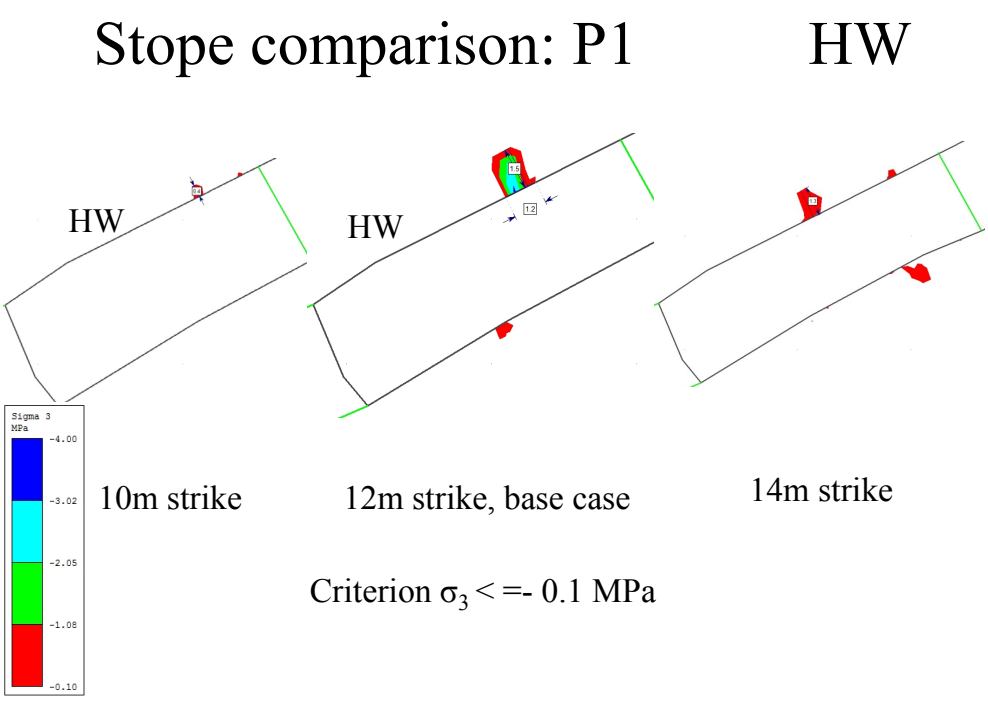


**Figure 6.9** HW comparison for P1

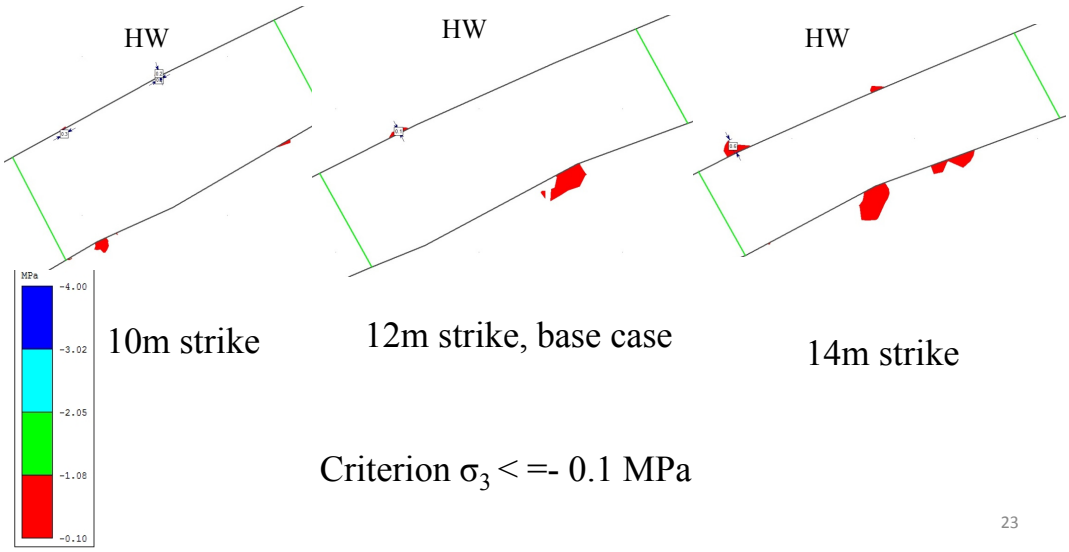


**Figure 6.10** HW comparison for S1

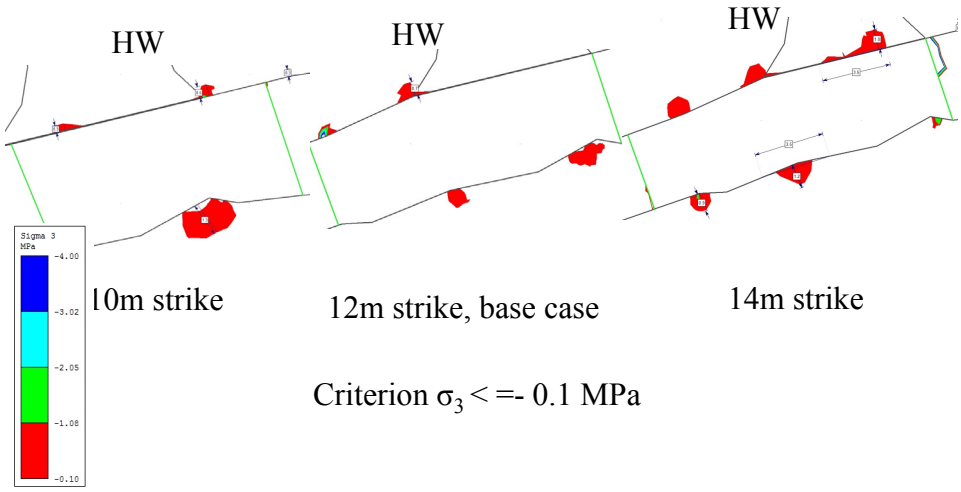


**Figure 6.11** HW comparison for S2

Wall convergence increases with the longer strike and when the stope is surrounded by backfill, stope type S2, as plotted on Figure 6.12.

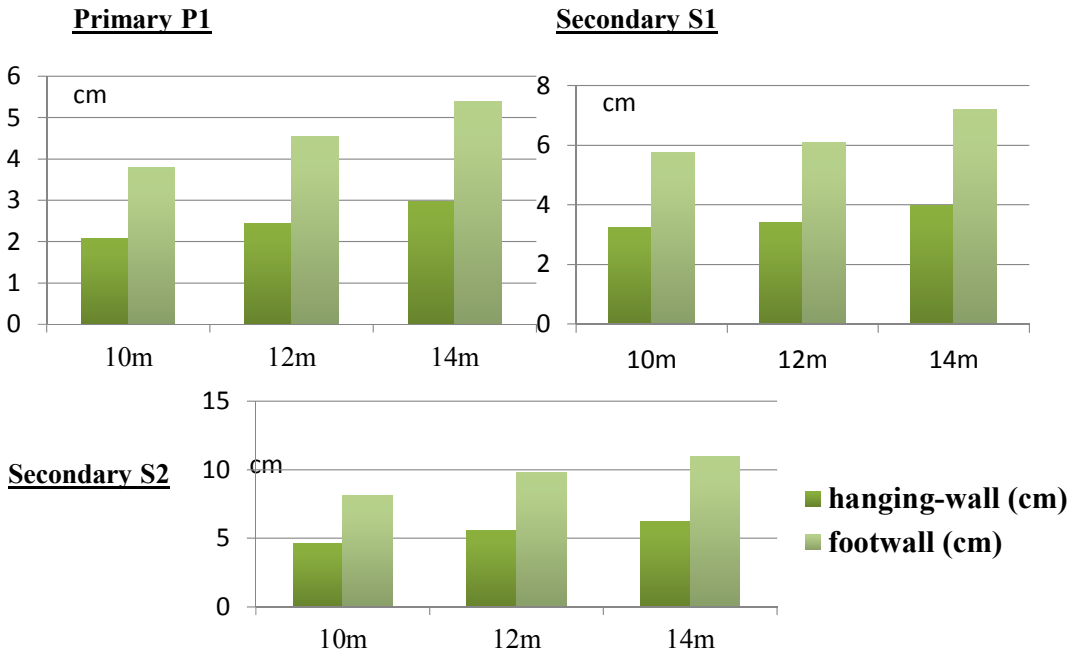


**Figure 6.12** Wall convergence on level 104

### 6.3.3 Discussion and conclusion

In conclusion, longer stope strike increases overbreak and at the Lapa Mine, it was observed that the footwall overbreak is greater than hanging-wall overbreak. Yielding is maximum at mid-stope length and tension is greater when irregularity in geometry is along the strike.A decrease in strike length from 12m to 10m should cause a reduction of overbreak by 46% on hanging-wall .An increase in strike length to 14 m on the other hand is likely to create more overbreak from the stope walls by approximately 2% on hanging-wall and 56% on the footwall according to the $\sigma_3 \leq 0$ MPa,see Figure 6.13.

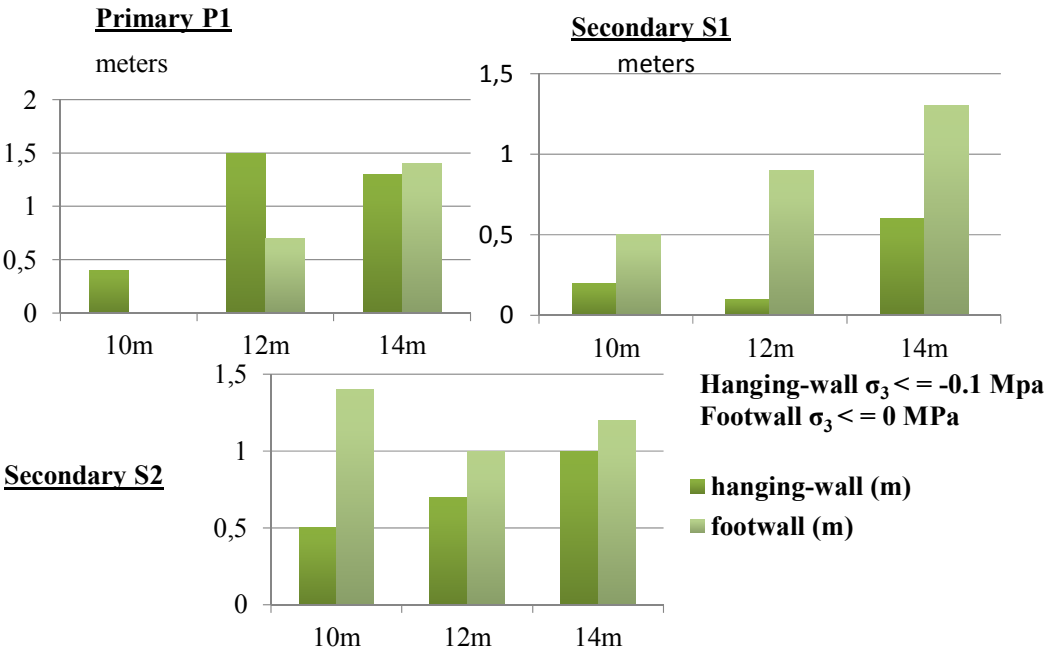


**Figure 6.13** Wall sloughage on level 104

## 6.4 Effect of stope width

Dilution is particularly critical for narrow stopes whereby the narrower the stope the higher the dilution for the same amount of wall slough, Pakalnis et al(1995). Six stopes widths were examined starting 2.5m ore width to 7.5m with an increment of 1m ore width starting from 2.5m.

### 6.4.1 Numerical modelling set-up

Models from 3.5m width to 7.5m have a footwall undercut of 0.3m and a hanging-wall undercut of 0.4m. The 2.5m ore width model has a greater undercutting since a minimum

clearance for a scoop is 4m, and therefore the hanging-wall undercut is 0.8m and the footwall is 0.7m. Stope height is 30m with a dip of 85 degrees. Figure 6.14 shows the geometry of a 7.5m ore width stope.

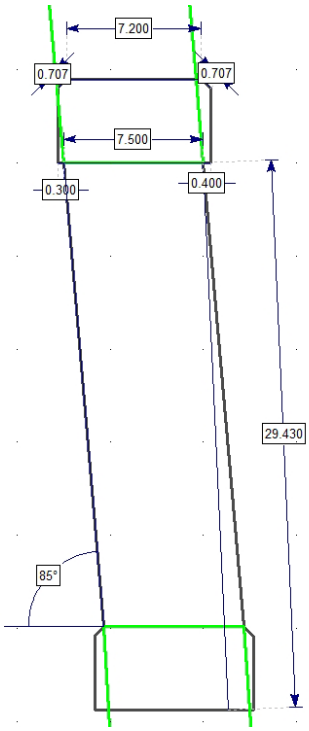


**Figure 6.14** Stope construction geometry

The geomechanical properties used are summarized in Table 6.3.

**Table 6.3** Geomechanical properties based on level 80

| Rock mass | GSI | $E_{rm}$ GPa | $\sigma_t$ MPa | c Mpa | φ ° | ψ° | ν |
|---|---|---|---|---|---|---|---|
| Hanging wall | 60 | 23.2 | 8.6 | 3.67 | 44.7 | 11.2 | 0.16 |
| Ore | 56 | 9.1 | 0.12 | 3.26 | 34.7 | 8.7 | 0.18 |
| Footwall | 56 | 15.9 | 6.5 | 2.93 | 41 | 10.2 | 0.18 |

### 6.4.2 Model results

The first results concern the footwall where the dilution criterion is $\sigma_3 \leq 0$ MPa. In cases from 3.5m to 7.5m ore width, the tension in the overcut is averaging 1.9m compared to 2.9m in the 2.5m ore width case. It was observed that tension developed on the stope undercutting is more severe on the narrow ore width 2.5m where the undercutting tension is 14% less when the ore width is greater than the 2.5m ore width.

Larger is the stope, less dilution is created from the footwall. Figures 6.15 and 6.16 illustrate observed tension results.

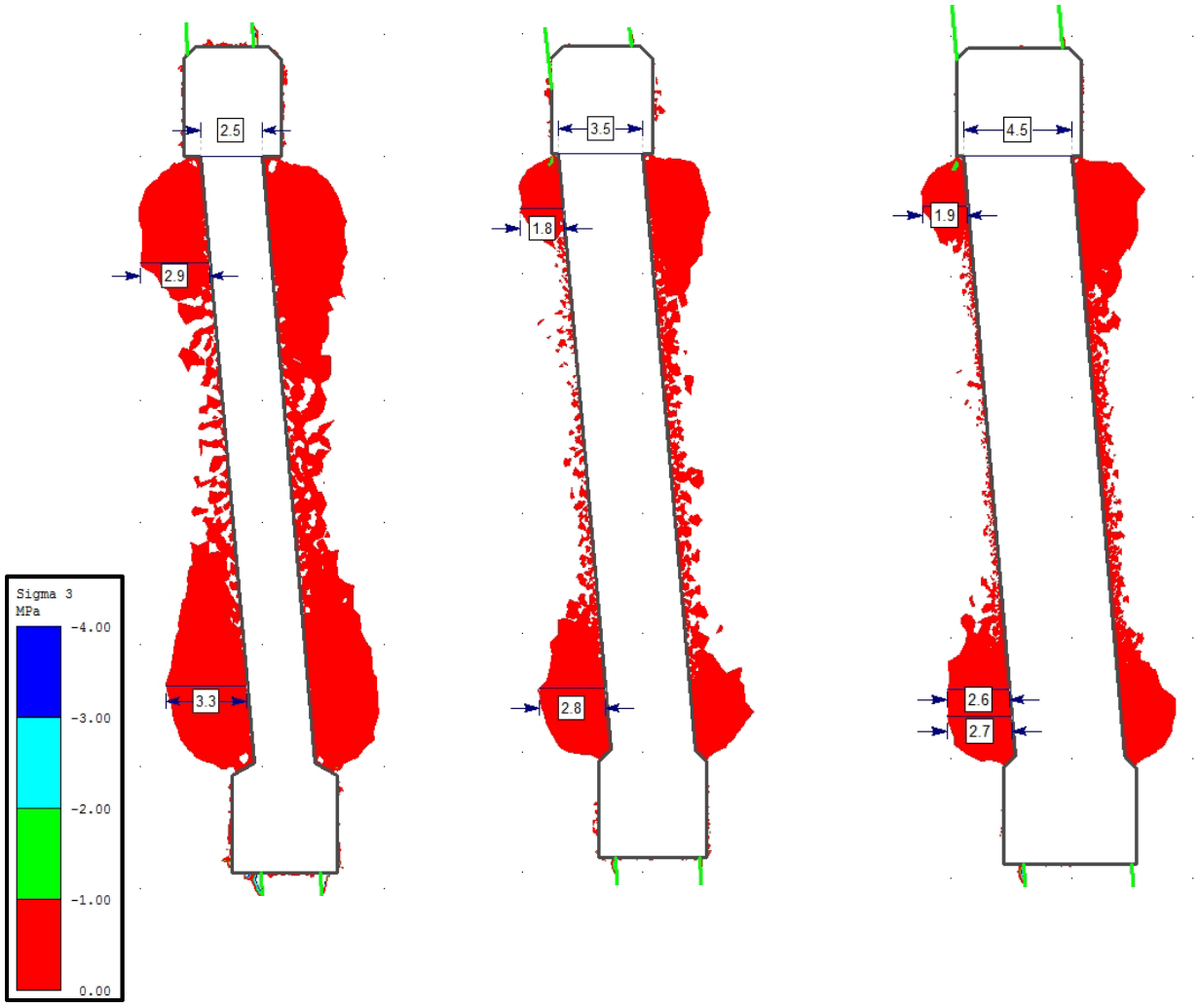


**Figure 6.15** Footwall tension in stopes with ore width ranging from 2.5m to 4.5m

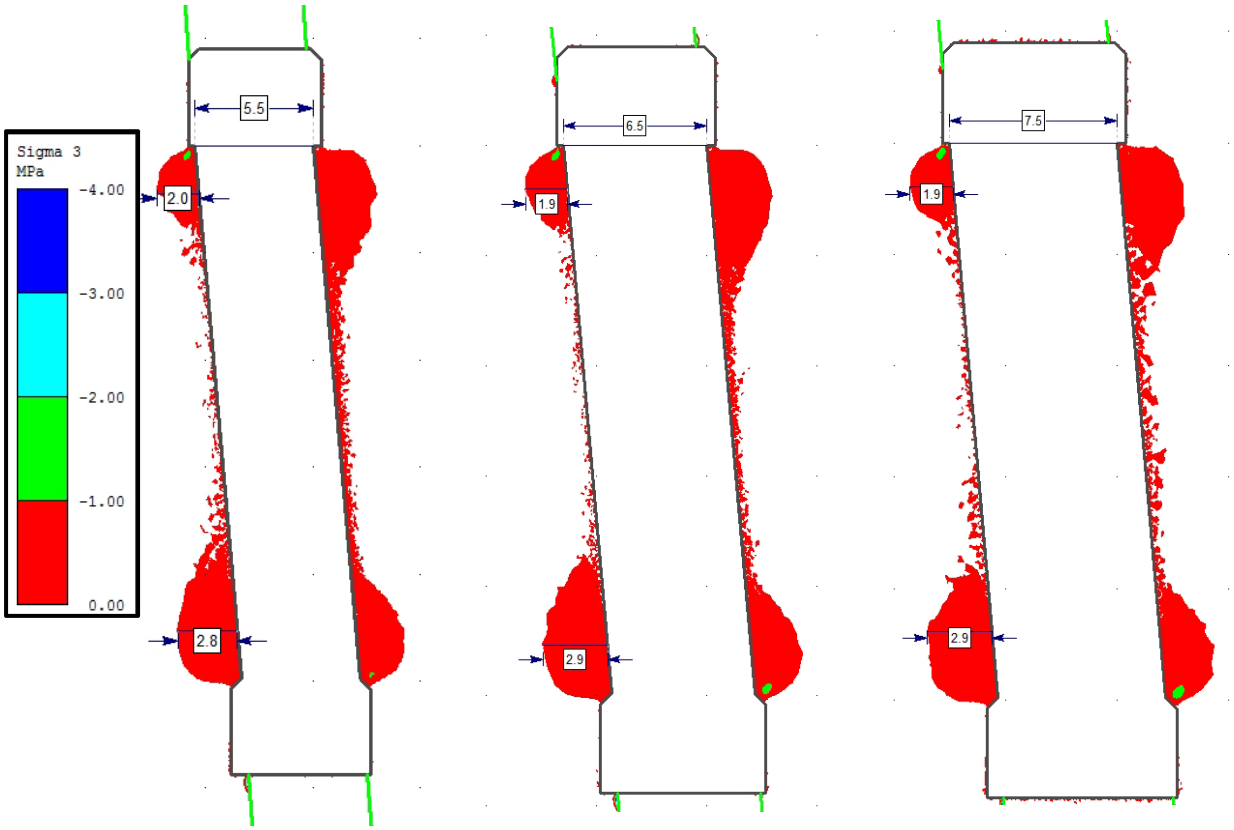


**Figure 6.16** Footwall tension in stopes with ore width ranging from 5.5m to 7.5m

The second results concern the hanging-wall where the tension criterion $\sigma_3 \leq$ -0.1 MPa Stopes with an ore width from 3.5m to 7.5m, the tension in the overcut is between 2.2m and 2.5m compared to 2.9m in the 2.5m ore width case. Tension area in stope undercutting is greater in the narrow ore width 2.5m.

By comparing footwall and hanging-wall results, the amount of dilution from the hanging-wall is minimal compared to the footwall. Figure 6.17 and 6.18 illustrates observed tension in the six studied cases.

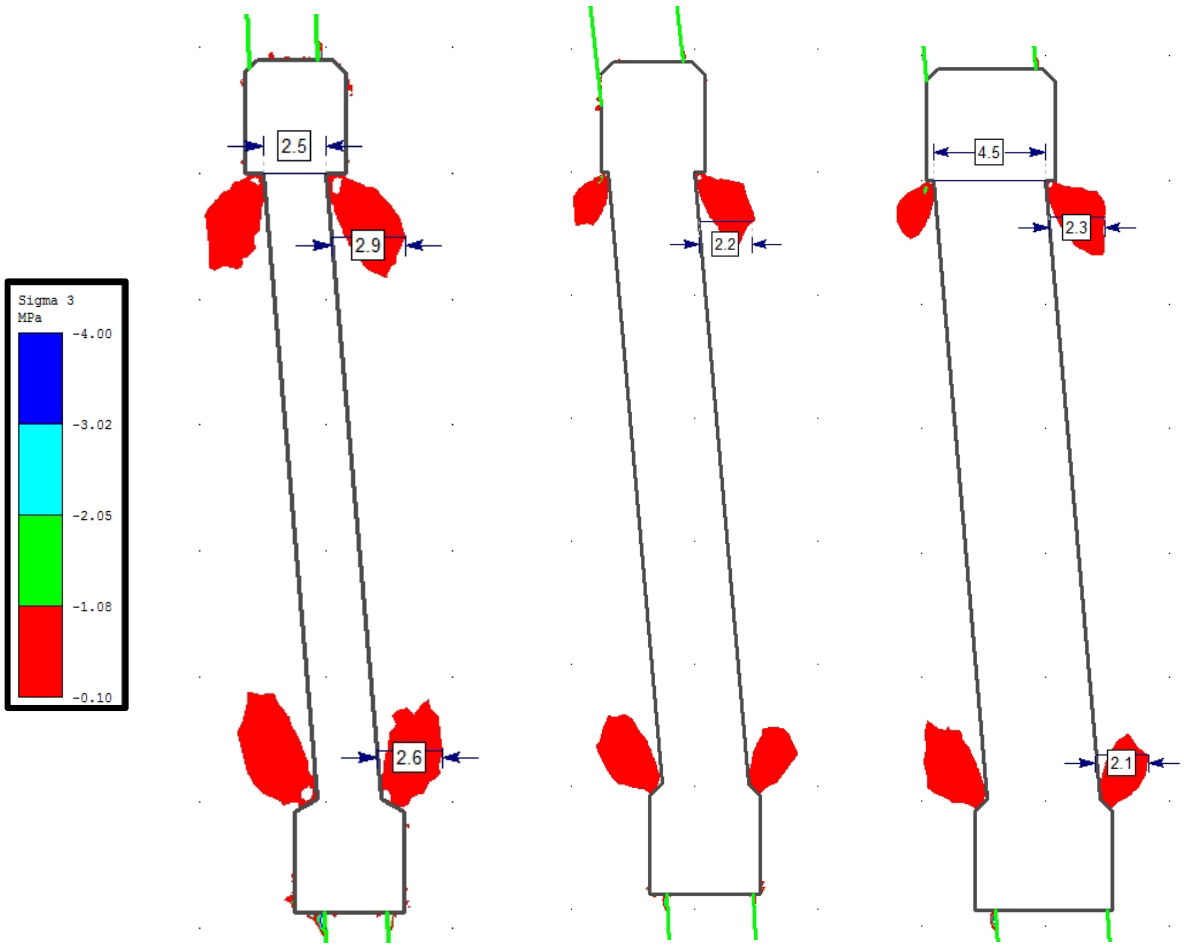


**Figure 6.17** Hanging wall tension in stopes with ore width ranging from 2.5m to 4.5m

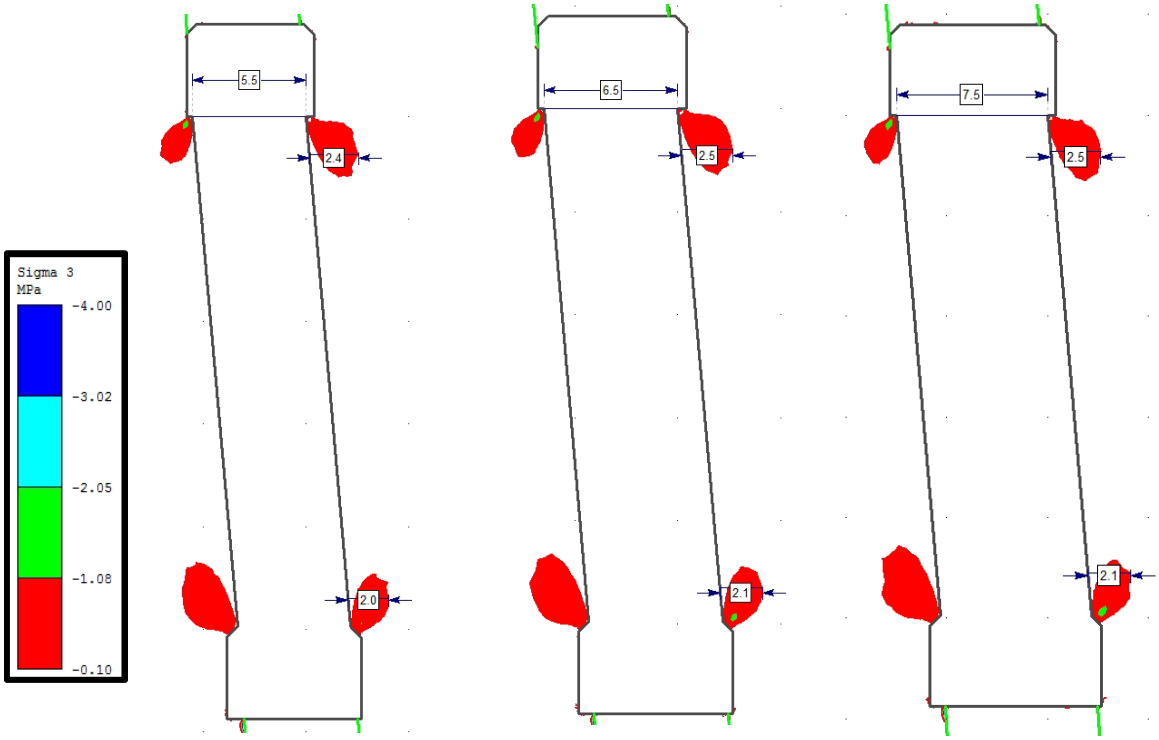


**Figure 6.18** Hanging wall tension in stopes with ore width ranging from 5.5m to 7.5m

Displacements and tension were summarized in Figure 6.19. It is noted that the stope convergence is comparable and the displacement does not increase significantly with larger ore width.

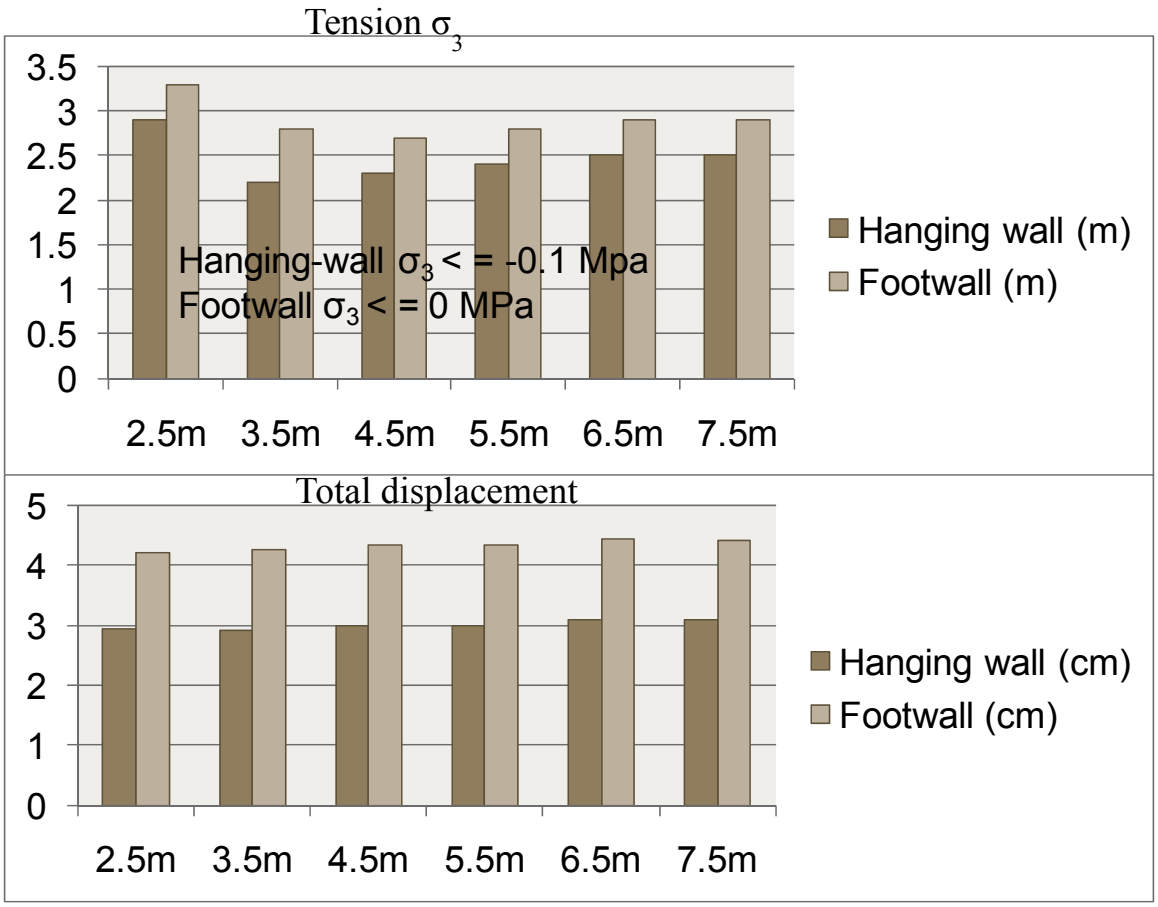


**Figure 6.19** Total displacement and wall tension summary

### 6.4.3 Discussion and conclusion

Dilution is particularly critical for narrow stopes whereby the narrower the stope the higher the dilution for the same amount of wall slough. The hanging-wall tension increases with the ore width. Finally, stope width does not affect drastically the wall stability in a low stress environment unless the vein is very narrow (2.5m ore width).

## 6.5 Effect of wall dip

Unplanned ore dilution (overbreak) is sensitive to the ore dip. Henning & Mitri (2007) noted that in the situation of steep hanging-wall dip, the disturbance of low σ3 stress contours becomes irregular and favorable for a release of an unstable wedge. Moreover, with an inclined hanging wall dip, the gravity effect has the tendency of increasing the overbreak.

### 6.5.1 Numerical modelling set-up

Three models were carried out from 80°, 85°, and 90°. Tension criterion for sub-vertical and vertical dip is footwall $\sigma 3 \leq 0$MPa and hanging-wall $\sigma 3 \leq -0.1$MPa excluding the 80 degree dip model where both footwall and hanging-wall is $\sigma 3 \leq 0$MPa. Stope height is 30m with a footwall undercut of 0.3m and 0.4m undercut of hanging-wall. The ore width is 3.5m. The geomechanical properties used are presented in Table 6.4.

**Table 6.4** Geomechanical properties

| Rock mass | GSI | $E_{rm}$ GPa | $\sigma_t$ MPa | c Mpa | φ ° | ψ° | ν |
|---|---|---|---|---|---|---|---|
| Hanging wall | 60 | 23.2 | 8.6 | 3.67 | 44.7 | 11.2 | 0.16 |
| Ore | 56 | 9.1 | 0.12 | 3.26 | 34.7 | 8.7 | 0.18 |
| Footwall | 56 | 5.16 | 0.1 | 1.93 | 30.15 | 7.53 | 0.18 |

### 6.5.2 Model results

Tension in hanging-wall is pronounced on the case of 80° dip, the expansion of tension goes to 2.8m from the stope wall compared to the vertical dip where tension on the hanging wall is 1.9m, see Figure 6.21.

In the other hand, tension in the foot wall is pronounced on the 80° dip, 3.2m compared to the vertical dip where tension on the hanging wall is 2.5m with a smaller area by tension. Area affected by the tension is smaller when the ore dip is vertical,see Figure 6.20.

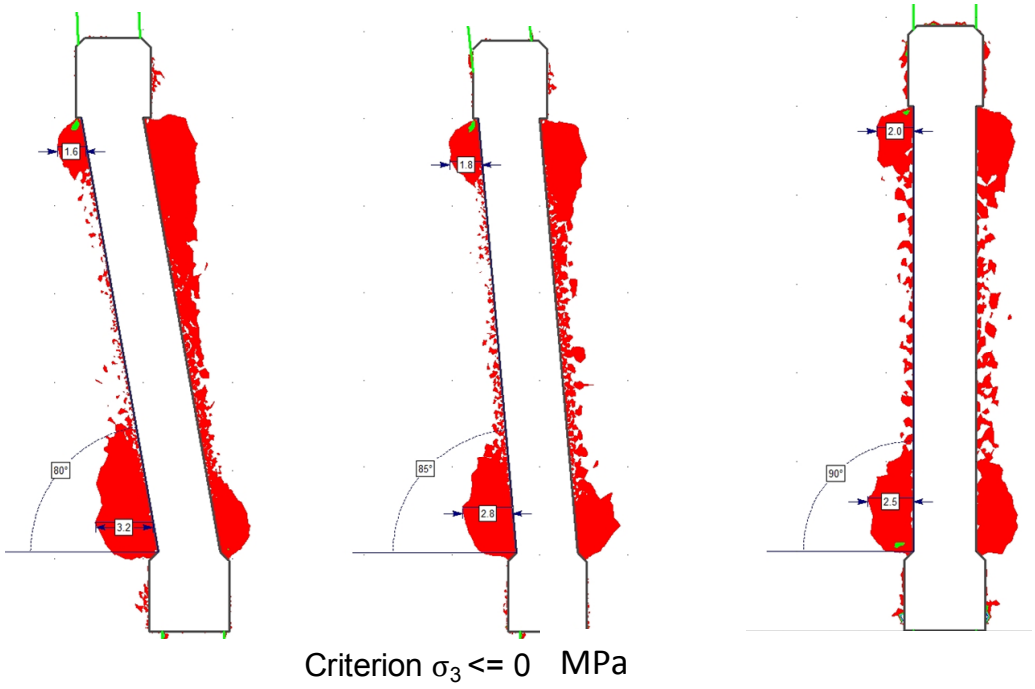


**Figure 6.20** Footwall dip results comparison

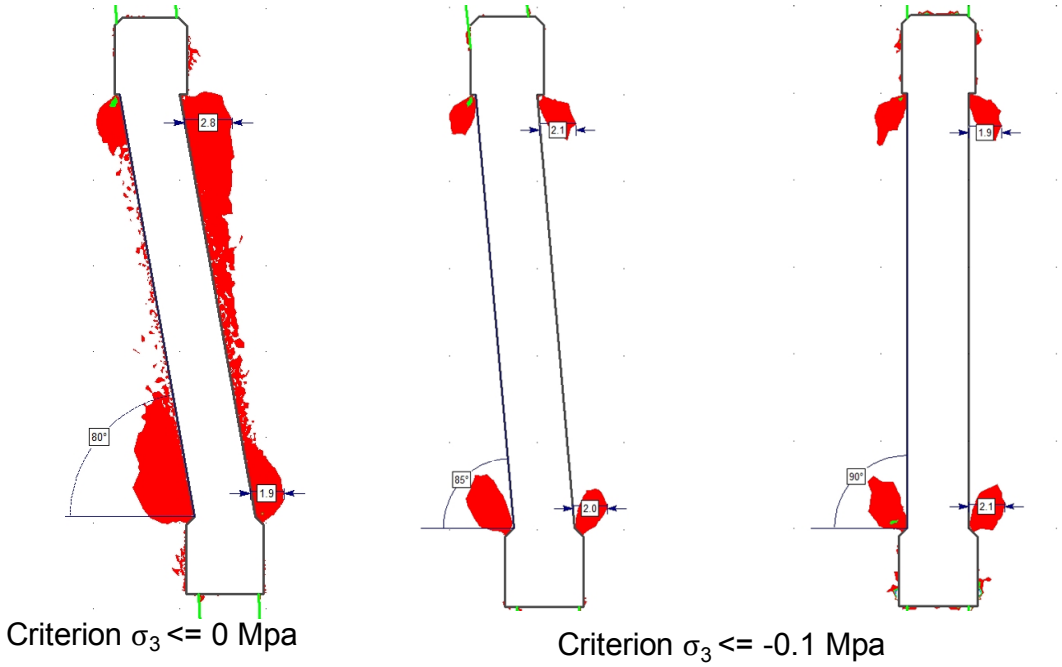


**Figure 6.21** Hanging-wall dip results comparison

### 6.5.3 Discussion and conclusion

On the whole, a change in vein dip in Lapa Mine causes an increase in overbreak. Tension hanging-wall increases with dip where 33% overbreak are experienced in the case of 80 degrees due to the gravity effect, see Figure 6.22. Dip with wall undercutting affects the severity of overbreak on both walls.

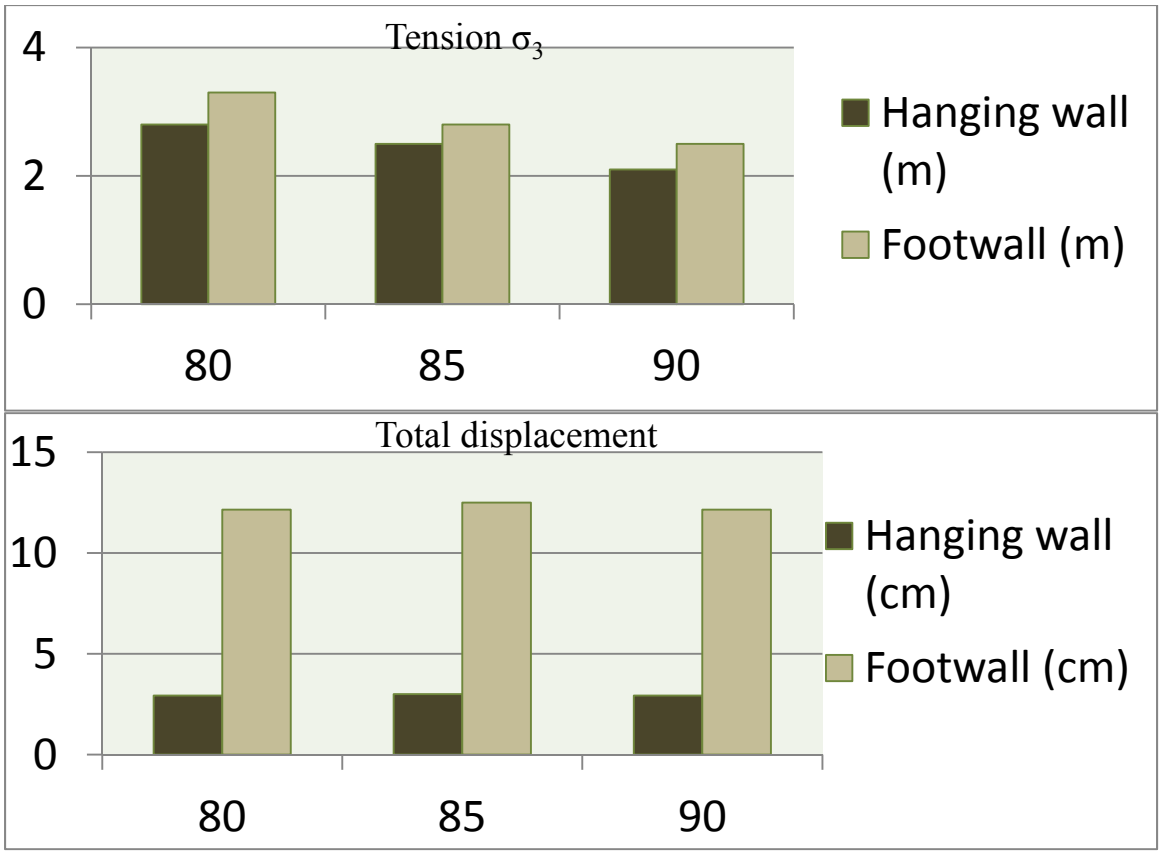


**Figure 6.22** Walls displacement and tension

## 6.6 Conclusion

An increase in strike length to 14 m is likely to create more overbreak from the stope walls by approximately 2% on hanging-wall and 56% on the footwall according to the $\sigma_3 \leq 0$ MPa.

Unplanned dilution is particularly critical for narrow stopes whereby the narrower the stope the higher the dilution for the same amount of wall slough. Finally, dilution has the tendency of increasing under the gravity effect with dipping hanging-wall.

# Chapter 7 Summary and conclusion

## 7.1 Summary of results

Unplanned ore dilution in narrow vein mines affects project profitability. Understanding the reasons for unplanned dilution is key to the reduction and control of ore dilution. The first part of this study focused on a detailed literature review of the various sources of ore dilution and methods currently available for its estimation. A case study of the Lapa Mine, a gold mining operation in the Abitibi region of Quebec, is the scope of this study. Field data was compiled to estimate the rock properties from diamond drill holes. Stope geometric details were recorded and calculated dilution values were added to the database. All gathered data was put in a preliminary database and the maximum dilution density (DD) and ELOS were plotted against the actual stope surveyed profile. A detailed nonlinear finite element modeling study of stope strike, dip angle, ore width, and stope undercutting was conducted using the geomechanical data from the data base. Moreover, a model calibration was performed based on the surveyed stope profiles in order to validate the findings from the numerical modeling study. The following conclusions can be drawn from the study:

- A construction of a preliminary data at an early stage helped in assessing missing geotechnical data and in overcoming a future lack of information.
- Comparing DD max and ELOS against the stope profiles obtained from the CMS showed that DD max profiles are more representative of actual stope wall overbreak shapes.

- A CMS calibration of LAPA mine was conducted to assess the dilution occurrence. The resulting criterion is, $\sigma_3 \leq$-0.1 MPa is the overbreak criterion for hanging wall and $\sigma_3 \leq$0 MPa for footwall.
- Stope construction geometry affects the amount of resulting overbreak. Strike length influences the overall walls stability; such overbreak is greater with longer stope strike length. Secondly, ore dip is another factor where gravity amplifies the hanging wall overbreak when the ore dip gets shallower. Finally, narrower stope (less ore) exhibits higher dilution figures.
- Stope undercutting at Lapa is a major problem and by examining the blast pattern, a change made on it by offsetting the footwall column gave positive results. By undercutting the hanging-wall, the resulting extra amount of waste is not signification compared to the footwall results.

## 7.2 Suggestions for further research

Recommendation for future work at the LAPA mine are:

- Examination of blasting vibration effect on a weak footwall in the vicinity. A tight pattern drilling pattern and drill deviation or high powder factor are likely causes for overbreak.
- Ore dilution due to backfill failure has to be investigated since backfill dilution is recorded in the CMS stope profiles. This is another important aspect that could negatively affect the economics of the operation.

# References


Anderson, B. and B. Grebenc (1995). Controlling dilution at the Golden Giant Mine. CIM Mine Operator's conference. Timmins, Ontario,Canada: 14.

Barton, N. R. L., R.; Lunde, J. (1974). "Engineering classification of rock masses for the design of tunnel support." Rock Mechanics and Rock Engineering 6(4): 189–236.

Bawden, W. F. (1993). The use of rock mechanics principles in Canadian underground hard rock mine design. Comprehensive Rock Engineering: Principle,Pratice and Projects. Oxford, Pergamon Press: 247-290.

Bawden, W. F. (1995). Innovations in cable bolt design for underground hard rock mines. CIM Mine Operators Conference. Timmins,Ontario,Canada: 25.

Bedard, B., Cousin, Lombardi,Mercier, Prince (2006). Lapa project feasibility study. Cadillac, Angico-Eagle Limited: 185.

Bieniawski, Z. T. (1976). Rock mass classification in rock engineering. Exploration for Rock Engineering, Proc. Of the Symp. Cape Town, Balkema.: 97-106.

Bieniawski, Z. T. (1989). Engineering rock mass classifications. New York, Wiley-interscience publication.

Clark, L. M. and R. Pakalnis (1997). An empirical design approach for estimating unplanned dilution from open stope hangingwalls and footwalls. 99th CIM Annual General Meeting, Vancouver, British Columbia.

Connors, C., Wheeler, L., Forsyth, B., and Clark, L., (1996). "Determination of blast damage mechanisms in low quality rock masses".CANMET.

De La Vergne, J. (2000). Hard Rock Miner's Handbook, McIntosh Engineering:330 .

Diederichs, M. S., Kaiser,P. (1996). "Rock instability and risk analyses in open stope mine design." Canadian Geotechnical Journal 33(3): 431-439.

Dunne, K., and R. Pakalnis. (1996). Dilution aspects of a sublevel retreat stope at Detour Lake Mine.

Hadjigeorgiou, J., Lessard, J.F. (2006). Dimensionnement préliminaire des chantiers, Georock Inc.: 18.

Hassani,F.P., Archibald J. P. (1998). "Mine backfill". Canadian Institute of Mining and metallurgy, CD-ROM.

Henning, J. G. (2007). Evaluation of Long-Hole Mine Design Influences on Unplanned Ore Dilution. Mining department. Montreal, Quebec, McGill. Ph.D: 363.

Henning, J. G. (2008). "Assessment and control of ore dilution in long hole mining: Case studies." Geotechnical and geological engineering 26(4): 349-366.

Henning, J. G., Mitri, H. S. (2007). "Numerical modelling of ore dilution in blasthole stoping." International Journal of Rock Mechanics and Mining Sciences 44(5): 692-703.

Hoek, E., Carranza-Torres,C.,Corkum, B. (2002). Hoek-Brown failure criterion - 2002 edition Proceedings of the Fifth North American Rock Mechanics Symposium and 17th Tunneling Association of Canada Conference. Toronto: 267-273.

Hoek, E., Diederichs, M. S. (2006). "Empirical estimation of rock mass modulus. " International Journal of Rock Mechanics and Mining Sciences 43(2): 203-215.

Hoek, E., Marinos, P. (2000). "Predicting tunnel squeezing problems in weak heterogeneous rock masses." Tunnels and Tunnelling International.

Hustrulid, W., Bullock,R., Bullock,R. (2001). Underground Mining Methods: Engineering Fundamentals and International Case Studies, SME: 718.

Martin, C. D., Kaiser,P.K.,D.R. McCreath (1999). "Hoek–Brown parameters for predicting the depth of brittle failure around tunnels." Canadian geotechnical 36: 136-151.

Mathews, K. E. et al. (1981). Prediction of stable excavation spans for mining at depths below 1000m in hard rock, CANMET.

Mitri H.S., J. M., Marwan M. Mohammed,Bouteldja,M. (1998). Design of cable bolts using numerical modelling. ISRM Regional Symposium, Santos, Brazil.

Mitri, H. S., R. Hughes, et al. (2011). "New rock stress factor for the stability graph method." International Journal of Rock Mechanics and Mining Sciences 48(1): 141-145.

Pakalnis R. (1986). "Empirical stope design in Canada" . Ph.D. thesis.University of British Columbia. :276.

Pakalnis, R., Poulin,R.,Hadjigeorgiou, J. (1995). "Quantifying the cost dilution in underground mines." Mining Engineering 47(12).

Pakalnis, R., Poulin,R.,Vongpaisal, S. (1995). Quantifying Dilution for Underground Mine operations. 97th Annual general meeting of the Canadian Insitute of Mining Halifax.

Palmstrom, A. (1982). The volumetric joint count - A useful and simple measure of the degree of rock mass jointing. IAEG Congress. New Delhi pp V.221 – V.228.

Perron, J. (1999). Simple solutions and employee's involvement reduced the operating cost and improved the productivity at Langlois mine. Proceeding 14th CIM Mine Operator's Conference. Bathurst,New Brunswick.

Potvin, Y. (1998). Rock Mechanics Principles for Open Stope Mining at Mount Isa Mines. CIM.

Potvin, Y., and Hadjigorgiou, J. (2001). The stability graph method for open stope design. Underground mining methods: engineering fundamentals and international case studies. Colorado, Society for Mining, Metallurgy, and Exploration: 513-520.

Ran, J. (2002). "Hangingwall sloughing mechanism in open stope mining." CIM Bulletin 95(1064): 74-77.

Scoble, M.J., and Moss, A. (1994). "Dilution in underground bulk mining: Implications for Production Management, mineral resource evaluation II, methods and case histories." Geological Society Special Publication 79: 95-108.

Yao, X., G. Allen, et al. (1999). Dilution evaluation using the cavity monitoring system at HBSM-Trout Lake Mine. 101th Annual General Meeting, Calgary,Alberta.

Wang, J. (2004). Influence of stress, undercutting, blasting and time on open stope stability and dilution, Saskatchewan. Ph.d: 279.

Wang, J., Milne,D., Yao, M. and Allen, G. (2002). Quantifying the Effect of Hanging Wall Undercutting on Stope Dilution. 104th CIM annual General Meeting, Vancouver, British Columbia, Canada.

Zniber El Mouhabbis, H., Mitri,H.S., Bedard,N.,Lecomte,E. (2009). Effect of stope undercutting on itswall overbreak. Proc. 43rd us Rock Mechanics Symposium. Ashville, North Carolina.